Investigations on electrical conducting magnetic hybrid materials for sensor and actuator systems

Bachelor: Jhohan Harvey Chávez Vega

Thesis submitted for the degree of
Master of Science in Mechanical Engineering

Advisors, Ilmenau:
M.Sc. Tobias Kaufhold
Dr.-Ing. Valter Böhm

Advisors, Lima:
Dr. Ing. Francisco Rumiche

Supervising Professor, Ilmenau:
Univ.-Prof. Dr.-Ing. habil. Klaus Zimmermann

Ilmenau – Germany
2016

PONTIFICIA UNIVERSIDAD CATÓLICA DEL PERÚ

TECHNISCHE UNIVERSITÄT ILMENAU

Fakultät für Maschinenbau

Technical Mechanics Group

Task for master's thesis

of Jhohan Harvey Chavez Vega

Topic: Investigations on electrical conducting magnetic hybrid materials for sensor and actuator systems

The use of magneto sensitive materials for sensor and actuator systems is an actual research field. These materials offer new advantages like mechanical compliance, shape variability and more, in contrast to conventional systems. Also these hybrid materials are composed of magnetic particles as suspended component and complex substrates with or without reversible variable properties. In the focus is the use of compliant magnetic hybrid materials based on elastomers as matrix material. The reversible variable mechanical behavior of technical functional elements can be realized and specifically controlled by magnetic fields using particle matr x interactions.

This work will focus on electrical conducting magneto sensitive materials. Through the implementation of electrical conductivity as an additional material property combined sensor-actuator systems can be realized. The change of the electrical resistance, due to magnetic fields and/or mechanical loads, is dependent on the fraction of magnetic and electrical conductive particles.

Main tasks for this thesis are:

- Literature overview, state of the art
- Development of mixtures with specific properties: high electrical conductivity and sensitivity to magnetic fields / mechanical loads
- Realization of an experimental test stand, measuring the considered properties
- Documentation and oral presentation of the work

Start date:	01.10.2015
Supervising Professor, Ilmenau:	Univ.-Prof. Dr.-Ing. habil. Klaus Zimmermann
Advisor, Lima:	Ph.D. Francisco Rumiche
Advisor, Ilmenau:	Dr.-Ing. Valter Böhm
	M.Sc. Tobias Kaufhold

5.10.15
Place, Date

02/12/2015
Place, Date

5.10.15
Place, Date

Signature, supervising Professor, Ilmenau

Signature, Advisor, Lima

Signature, M.Sc. Candidate

Statement

Hereby, I declare that I have elaborated the present work without any non-specified assistance. The people involved on this research, literature, as well as any other resource used in this thesis, has been completely specified throughout and at the end of the text.

31st March 2016. Ilmenau

Jhohan Harvey Chavez Vega

Acknowledgements

First of all, I thank God for life and all the opportunities he gives us. With his blessing and some effort, we can achieve great results.

I also want to thank my parents, because I was taught from them that things in this life are not easy and one have to work constantly to succeed and be satisfied. To my sister Sthephanie who has made feel that the distance between us did not exist. To them it is dedicated each hour invested in this work.

A very special thanks to my advisors at TU-Ilmenau: M.Sc. Tobias Kaufhold, from whom I have learned many things in this little time for research, for his patience, readiness and good ideas at work; and to Dr. Valter Böhm for his good mood and humor, besides his relevant suggestions for the thesis. To Prof. Zimmermann, for have given me so openly the opportunity to work in his department. And all his staff, for the almost familiar treatment that handle between them and their kindness despite the difficulties of communication due to the difference of languages.

Definitely I also thanks a lot to the PUCP team, especially my advisor Dr. Francisco Rumiche who accepted instantly and with great scientific interest the thesis topic, and to directors of the master studies, Dipl.-Ing. Benjamin Barriga and Dr. Julio Tafur for give to many students the option to this fruitful double degree program.

Finally, thanks to all my Peruvian and foreign colleagues, for every constructive criticism to this work and also shared experiences.

Zusammenfassung

Wissenschaftler und Ingenieure sind motiviert, neue Elemente und Materialien zu untersuchen und zu verstehen. Materialien mit neuen Eigenschaften wecken besonderes Interesse der Forschung und daraus entstehen zumeist auch innovative Anwendungsmöglichkeiten.

Einer dieser modernen Stoffe sind Ferrofluide. Diese weisen ein spezielles, smartes Verhalten unter dem Einfluss von magnetischen Feldern auf. Daraus ergeben sich zahlreiche Anwendungsmöglichkeiten wie beispielsweise für Stoßdämpfer bei Automobilen sowie unter anderem für die Messung der Viskosität von Flüssigkeiten.

Magneto-sensitive Elastomere (MSE) sind Materialien, die ähnliche Eigenschaften wie Ferrofluide aufweisen. Der wesentliche Unterschied liegt in dem festen Zustand des Materials, unabhängig von der An- oder Abwesenheit eines magnetischen Feldes. MSE weisen eine Polymer-Matrix auf, die magnetische Partikel enthält. Diese ermöglicht dem Material intelligentes Verhalten bei magnetischen Feldern. Im vorliegenden Projekt waren die magnetischen Partikel Eisenpulver und einige Mengen Graphit, die hinzugefügt wurden, um elektrische Leitfähigkeit zu ermöglichen.

Mehrere Proben magneto-sensitiver Elastomere wurden auf ihre elektrischen und mechanischen Eigenschaften hin bei Einfluss eines magnetischen Feldes untersucht. Das magnetische Feld wurde mit Hilfe von Permanentmagneten induziert und durch die variierendere Position der Magnete mit einem motorisierten Positionierungssystem verändert. Die aus den Ergebnissen gewonnenen Schlussfolgerungen können im Design und Bau von Sensoren und Stellteilen Anwendung finden.

Abstract

Scientists and engineers feel motivated in the presence of new elements or materials they cannot comprehend. That is why when a material with a new properties or behavior arises, they do the best to investigate on them until understand them and give some applications.

One of these kind of moderns materials are the ferrofluids, which have a special and very different behavior when are induced under magnetic field and when not. These materials have plenty of applications nowadays. Due to their smart behaviour they are used on dampers for automobile suspensions, for measurement of fluid's viscosities, acoustics and several more tasks.

Magneto sensible elastomers (MSE) are materials that own similar properties to ferrofluids, with the substantial difference of being in solid state independently of the presence or absence of magnetic field. MSE are composed on a polymer matrix that has magnetic particles that provide them a smart behaviour under magnetic fields. For this project the magnetic particles were iron powder and certain amounts of graphite were also added to give electrical conductivity.

In the current work it was fabricated several samples of MSE to study the behaviour of their electrical and mechanical properties under the effect of a magnetic field. Permanent magnets were used to induce the magnetic field on the probes and this field was changed by moving the magnets away and close to the probes through a motorized positioning machine. The results obtained from the experiments are summarized on conclusions that can be used in future to the design and building of sensors and actuators.

Contents

1 Introduction

Smart materials have been a topic of interest to engineers for a long time. Each time there is a material that behaves in an unconventional way, the scientific community has devoted time and money to study them and after understood their behaviour they can give a novel application [1].

1.1 Motivation of Work

Magneto sensitive materials (MSM) are used in many applications today. One of the magneto-sensitive materials widely known and studied in science are ferrofluids. These are non-Newtonian fluids which being under a magnetic field behave differently when free from the effect of this field.

The particularity in working with ferrofluids is that when they are not influenced by a magnetic field, they adopt the shape of its container and this property is sometimes not convenient. In contrast, magneto sensitive elastomers (MSE) have a shape defined by the container that held them during the curing process.

The MSE are constructed from a matrix, which is normally gel or silicone, inclusions of magnetic particles [1,2]. The magnetic particles added to the matrix allow the the external magnetic field flow into the MSE, the magnetic material commonly used is carbonyl iron. Carbonyl iron particles can be of different sizes or shapes, but the most used range goes from hundreds of nanometers to some micrometers size particles [2,3].

There are several applications for magneto sensitive materials, one of the most interesting is in vehicles suspension, where the oil that is usually used in dampers can be replaced by ferrofluid or MSE, surrounding the device with an electromagnet and varying the magnetic field induced by it, the viscosity of the MSM is varied, the change in viscosity can be used by the user when the vehicle bears a greater load or to provide better stability while driving on a uneven road [2,4,5].

The use of magneto sensitive materials for sensor and actuator systems is an actual research field. These materials offer new advantages like mechanical compliance, shape variability and more, in contrast to conventional systems. Also these hybrid materials are composed of magnetic particles as suspended component and complex substrates with or without reversible variable properties. In the focus is the use of compliant magnetic hybrid materials based on elastomers as matrix material. The reversible variable mechanical behaviour of technical functional elements can be realized and specifically controlled by magnetic fields using particle matrix interactions.

In this work it is studied macroscopically the composition of some MSE mixtures built in a laboratory and their electrical, elastic and magnetic memory properties. The purpose of the experiments and conclusions presented is to apply them in future design and construction of sensors and actuators.

1.2 Goals of the project

This work will focus on electrical conducting magneto sensitive materials and field-induced plasticity (magnetic shape-memory). Through the implementation of electrical conductivity and field-induced plasticity as an additional material property combined sensor-actuator systems can be realized. The change of the electrical resistance, due to magnetic fields and/or mechanical loads, is dependent on the fraction of magnetic and electrical conductive particles. The quality of objects shape recorded depends on the fraction of magnetic particles and the composition of the polymer matrix.

The specific objectives for the current work are:

- Development of mixtures with specific properties: high electrical conductivity and sensitivity to magnetic fields / mechanical loads.
- Development of field-induced-plasticity alloys to study their behaviour under the effect of magnetic field.
- Development of an experimental test stand, measuring the considered properties.
- Conclusions of the results obtained in the experiments executed.
- Recommendations for improvements of the set up of tests, fabrication of mixtures and measurement.

1.3 State of art

On this chapter are presented some basic knowledges that should be considered while working with MSE and some researches of theoretical studies and experimental works related to this thesis.

Magnetization curves for ferromagnetic materials

On the experiments of this project, a key component on the samples is iron. Such that iron is a ferromagnetic material, it is important to know the magnetization curves for the ferromagnetic materials [6-7]. In the figure 1.1 it is shown the hysteresis loop for these materials.

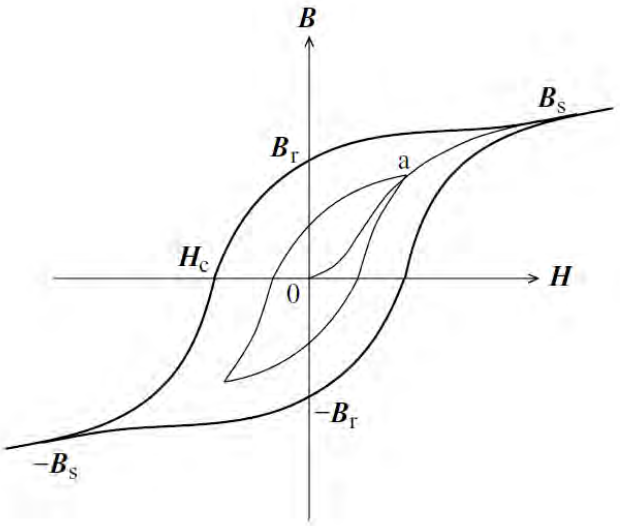

Figure 1.1: Hysteresis loop for a ferro- or ferri-magnetic materials [6].

In the figure 1.1, the curve of hysteresis for ferro-magnetic materials starts on the origin of coordinates for H-axis (magnetic field strength) and B-axis (magnetic flux density), then the induced magnetic field reaches the value B_s that is denominated the saturation because although more magnetic field is applied, the induced field on the material cannot be higher than this value. Then when the magnetic field is released, the induced one does not go back to the initial of coordinates, instead of that it saves a remaining value of induced magnetic field equal to B_t. If it is needed a induced magnetic field equal to zero as in the beginning, some negative magnetic field (H_c) is needed to reach that. With the same procedure for negative magnetic field, the loop is completed. [6-7]

Stress relaxation on viscoelastic materials

As shown in some literature for viscoelastic materials' behaviour [8], for classic elasticity, mostly studied for metals, there is no time delay between the application of a force and the deformation made from that. For many materials, however, there is additional time-dependent deformation that is recoverable. This is called viscoelastic deformation. When

a load is applied to those materials, there is an instantaneous elastic response, but the deformation also increases with time. And when a deformation is imposed, the load on that material decreases with time.

The best rheological model for viscoelastic materials, that describes the force (or stress) and deformation (or strain) relaxation for viscoelastic materials, is a combined series parallel model for springs and dashpot or also called Voight-Maxwell model [8], this model is shown in the figure 1.2.

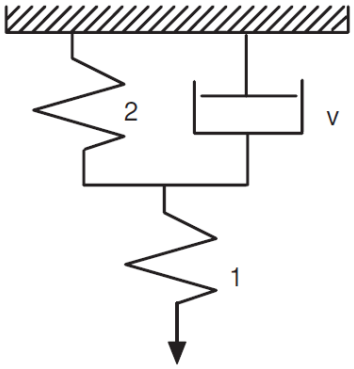

Figure 1.2: Combined series parallel model (Voight-Maxwell model) [8].

The basic equations for the behaviour of a spring is described by equation 1.1, where e_e is the length change of the spring, K_e is the constant of the spring and F_e the force on the spring.

$$e_e = \frac{F_e}{K_e} \tag{1.1}$$

The basic equations for the behaviour of a dashpot is described by equation 1.2, where e_v is the length change of the dashpot, K_v is its constant and F_v the force on it.

$$\dot{e}_v = \frac{F_v}{K_v} \tag{1.2}$$

The equations of force and elongation for this model are:

$$F = F_1 = F_2 + F_v$$

$$e = e_v = e_1 = e_2$$

When a force, F, is suddenly applied to the viscoelastic material at time 0 (see figure 1.3) The equations of the behaviour are as follow [8]:

$$\frac{de_v}{dt} = \frac{F_v}{K_v} = \frac{F - F_2}{K_v} = \frac{F - K_2 e_2}{K_v} = \frac{F/K_2 - e_v}{K_2/K_v}$$

Rearranging, the following equation is obtained:

$$\int \left(\frac{F}{K_2} - e_v\right)^{-1} de_v = \frac{1}{\tau_e} \int dt$$

Where $\tau_e = K_v/K_e$ is the relaxation time for strain relaxation. After integrating the previous equation, the following one is obtained.

$$e_v = \left(\frac{1}{K_2}\right) F \left(1 - e^{(-t/\tau_e)}\right)$$

Substituting $F/K_2 = e_\infty - e_o$, where e_∞ and e_o are the relaxed and initial (unrelaxed) elongations, $e_v = (e_\infty - e_o)\left(1 - e^{(-t/\tau_e)}\right)$. The total strain is $e = e_v + e_1$, so the equations for elongation can be summarized in the equation 1.3. At time zero the elongation is equal to e_o and at infinite time is e_∞.

$$e = e_\infty - (e_\infty - e_o)\left(1 - e^{(-t/\tau_e)}\right) \tag{1.3}$$

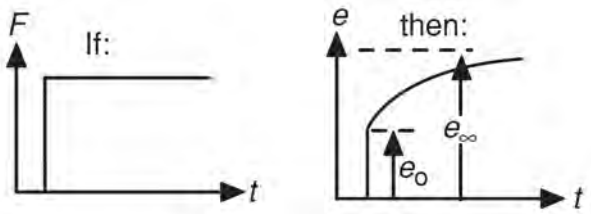

Figure 1.3: Strain relaxation predicted by the series parallel model. The strain saturates at e_∞ [8].

Now, when an elongation, e, is suddenly applied to the viscoelastic material (see figure 1.4) Immediately after stretching, the strain occurs in spring 1, so $e = F/K_1$ and the initial force is $F_o = eK_1$. After an infinite time, the dashpot carries no load, so:

$$e = F\left(\frac{1}{K_1} + \frac{1}{K_2}\right)$$

$$F_\infty = \left(\frac{K_1 K_2}{K_1 + K_2}\right) e$$

The general force equation is shown in equation 1.4.

$$F = F_o - (F_o - F_\infty)\, e^{(-t/\tau_\sigma)} \tag{1.4}$$

Where the relaxation time, τ_σ, is given by:

$$\tau_\sigma = K_v/(K_1 + K_2)$$

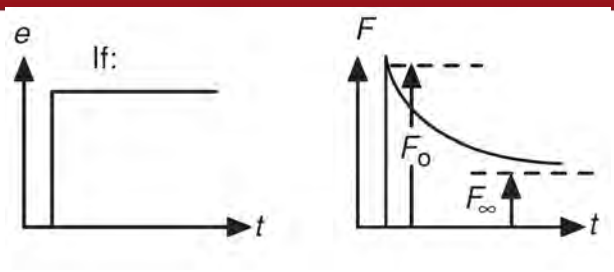

Figure 1.4: Stress relaxation with the series parallel model. The stress decays to F_∞ [8].

This behaviour is seen later on section 2.3 for experiments of deformation of silicone matrix samples.

Scientific studies on MSE

Some works studied some properties of MSEs under the effect of magnetic fields and mechanical loads. In a similar configuration of the one used on the present work, the impedance was analysed on some previous works like the one from Wang et al. [13]. The setup of the experiments are shown on the figure 1.5. There the electrical resistance of the MSE was measured under a certain compression pressure, and the dependence between resistance, magnetic field intensity and compression pressure was determined [13]. This configuration served up as a precedent for the setup of this thesis.

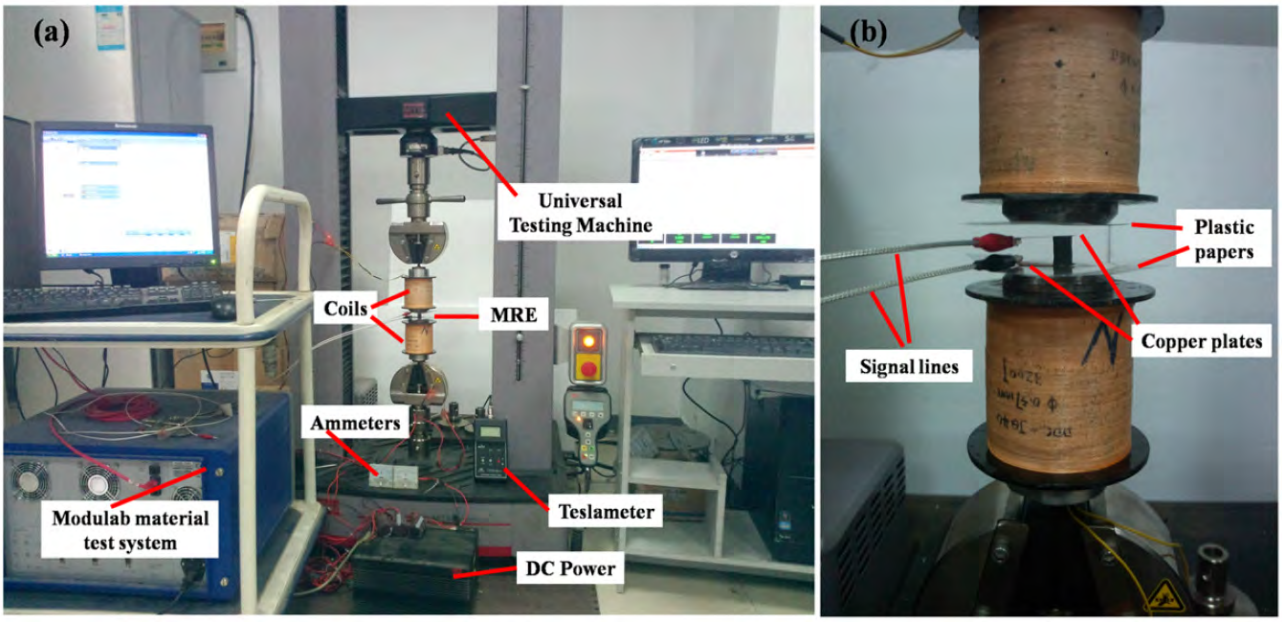

Figure 1.5: (a)The electrical test system and (b)the placement details of the MRE sample [13].

The relationship between shear storage modulus and magnetic field strength is shown on figure 1.6. Because of the high content of iron particles, the shear modulus increases greatly as the magnetic field strength is raised [13].

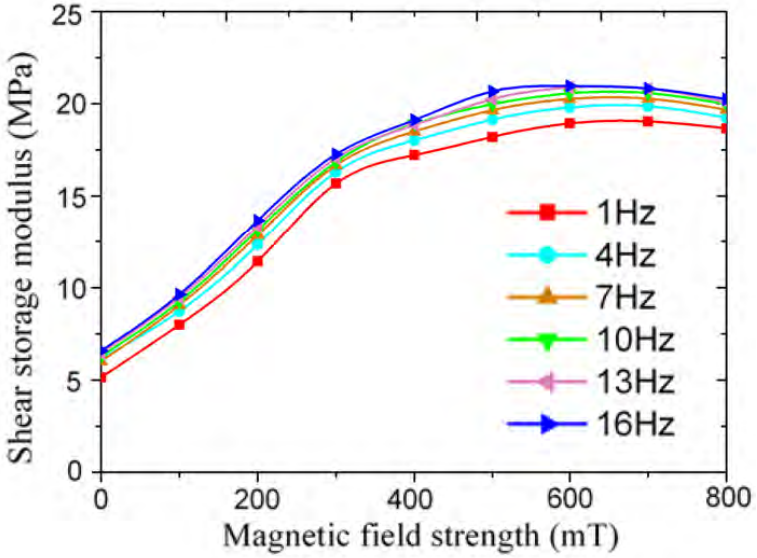

Figure 1.6: Magnetic field strength dependency of shear storage modulous [13].

If a mechanical load is applied on the MSE, the particles would change they location and spacial arrangement [38-40], afecting in this way the rheological properties.

On the figure 1.7 is shown the variation of the electrical resistance for 60%, 70% and 80% volume fraction of iron after applying some and the figure 1.8 shows a mathematical representation of the behaviour of the electrical resistance through one approximation with a power function for the sample's electrical resistance over the mechanical load [17].

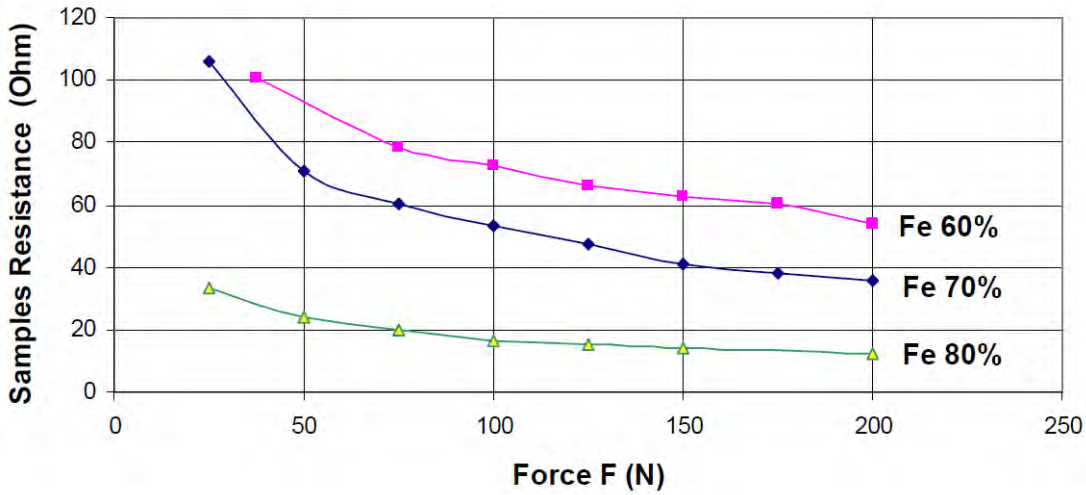

Figure 1.7: The electrical resistance variation for particle reinforced composite material having iron particles (100μm) with volume fraction of 60%, 70% and 80% under the effect of external force [17].

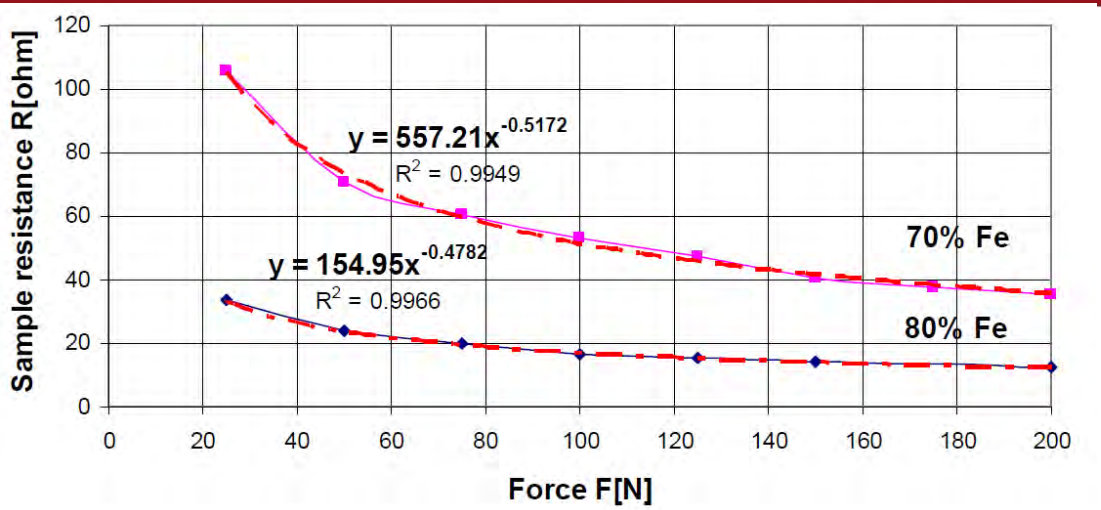

Figure 1.8: The sample's electrical resistance dependence on force, approximate by power function [17].

When a magnetic field is induced on the MSE, the same result as with mechanical load occurs, the arrangement of the magnetic particles changes [40-42]. A representation of this change is shown on figure 1.9.

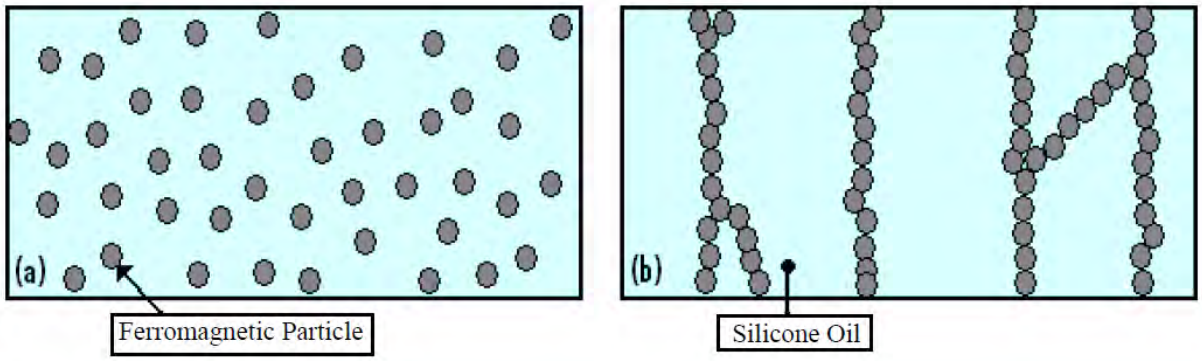

Figure 1.9: Structure of MSE, ferromagnetic particles in a silicone oil suspension; (a) under no magnetic field, and (b) with magnetic field applied [21].

This representation is proved in some experiments of scientific works [9] like the one shown on figure 1.10.

The effect of the induced magnetic field on the MSE is returned as a force in the MSE (or MRE, magneto rheological elastomer), as presented on the sequence of figures 1.11 to 1.13. On the figure 1.11 is shown the mesh profile of a cross-section of a model of a cylindrical MSE close to a cylindrical coil, the MRE is attracted to the electromagnet. Figure 1.12 shows the magnetic flux density distribution, the maximum magnetic flux density is 0.75T in the iron core and the maximum magnetic flux density in the MRE is about 0.01T. The figure 1.13 shows the magnetic forces acting on the nodes of the MRE, the inner magnetic force distribution in the MRE is calculated: the maximum magnetic force is 9.89E-4N in the MRE underside surface and is rapidly decreased [28].

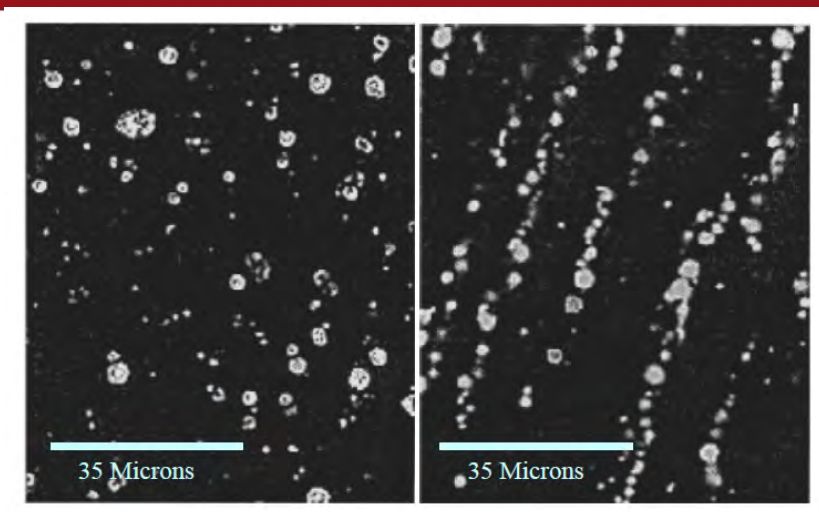

Figure 1.10: Scanning electron Micrographs (SEMs) images of particles in an elastomer; (left) randomly dispersed particles, (right) particles aligned by applied magnetic field [9].

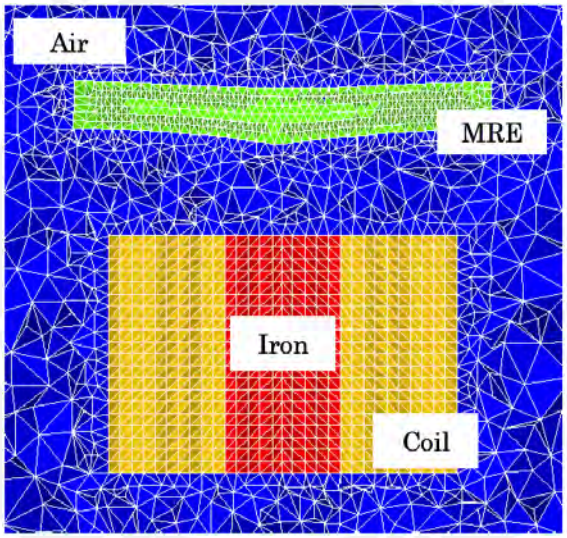

Figure 1.11: The mesh profile of a cross-section of a cylindrical model for a MRE [28].

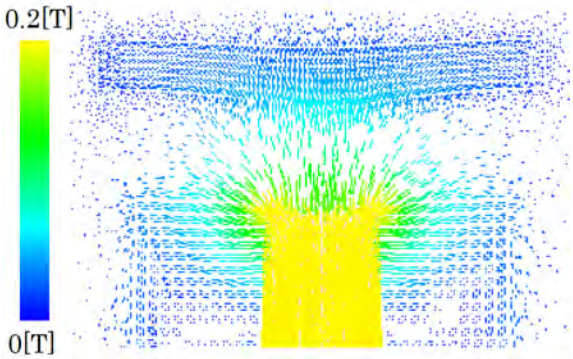

Figure 1.12: Magnetic flux density distribution [28].

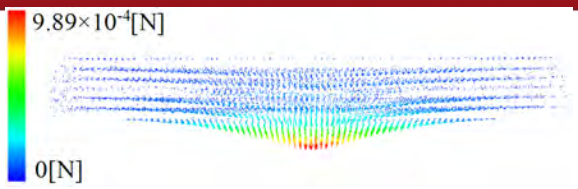

Figure 1.13: Magnetic force distribution in the MRE [28].

An interesting experiment using the results of the influence of the mechanical load and the force created by the induced magnetic field on the samples, is shown also in one work [17]. On the figure 1.14 is shown the variation of the electrical resistance of a MSE when magnetic pulses are applied on it.

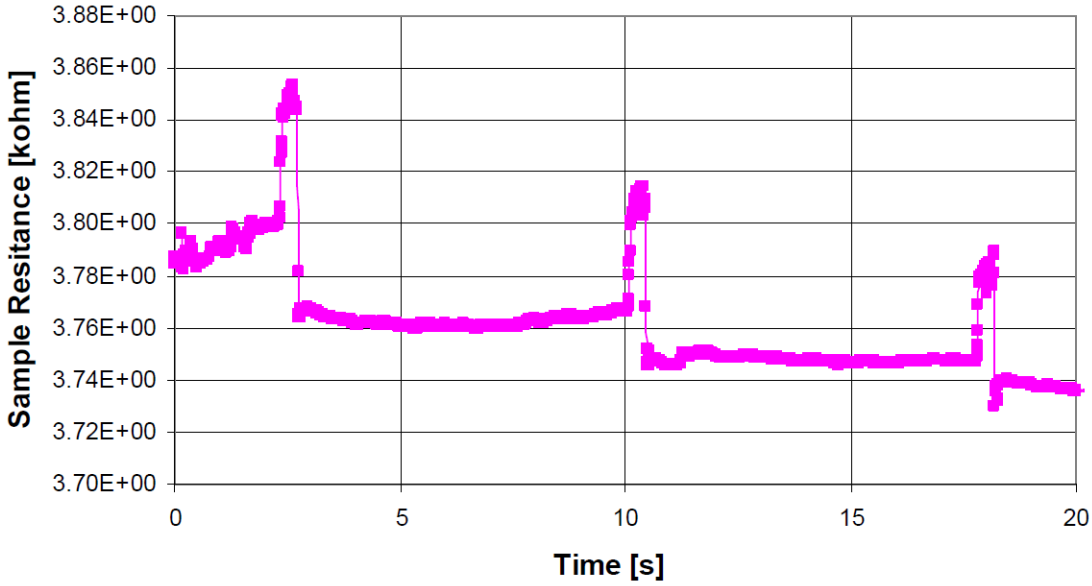

Figure 1.14: Variation of sample's electrical resistance with magnetic pulses [17].

The works, experiments and configuration of the tests presented above have somehow emboldened the present thesis for the fabrication of samples and the set up used in each kind of experiment presented in the following chapter.

2 Fabrication of samples, testing and measurement

During this thesis project several samples were produced to study of different properties. In this chapter are presented first the materials used to produce the samples and from the section 2.2 to the end are described the way of preparation of the samples, the set up for the tests and the results obtained.

2.1 Materials used for the fabrication of samples

Some of the materials presented in the following paragraphs were used indispensably to make the samples, as silicone for the base matrix, and others were used to give some special properties to the sample and to make them suitable for the kind of test.

Silicone
The matrix used to where the magnetic particles and semiconductor element were included, is silicone. The type of silicone used is Polydimethylsiloxane, these kind of silicone are known for its non-common rheological properties [11].
The silicone used is Alpa-Sil Classic provided by Alpina Technische Produkte GmbH. Alpa-Sil Classic has two components: the first component (component A) is a translucent liquid with density 1.05g/cm^3 and the second component (component B) is a blue liquid with density 1.10g/cm^3 added to the first for the curing process. The ratio of components A and B needed for curing is 10:1 respectively. The silicone reaction for the curing process is by adhesion, where no sub-products are released, the two components stick together and the mixture has a good dimensional stability.
The first component added on the mixtures was the component A, then the other components or particles, and at the end was added the component B. After that adding the second component, the mixture can be keep being mixed for 7 minutes, after 30 minutes is starts to cure. One more important property of the silicone used is its hardness that is between 6 and 8 in the Shore A scale, this result is obtained after 14 days of vulcanisation in a normal climate. However, these specifications could change when other components are used in the mixture, furthermore in all the test presented later we waited for just one day of curing after adding the component B because it was hard enough for our tests.
To review all properties for both components of Alpa-Sil Classic, review appendix A.

Silicone oil
Component added to the component A Alpa-Sil Classic. Two types of silicone oil were used, each one with a particular viscosity and both a transparent appearance and from the same laboratory (XIAMETER®). The viscosity and density for those oils, at a temperature of 25°C, are:

- Silicone Oil 1000cSt: 0.970g/cm^3
- Silicone Oil 5cSt: 0.913g/cm^3

For all the samples used in the project, the silicone oil replaced some amount of component A Alpa-Sil Classic on the mixture, and the needed component B needed to cure was calculated as the tenth part of the combined mass of component A and silicone oil.
To check the data sheet of the supplier of silicone oils, with all its properties, review the appendix B for the 1000cSt oil and the appendix C for the 5cSt oil.

Iron powder
The iron used was carbonyl iron powder from BASF Company, grade CEP CC with 99.5% purity iron. The highest size of particles is equal to 10 microns. This iron has the characteristic of being not conductive, nor alone nor in a polymer matrix. The iron has a density of 7.87g/cm^3 and the carbonyl iron has a apparent density of 4.20g/cm^3 [8].
Although several sources of information and literature was reviewed for finding a explanation for its non-conductive behaviour [12,14-18,34,36], it had not success and just can be affirmed by experiment. To review other technical data of the iron used, review appendix D.

Graphite
To provide conductive characteristics to the samples, it was used graphite PRINTEX®XE2-B from Orion Engineered Carbons. Its initial shape was in beads or spheres, this shape is used to transport easily the graphite, compared to working with graphite powder. The initial size of graphite spheres of diameter was around 1mm. A mesh of 100 micrometers and for some tests also a mesh of 25 micrometers were used to sieve the initial spheres before adding to the mixture. All the properties given by the dealer of the graphite can be found on its data sheet in appendix E.

Silicone glue
The silicone glue (rubber) used was ELASTOSIL®E41 from Wacker Laboratories. It is a paste with good mechanical properties and can adhered strongly to other silicone compounds. The most outstanding properties are the density equal to 1.078g/cm^3 at 23°C and the hardness, Shore A 40.
To review more properties of this rubber, see appendix F.

Copper mesh
This mesh was used to create contacts with very low electrical resistance. The provider is Weisse & Eschrich GmbH. The size of its copper wires is 0.25mm and their were spacing 0.50mm in both directions of the mesh.

2.2 Test for change in el. resistance under magnetic field and mechanical load

On a silicone matrix, it was added graphite and iron to give electrical conductive and magnetic properties to the mixture. When the mixtures were cured, some tests were made to see the influence of magnetic field and external pressure on changing their electrical resistance.

2.2.1 Fabrication of samples

The silicone matrix was composed of Alpa-Sil Classic and silicone oil of viscosity 1000cSt. To this matrix of silicone and silicone oil it was added some graphite particles. All the components added to the mixture were weighed in a balance with 0.001g of resolution. Because of the great sensibility of the balance, the last digit of the weight measured normally was fluctuating, that is why the error for each component was of +/- 0.01g.
The initial shape of graphite, as presented before, was in spheres of about 1mm size. To get a better distribution of the graphite in the sample, the initial spheres were crushed and then sieved with a steel mesh of 100 microns of separation of tissues.
After sieving the crushed graphite, the necessary amount was added to the mixture. To dissolve easily the graphite in the silicone matrix some hexane was used, only in the amount needed (between 0.5g and 1.5g of hexane per 4g of mixture silicone - silicone oil - graphite). When the graphite was already dissolved in the silicone matrix, the mixture was sieved again with a finer steel mesh, of 25 micron size. The set up to sieving the graphite with the 25 microns mesh is shown in the figure 2.1, when this mesh was used to sieve, more hexane was added at the same time to avoid the graphite get stuck to the mesh. The set up for sieving with 100 microns mesh was similar to the figure 2.1, but no hexane was necessary for sieving with it.

Figure 2.1: Set up for sieving graphite with the 25 microns size mesh.

The figure 2.2 shows a comparison between a cured mixture made using sieved graphite and unsieved graphite, both cured mixtures shown were cut by the middle.

Figure 2.2: Difference between a sample with unsieved graphite (left) and sieved graphite (right). Photo made by Tobias Kaufhold.

To the mixture sieved with 25 micron mesh, some iron particles were added to give magnetic property to the mixture. Then, the mixture was left to dry until the hexane was evaporated entirely. This could be controlled by checking the total weight or empirically by the mixture's smell (hexane has a characteristic smell that made known its presence). During the evaporation of the hexane, eventually a vacuum pump was used to release the gas from the mixture to avoid having gaps containing air in the sample.

Before the mixture was put into the cast, the electrical contacts for the samples were cleaned and placed on each side of the cast, as shown in the figure 2.3. The contacts were made of a bronze plate and welded to the wires with tin.

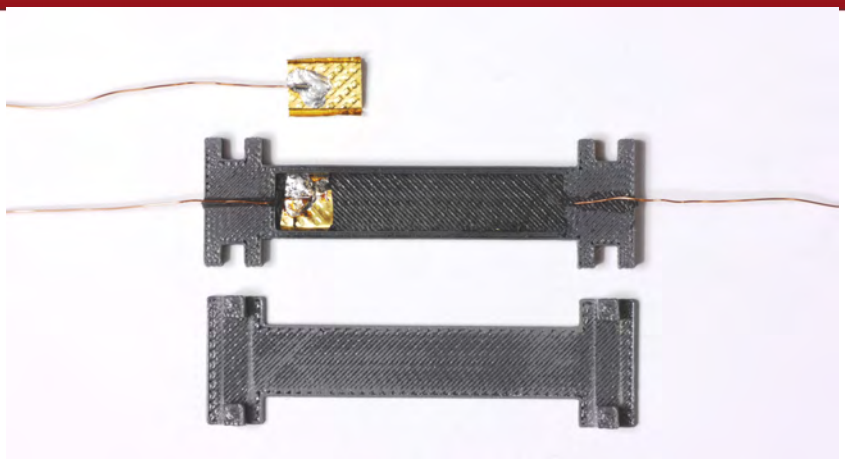

Figure 2.3: Electrical contacts used in the samples. Top: a single contact, middle: a contact placed on the cast, bottom: cast's cover.

Once the hexane was evaporated, the component B Alpa-Sil Classic was added. After using for last time the vacuum pump, the mixture was poured into the cast, this step needed to be fast. After seven minutes of had added the component B, the sample started to cure. The housings were filled entirely with the mixture and then, to be sure the cast was closed completely, they were exposed under pressure using a 15kg standard weight onto the two samples. After one day, the sample was ready to be tested.
All the samples tested were inside their casts and the condition to be available for these tests was to be closed before and during the experiments.

An opened sample, is shown in the figure 2.4. The sample and its cast's dimensions are also shown in the same figure.

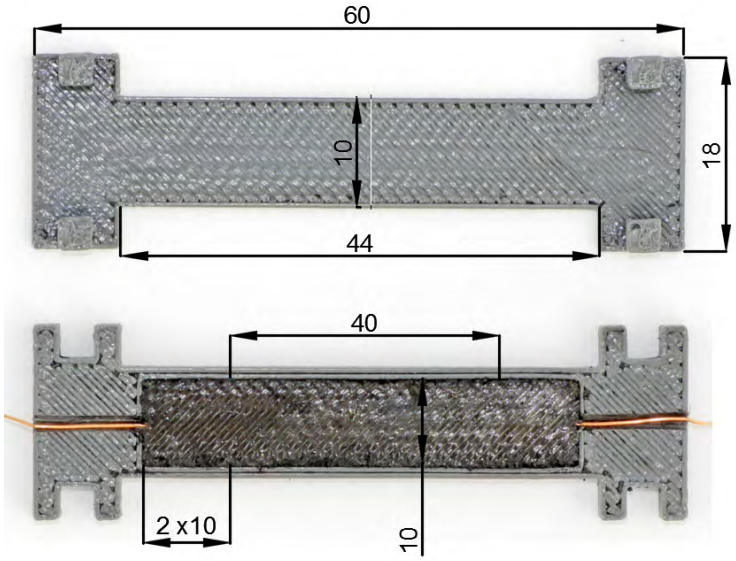

Figure 2.4: Dimensions of one sample and its cast on millimeters.

As presented in section 2.1, the pure iron powder used was not electrical conductive. The

graphite added to the mixture provided a better electrical conductivity. The more graphite concentration the mixture had, the better electrical conductivity was. For these tests, five samples were made with a specific amount of graphite, to study its electrical behaviour under the influence of magnetic field. From those samples, later will be shown the results for just one of them. The composition of the mixtures from where each sample was fabricated was the following:

- 3.00g component A Alpa-Sil Classic
- 1.00g silicone oil 1000cSt
- 0.15g graphite, mesh size for sieve: 25 microns
- 6.00g carbonyl iron powder
- 0.40g component B Alpa-Sil Classic

The reason for have used that composition is the recommendation from the department of Technische Mechanik in TU-Ilmenau, after the results of previous investigations.

From section 2.1, the density of the components used to fabricate the samples is summarized in the table 2.1.

Table 2.1: Density of components used in the fabrication of samples.

Component	**Density [g/cm^3]**
Component A Alpa-Sil Classic	1.050
Component B Alpa-Sil Classic	1.100
Silicone oil 1000 cSt	0.970
Silicone oil 5cSt	0.913
Graphite	2.150
Iron	7.870
Silicone rubber	1.078

With the list of components for making the samples, and the table 2.1, can be obtained the volume fraction of each component, as shown in the table 2.2.

Table 2.2: Volume fraction of components for samples of electrical resistance change.

Component	**Density [g/cm^3]**	**Weight [g]**	**Weight fraction**	**Volume [cm^3]**	**Volume fraction**
Component A Alpa-Sil Classic	1.05	3.00	28.4%	2.86	56.2%
Silicone oil 1000cSt	0.97	1.00	9.5%	1.03	20.3%
Graphite	2.15	0.15	1.4%	0.07	1.4%
Iron powder	7.87	6.00	56.9%	0.76	15.0%
Component B Alpa-Sil Classic	1.10	0.40	3.8%	0.36	7.2%
TOTAL		10.55	100.0%	5.08	100.0%

The most important volume fraction are the ones for graphite and iron, which are the particles added to the silicone matrix that gave electrical and magnetic properties respectively. From the table 2.2, these fractions are 1.4% and 15% respectively.

2.2.2 Configuration of the test

Each fabricated sample was placed firmly on a housing. To this sample, two permanent magnets came closer during the test. In the initial position both magnets were 23mm away from each side of the sample. In the final position, the magnets were only 0.5mm distant from each side of the sample, to avoid contact. Besides, it was applied an external pressure to the samples, through a cylinder connected to a force sensor. The force sensor was used only to reach 10N for the pressure on the sample, but the force was not measured during the test. The velocity of all the axes was equal to 5mm/s. This configuration is illustrated in the figure 2.5.

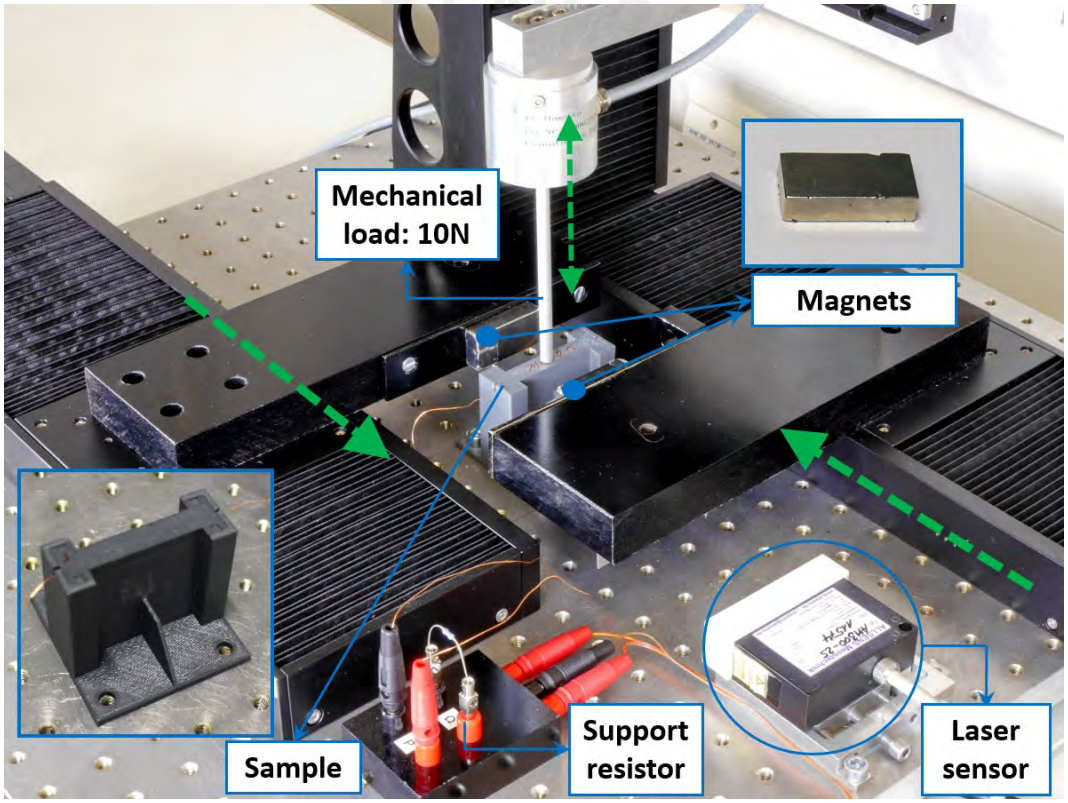

Figure 2.5: Experiment setup: the permanent magnets were moved closer to the sample to increase the induced magnetic field and a vertical travelling cylinder applied external pressure. Photo modified from the original made by M.Sc. Tobias Kaufhold.

For the movement of the magnets and the cylinder, it was used a motorized positioning machine branded OWIS. The resolution of this machine is 5 microns.

The magnets were anchored to the axes with horizontal movement. The electrical motors of each axis in the machine did not have an encoder that could indicate the position during

movement. Therefore a laser sensor was used to indicate one magnet's position during the movement of the axis. Because the configuration was symmetrical from the middle of the sample, the second magnet's position was also known.

In the figure 2.6 is shown the measured magnetic field on the center of the samples, when the magnets were moved. When the distance between the magnets and each side of the sample was 23mm, the magnetic field on the middle of the sample was approximately 78mT. When the gap between magnets and the sample was only 0.5mm, the magnetic field increased to approximately 586mT.

For the explanation of the results of these tests, it is considered that there was not magnetic field on the samples when the magnets were 23mm away, because of the low field measured in comparison when they were close.

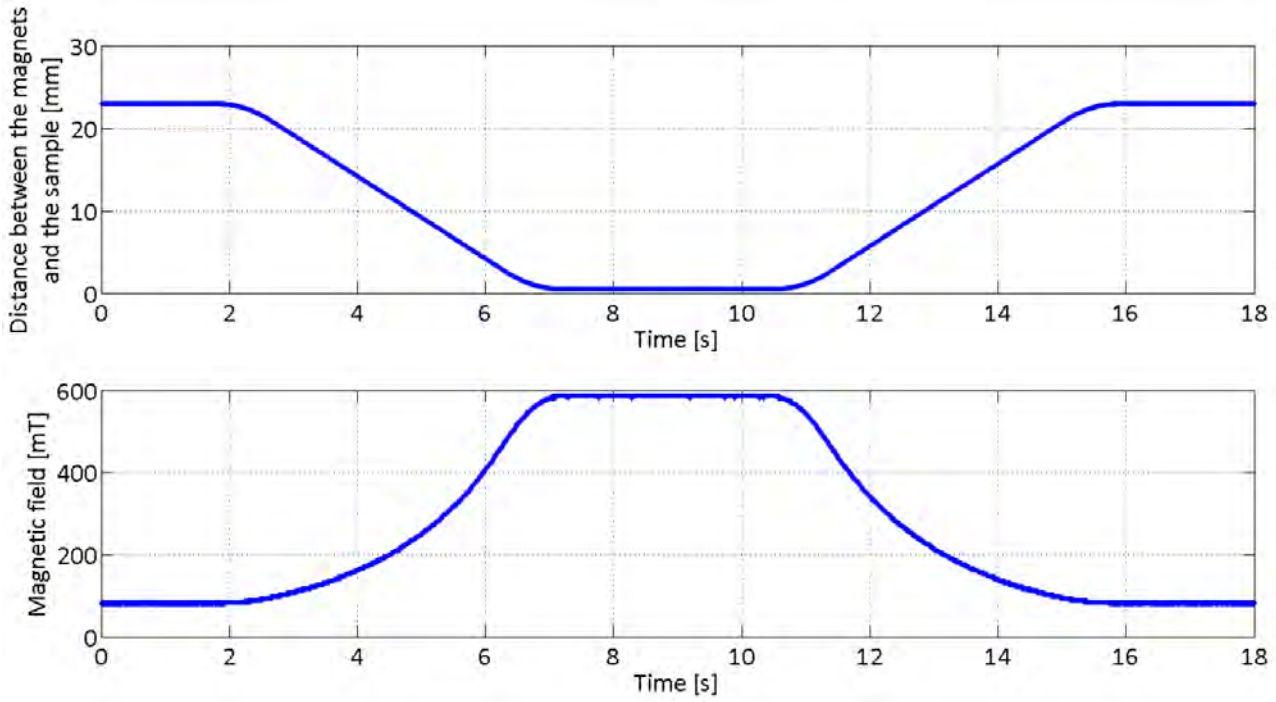

Figure 2.6: Magnetic field measured on the center of the samples while the magnets where moving.

A National Instrument (NI) device was used to make connections for voltage input and digital output signal. The device model used is SCB-68 (Shielded I/O Connector Block for DAQ Devices With 68-Pin Connectors). The card connected to the PC is PCJ-6024E model.
For this measurement, a support resistor was needed (see figure 2.5). A sample and the support resistor were connected to the NI device, a simple electric diagram for this connection is shown in the figure 2.7.

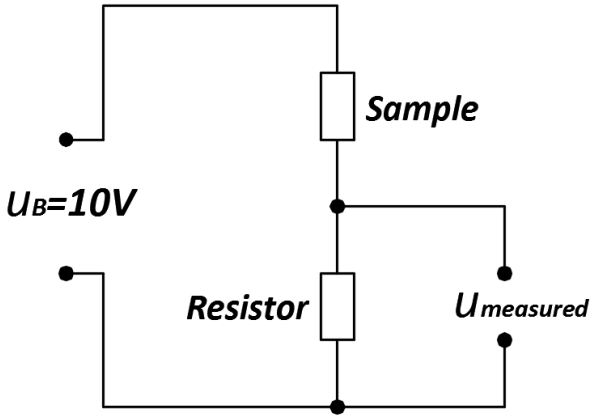

Figure 2.7: Electric diagram of the connection for the measurement of the resistance. A support resistor was needed.

The device NI SCB-68 was fed with 10V supply. The measurement of the sample's resistance was obtained by measuring the voltage across resistor support (in figure 2.5, a resistor is connected near to the sample's contact). The sample's resistance was calculated as shown in the following set of equations summarized on the equation 2.1.

R_{sample} : Resistance of the sample

$R_{resistor}$: Resistance of the support resistor

u_B : Voltage of input = 10V

u_m : Voltage measured on the terminals of the support resistor

I: Current flowing on the resistor and sample

$$u_B = I\,(R_{sample} + R_{resistor})$$

$$u_m = IR_{resistor}$$

$$u_B = IR_{sample} + u_m$$

$$R_{sample} = \frac{u_B - u_m}{I}$$

$$R_{sample} = \left(\frac{u_B - u_m}{u_m}\right) R_{resistor} \tag{2.1}$$

2.2.3 Effect of magnetic field and mechanical load

As explained in the section 2.2.2, the initial and final position for the magnets were respectively 23mm and 0.5mm of distance from each side of the sample. A cycle of movement for

the magnets means to move them from their initial to their final position, and back to the initial position. Moreover, the external pressure on the center of the sample was approximately 354 kPa, by a force of 10N applied on a circular area of 6mm diameter.

To study the effect of the magnetic field and the external pressure on the change of the sample's electrical resistance, three type of tests were performed. Worth mentioning that for these tests, after each movement of the axes, the resistance was measured for three seconds with the new position.

The steps for the axes for each type of test on this section are summarized on the tables G.1 to G.3 on the appendix G for a better understanding.

Test type I: Effect of the magnetic field.
The magnets made two cycles of movement. The measurement of the sample's resistance was done during the whole test.

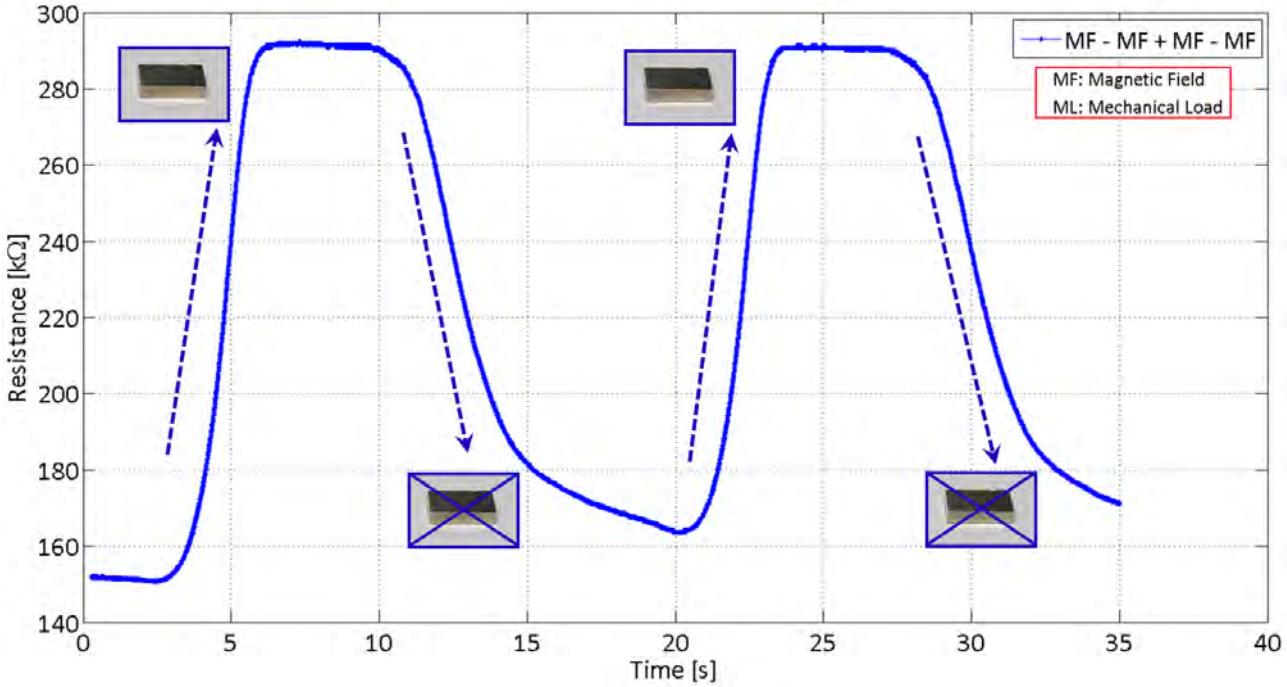

Figure 2.8: Results of electrical resistance for one sample on test type I.

Test type II: Effect of mechanical load during induced magnetic field.
The cycle of movement for the magnets had been done 5 times, after that immediately the measurement started. Then, the magnets were moved to their final position for sixth time. After that, the mechanical load was applied, and then relieved. Finally the magnets went back to their initial position.

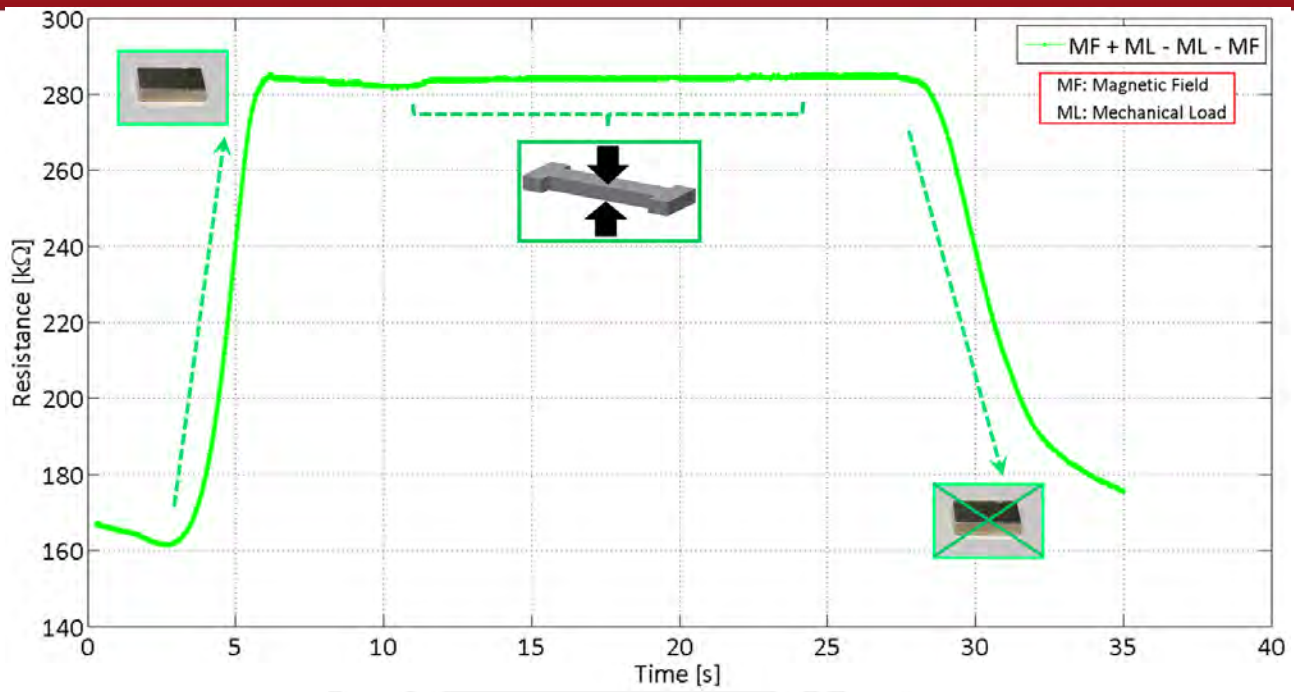

Figure 2.9: Results of electrical resistance for one sample on test type II.

Test type III: Effect of mechanical load after relieved magnetic field
The cycle of movement for the magnets had been done 5 times, after that immediately the measurement started. Then, the magnets moved a cycle for sixth time. After that, the mechanical load was applied, and then relieved.

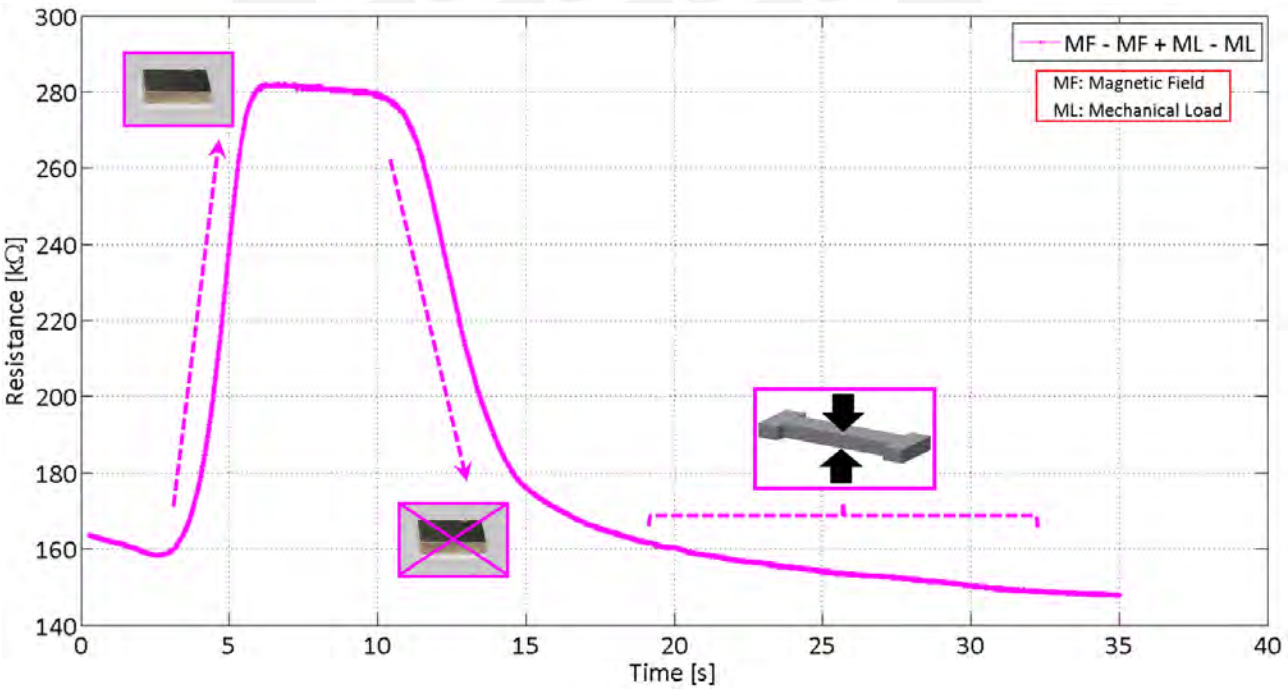

Figure 2.10: Results of electrical resistance for one sample on test type III.

In the figure 2.11 is shown just the results for one of the five samples with 1.4% and 15% of volume fraction of graphite and iron respectively. The initial resistance of the sample on each test was different because the sample already had a test before, to have the same initial value for all the tests it needed to be waited around 24 hours until the effect of the magnet was mostly mitigated, but the results of the curves after some seconds in the beginning would be very similar. The same effect of different initial resistance is observed on the figures 2.14 and 2.15.

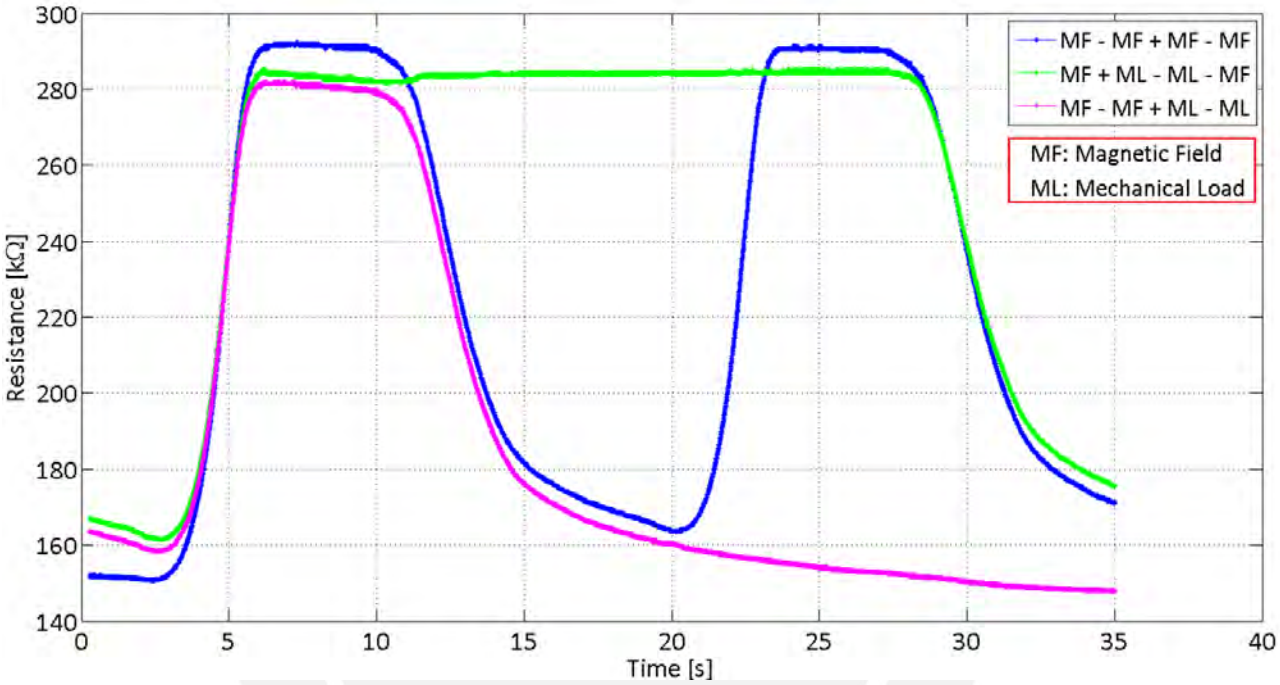

Figure 2.11: Results of electrical resistance for one sample with 1.4% volume of graphite and 15% volume of iron on tests type I to III.

From the figure 2.11 is concluded that the effect of the external pressure on the change of electrical resistance is low compared to the effect of the magnetic field. Therefore, henceforth, it will be studied the behaviour of the electrical resistance just under the effect of magnetic field.

The results of the experiments for the five samples with 1.4% volume of graphite and 15% volume for test type I are plotted on the figure 2.12. There is remarkably observed the difference between the initial and the maximum electrical resistance during the test for the five samples.

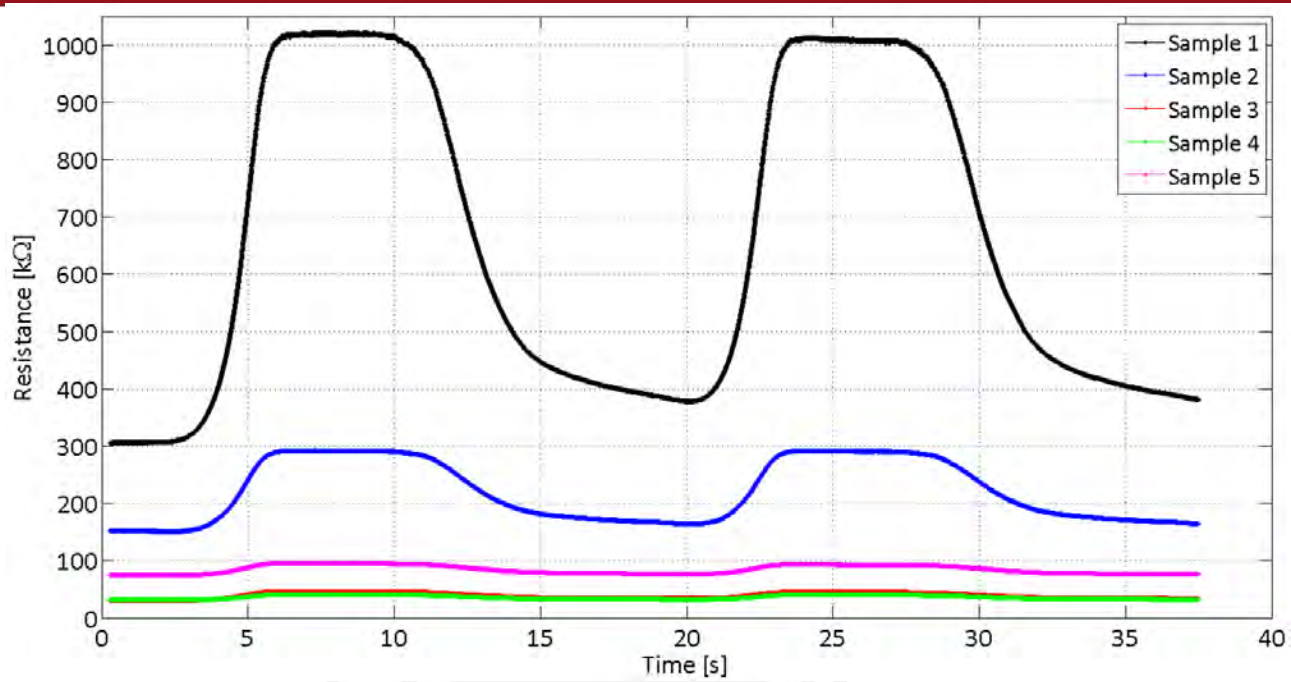

Figure 2.12: Results of electrical resistance on tests type I for the five samples with 1.4% volume of graphite and 15% volume of iron.

On the figure 2.13 is plotted the percentage of resistance's change, in respect to the initial resistance, during the test.

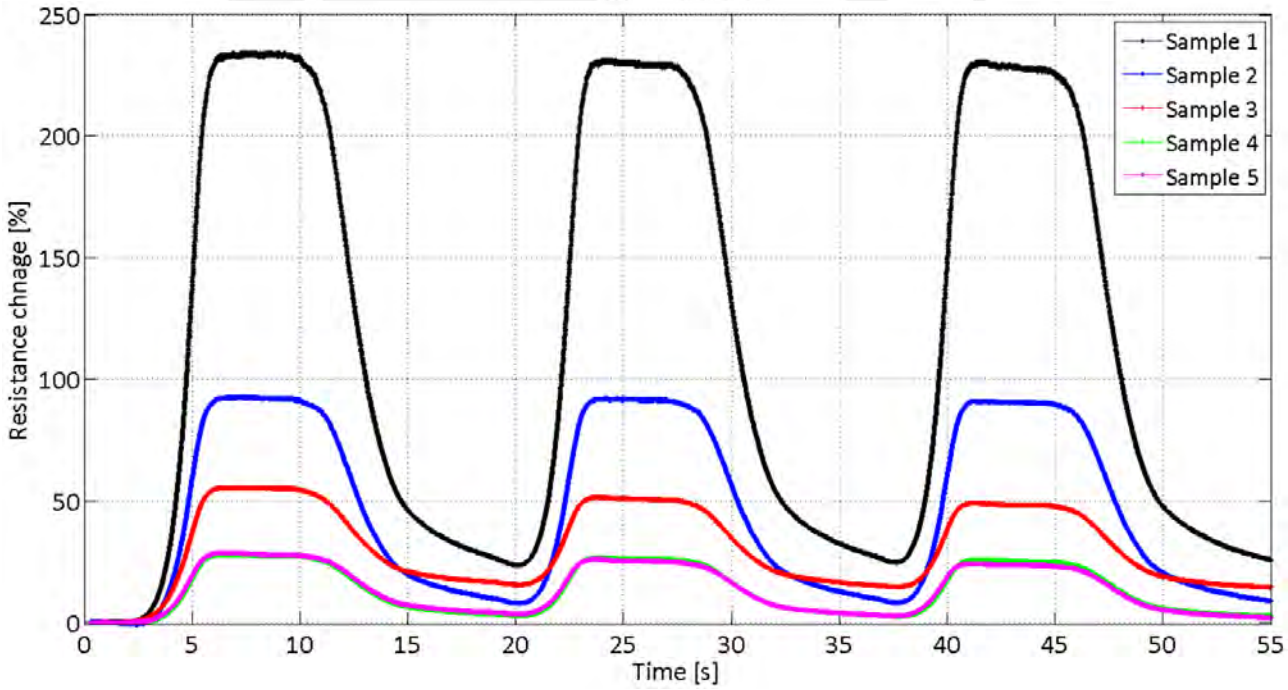

Figure 2.13: Electrical resistance increase on tests type I for the five samples with 1.4% volume of graphite and 15% volume of iron.

As mentioned previously, the five samples had the same behaviour, but not exactly the same increase of resistance under the maximum induced magnetic field, although the five samples had the same proportion of components (especially graphite) and had the same configuration and conditions for the experiments. Later in in section will be presented an improvement on the electrical contacts in order to solve this problem.

2.2.4 Effect of the speed of increment of magnetic field

In a cylindrical cast of 10mm diameter and 10mm height, some new samples were created. On the initial tests we varied the proportion of component A and silicone oil of the mixture. Then it was replaced the 1000cSt silicone oil by the 5cSt one.
Al the last, it was chosen the following composition because it was easy to take out from the cast and had a slightly higher stiffness.

- 2.00g component A Alpa-Sil Classic
- 2.00g silicone oil 5cSt
- 0.28g graphite, mesh size for sieve: 100 microns
- 6.00g carbonyl iron powder
- 0.40g component B Alpa-Sil Classic

With this composition, it was fabricated a new sample (in the closed cast of figure 2.03) to study its behaviour when the speed of movement of the magnets was varied. I.e., the tests were made for different speed of increment of the induced magnetic field on the sample.

In the figure 2.14 is shown the results of tests with three different speeds for the magnets. On the red ellipses we can see the way the sample reached its final resistance. When the magnet's velocity increased, the peak of the curves was higher.
Another annotation is that for these three tests, the resistance was very stable after 10 minutes after the magnets stopped at the closest position to the sample. But also it is clear that the reached resistance was different in those three experiments for the same sample, this issue could have also been improved with better electrical contacts.

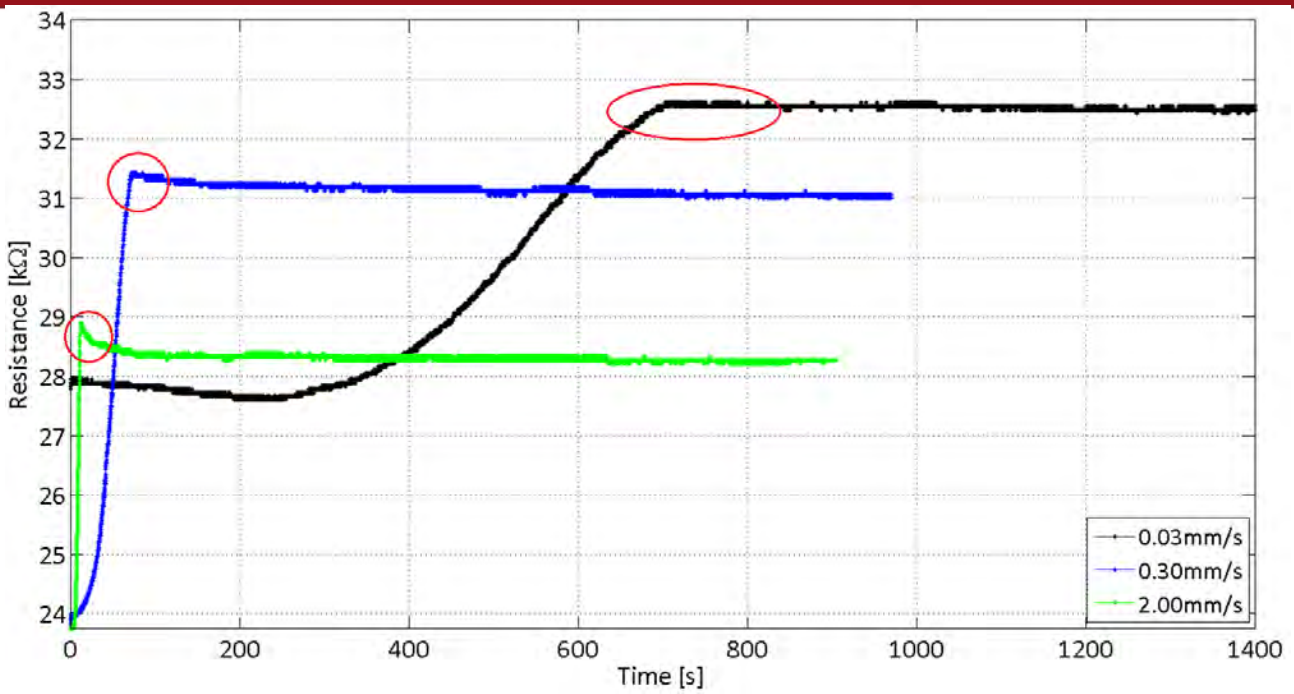

Figure 2.14: Resistance-time curves for the same sample with different speed of movement for magnets.

These results aroused the interest to know what would happen if the sample is exposed to alternated magnetic field.
After some previous test, it was measured the resistance over time for alternating magnets' movement, with velocities 6.0mm/s and 0.6mm/s. The results obtained are shown in figure 2.15. The initial resistance on the tests were different because the sample was tested before. After approximately 15 repetitions with 6.0mm/s and 6 repetitions with 0.6mm/s, the resistance was stable.

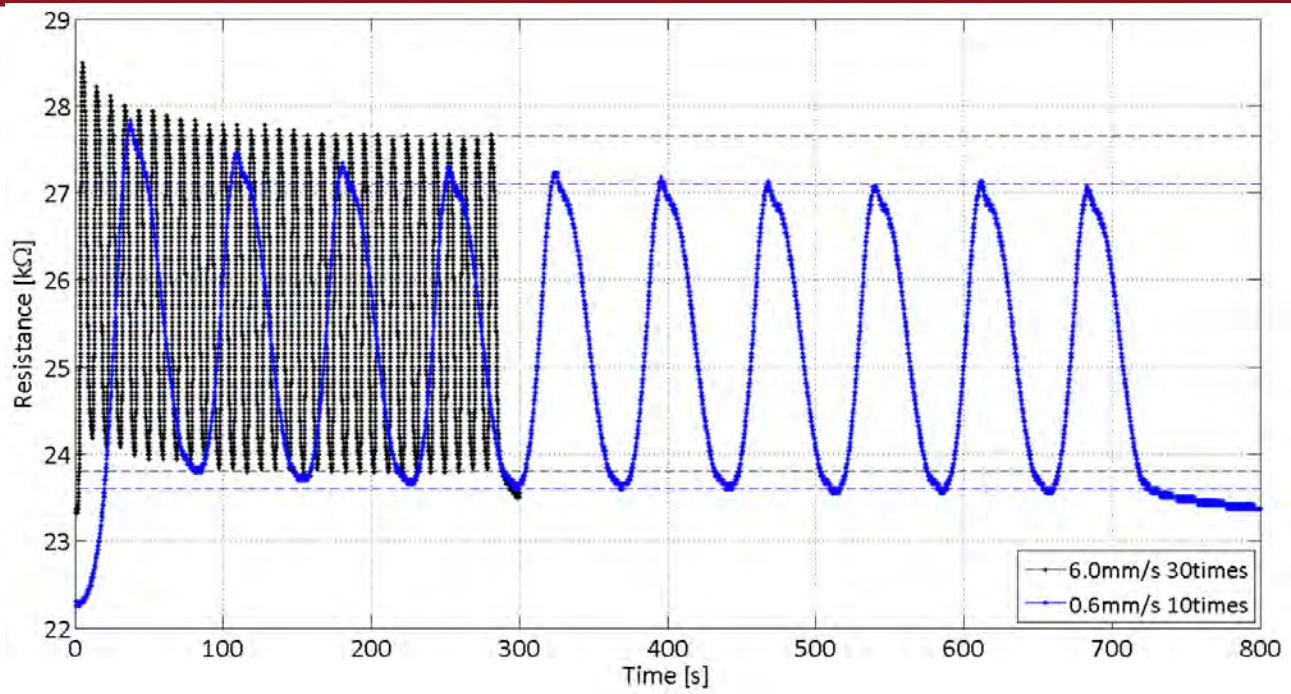

Figure 2.15: Test with alternating magnetic field with two velocities for the magnets.

With the figure 2.15 it is concluded that after some repetitions in the test with alternate magnetic field, the resistance oscillate between two stable values.

2.2.5 Improvement of electrical contacts

The results of the previous experiments showed that the behaviour under the effect of magnetic field or mechanical load was similar for samples with the same amount of graphite. However, the values were very different. I.e., for the samples made from the same mixture (same composition, specially the amount of graphite) and same shape and size, was not obtained a similar value for the electrical resistance in absence of magnetic field. This leads to the conclusion that there is something wrong in the samples or in the measurement of the resistance. After reviewing the experiments' configuration, it was concluded that the electrical contacts of the old samples (figure 2.3) were the sources of error for the measurement. Apparently in some samples the contact between the bronze plaque and the MSE it is better than in others.

For this reason it was decided to change the type of electrical contacts that are attached to the samples, it was replaced the bronze by copper to improve the contacts' conductivity. In addition to that, instead of using a plaque the contacts were made from copper mesh (specified on section 2.1) for a better contact since the MSE would be inserted between the gaps of the copper mesh. The mesh was soldered with tin in its whole edge to ensure all copper wires are connected for a good conductivity. Then, a electrical wire was also soldered to the mesh. For 40 new contacts fabricated it was verified the electrical resistance, for all of them it was lower than 1Ω, so they do not have influence on the final resistance.

The new samples were produced with the same procedure than the old ones, with the difference that in this case, only the 100 microns-size iron mesh was used to sieve the graphite. The mixture was poured in cylindrical recipients of 10mm high and 10mm diameter. For these new tests, the samples were taken out of their casts.

A glue silicone was used to stick the new electrical contacts to the samples. To glue them, it was used for each sample, a mixture of 1g silicone rubber E41, with enough hexane to solve that and 0.08g of graphite.

An example of the new fabricated contacts made of copper mesh and the new shape of samples are shown in the figure 2.16. On this figure is also shown one sample stuck to two contacts on its bottom and top.

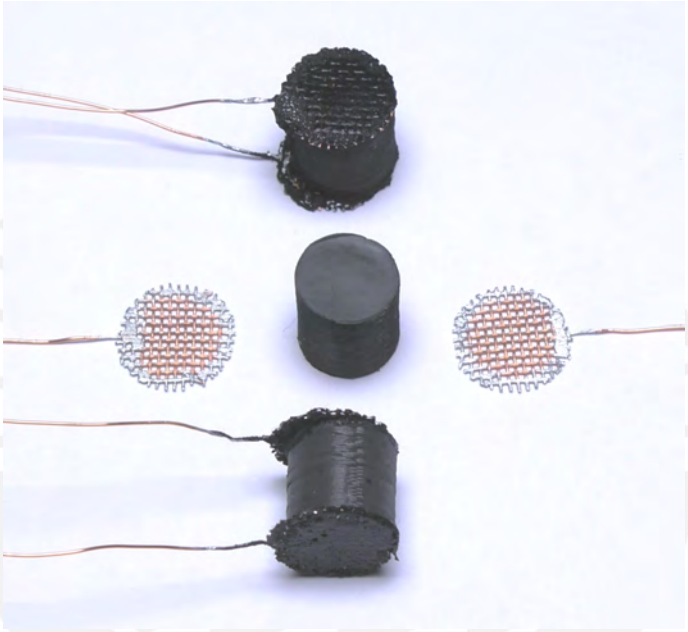

Figure 2.16: On the middle: contacts made of copper mesh and a new sample. On bottom and top: a sample glued to the new contacts.

The adhesion of the new samples glued to the new contacts was very good, they could be tensioned or twisted without separating them.

The glue's electrical conductivity is also good. To prove that, two electrical contacts were stuck, putting some mixture of glue and graphite in the middle. The result was lower than 50Ω.

With this improvement, it was fabricated 4 samples from the same mixture, that was made with following amount of components:

- 4.00g component A Alpa-Sil Classic
- 4.00g silicone oil 5cSt

- 0.5g graphite, mesh size for sieve: 100 microns
- 12.00g carbonyl iron powder
- 0.80g component B Alpa-Sil Classic

The electrical resistance of those samples were measured by a multimeter. The results were: 59kΩ, 59kΩ, 51kΩ and 65kΩ. That means that the mean value for them was 58.5kΩ with +/- 12.5% of margin of error.

With this improvement of new electrical contacts it was concluded that for the first new samples, with the same amount of graphite in composition, they had a near value of electrical resistance.

As a conclusion, this new samples have to be tested with the effect of magnetic field in a prospective project, because they promise to have better results. No more tests were done on this work because of its deadline.

A final observation was that the new samples were more sensible to mechanical loads. They had a big change of resistance with a little deformation. One of the possible reasons of this behaviour compared to the old samples that had no relevant effect under 354kPa of pressure, is that the old ones were cured under the pressure by 15kg of mass. Considering the old samples' area (see figure 2.4), the external pressure was around 101kPa while curing. The new experiments for resistance's change will need also a new configuration of the test stand.

2.3 Tests of stiffness change under magnetic field

From the section 2.2, it is known the behaviour of samples with graphite under the effect of mechanical loads and magnetic fields. For this section, it is studied the samples' mechanical properties, that is why the fabricated samples did not contain graphite on their composition since the electrical properties under the effect of magnetic field are already known.
For those new samples it was modified the proportion of components until have finding one proportion that had the biggest change of stiffness when exposed to magnetic field.

2.3.1 Fabrication of samples

The samples were manufactured with different amounts of components: component A Alpa-Sil Classic (and its respective amount of component B), silicone oil (1000 cSt) and carbonyl iron powder. The use of hexane is not necessary on the mixture because there is no need to solve graphite, however it is needed the vacuum pump before and after adding the component B of silicone to prevent air bubbles in the sample.

These samples needed to be deformed. For these reason, their casts were designed with a free surface, to let them being deformed. The shape of the fabricated samples for this section is shown in the figure 2.17, there are two samples, inside and outside the cast where their were cured. For the experiments it was necessary that the sample was held inside them.

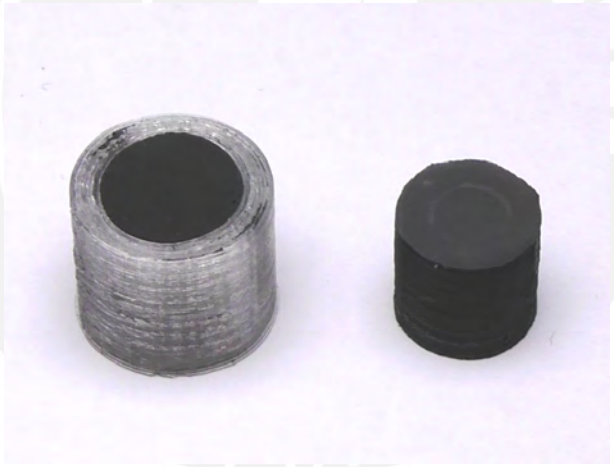

Figure 2.17: Samples fabricated for tests of stiffness change. On the left the samples as used in the experiments, inside the cast. On the right, a cast-free sample.

The fabricated samples are shown in the table 2.3, with amount in mass for each component used to made them. The last column of the table was calculated by using the information from the table 2.1 used in section 2.2.

Table 2.3: List of samples fabricated for tests of change in stiffness under magnetic field.

Ratio Silicone - Silicone oil	Sample Nr.	Silicone A [g]	Silicone oil 1000cSt [g]	Iron [g]	Silicone B [g]	Volume fraction of iron
1:1	Sample 1	1	1	5	0.2	22.7%
	Sample 2	1	1	6	0.2	26.0%
	Sample 3	1	1	7	0.2	29.1%
	Sample 4	1	1	8	0.2	31.9%
	Sample 5	1	1	10	0.2	37.0%
0.8:1.2	Sample 6	0.8	1.2	5	0.2	22.6%
	Sample 7	0.8	1.2	6	0.2	25.9%
	Sample 8	0.8	1.2	7	0.2	29.0%
0.5:1.5	Sample 9	0.5	1.5	5	0.2	22.4%
	Sample 10	0.5	1.5	10	0.2	36.6%

2.3.2 Configuration of the test

The set up for these tests was very similar to the one built on section 2.2 and it is shown on the figure 2.18.

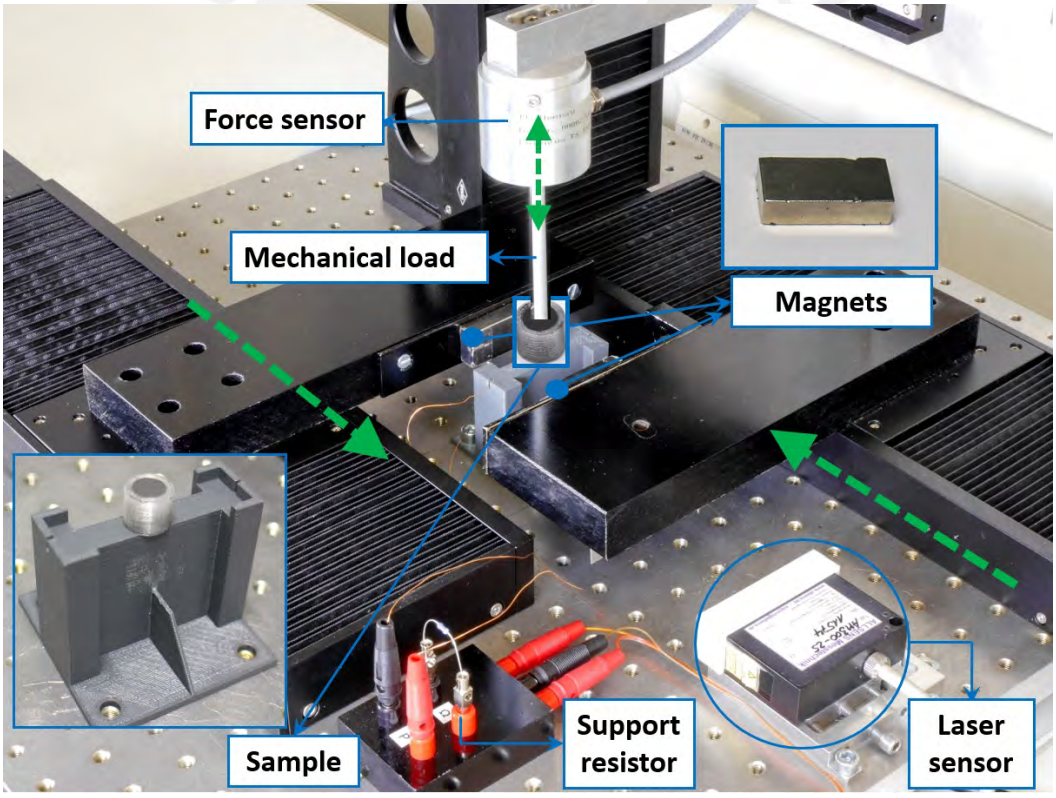

Figure 2.18: Experiment setup: the permanent magnets were moved closer to the sample to increase the induced magnetic field and a vertical travelling cylinder deformed 1mm the samples, the force sensor measured the force needed for the deformation. Photo modified from the original made by M.Sc. Tobias Kaufhold.

The magnets had horizontal movement in opposite directions. The force sensor was fastened to the axis with vertical movement. To the force sensor was anchored a slender cylinder of 6mm diameter that pressed and deformed the sample during its displacement. The bottom of the sample's cast was stuck to the platform to avoid movement from the attraction of the magnets or when the cylinder was disengaged.

For this tests, in the initial position both magnets were 19.5mm away from each side of the sample and the induced magnetic field on the center of the sample was approximately 105mT. In the final position, the magnets were only 0.5mm distant from each side of the sample to avoid contact, inducing approximately 586mT on the center of the sample.
For the explanation of the results obtained in these tests, it is considered that there was not magnetic field on the samples when the magnets were 19.5mm away, in order to make a contrast when the samples were affected by a strong field.

As in tests from the section 2.2, it was applied an external pressure to the samples, through the 6mm-diameter cylinder connected to a force sensor. The maximum measured value by the force sensor is 10N and its resolution is 1mN. The velocity of all the axes was equal to 5mm/s.

The steps of positions for these tests are mentioned below, considering that after each movement of the axes, the measurement of the force applied on the was done for five seconds with the new position.

- Position 1: Both magnets were 19.5 away from the sample's cast.
- Position 2: Measurement starts. The cylinder travelled 1mm deep on the sample. The position is kept for 5 seconds to measure the force.
- Position 3: The cylinder returned to its initial position and was kept there for 5 seconds.
- Position 4: The magnets travelled until 0.5mm distance from the sample's cast.
- Position 5: With the magnets close, the cylinder was inserted again 1mm deep on the sample. The position was kept for 5 seconds to measure the force.
- Position 6: With the magnets close, the cylinder returned to its initial position and was kept there for 5 seconds.
- Position 7: The magnets returned to their initial position, 19.5mm away and the measurement ended.

The steps presented for the experiment are summarized on the table 2.4.

Table 2.4: Steps for the experiments with waited time on each position.

	Distance of magnet 1 and the sample [mm]	Depth of the base of the cylinder on the sample [mm]	Distance of magnet 1 and the sample [mm]	Waiting time for measurement [s]
Position 1	19.5	0	19.5	0
Position 2	19.5	1	19.5	5
Position 3	19.5	0	19.5	5
Position 4	0.5	0	0.5	0
Position 5	0.5	1	0.5	5
Position 6	0.5	0	0.5	5
Position 7	19.5	0	19.5	0

2.3.3 Results

The first performed tests were for samples with 1g of component A of silicone, 1g of silicone oil 1000cSt and with different concentration of iron (see samples 1 to 5 from table 2.3). For each sample, the force-time curve was plotted, as shown in the figure 2.19. During the first 10 seconds of the graphic is shown the force needed for the deformation of 1mm in the absence of magnetic field, and on the last part, the force by deformation of 1mm under magnetic field.
Also on the figure 2.19 it is observed that there is some noise due to the vibration when the cylinder touches the sample and when gets separated of it without the presence of magnetic field (see the red circles). On the red ellipse it is observed a higher disturbance, due to the temporary adhesion between the surfaces of the sample and the cylinder. On this adhesion, the cylinder (connected to the force sensor) was pulled down when the two surfaces were getting separated and this seems reflected as negative force.

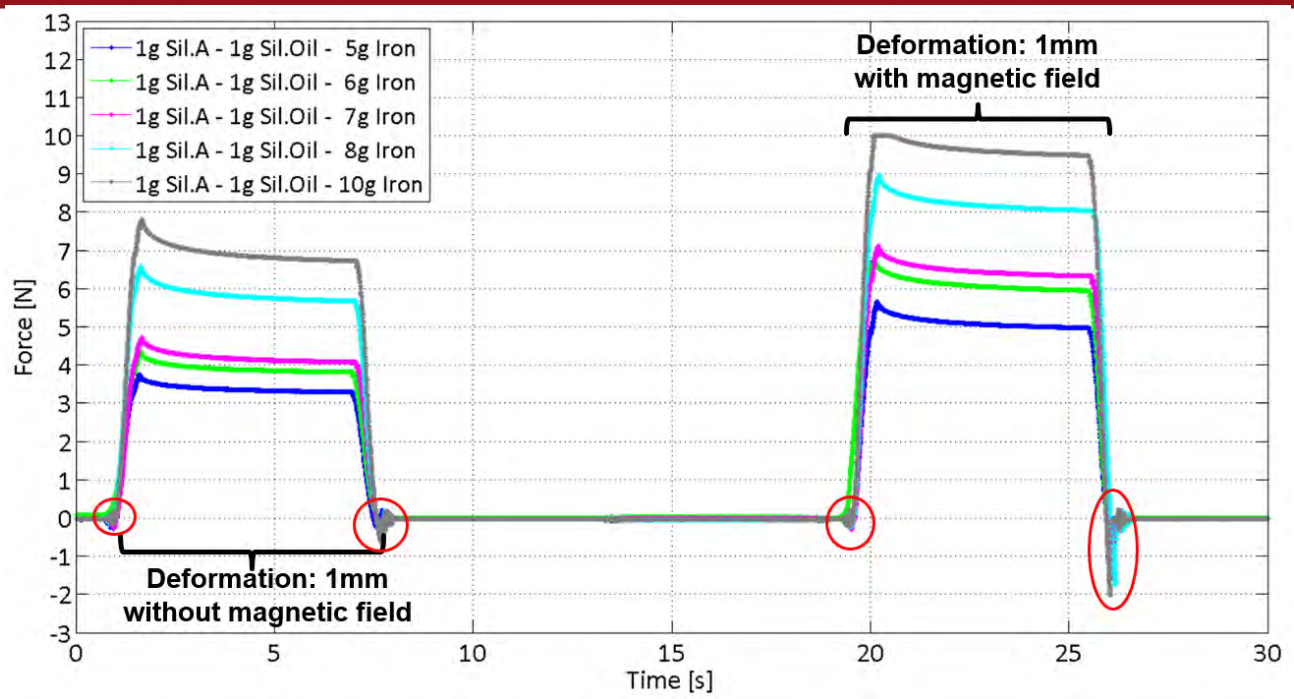

Figure 2.19: Curves force-time for samples 1 to 5, all of them with 1g component A and 1g silicone oil. The noise on the red circles is due to the system's vibration. The noise on the blue circle is because of the temporary adhesion.

As expected before the experiments, the samples with more iron were the most resistant to deformation in both cases, with magnetic field and without magnetic field.
For both deformations, with and without magnetic field, there is a peak at the beginning of the curve. This is due to the behaviour of viscoelastic materials (see figure 1.4).

Another observation is that for the sample with 38% volume of iron (10g) it was obtained a force greater than 10N (gray curve in figure 2.19) and, because the maximum value which can be measured by the force sensor is 10N, the curve was plotted truncated at its top.

From the results plotted on figure 2.19, the maximum forces achieved with 1mm deformation, with and without magnetic field, are compared on the table 2.5. On the last column it is shown the percentage of increase of the force by deformation of 1mm when the sample is under magnetic field, compared to the force by deformation without magnetic field.

Table 2.5: Force needed to deform 1mm the samples with 1g component A and 1g silicone oil, with and without the presence of magnetic field.

	Maximum force without magnetic field [N]	**Maximum force under magnetic field [N]**	**Change**
Sample 1	3.745	5.659	51.1%
Sample 2	4.341	6.777	56.1%
Sample 3	4.707	7.129	51.5%
Sample 4	6.582	8.970	36.3%
Sample 5	7.813	9.995	27.9%

From the figure 2.19 and the table 2.5 can be concluded:

- All samples had the same elastic behaviour in both parts of the curves.
- The sample with 6g of iron had the biggest change on the stiffness under magnetic field.
- The percentage of increment of force by 1mm deformation under magnetic field was very similar for samples with 5g, 6g and 7g of iron.

With these results we can not conclude in a certain volume fraction of iron that have the greatest increase of force by deformation under magnetic field, because the results were very close. Therefore it was decided to see what would be the effects if the proportion of component A and silicone oil are changed.

For this reason, the behaviour of three samples with the same amount of iron (5g) were compared, changing the proportions of silicone as follows:

- 1.0g silicone A + 1.0g silicone Oil
- 1.2g silicone A + 0.8g silicone Oil
- 1.5g silicone A + 0.5g silicone Oil

From the table 2.3, we used the samples 1, 6 and 9 which have the mentioned ratios, to make the new comparison. The result of the force-time measurements is shown in the figure 2.20.

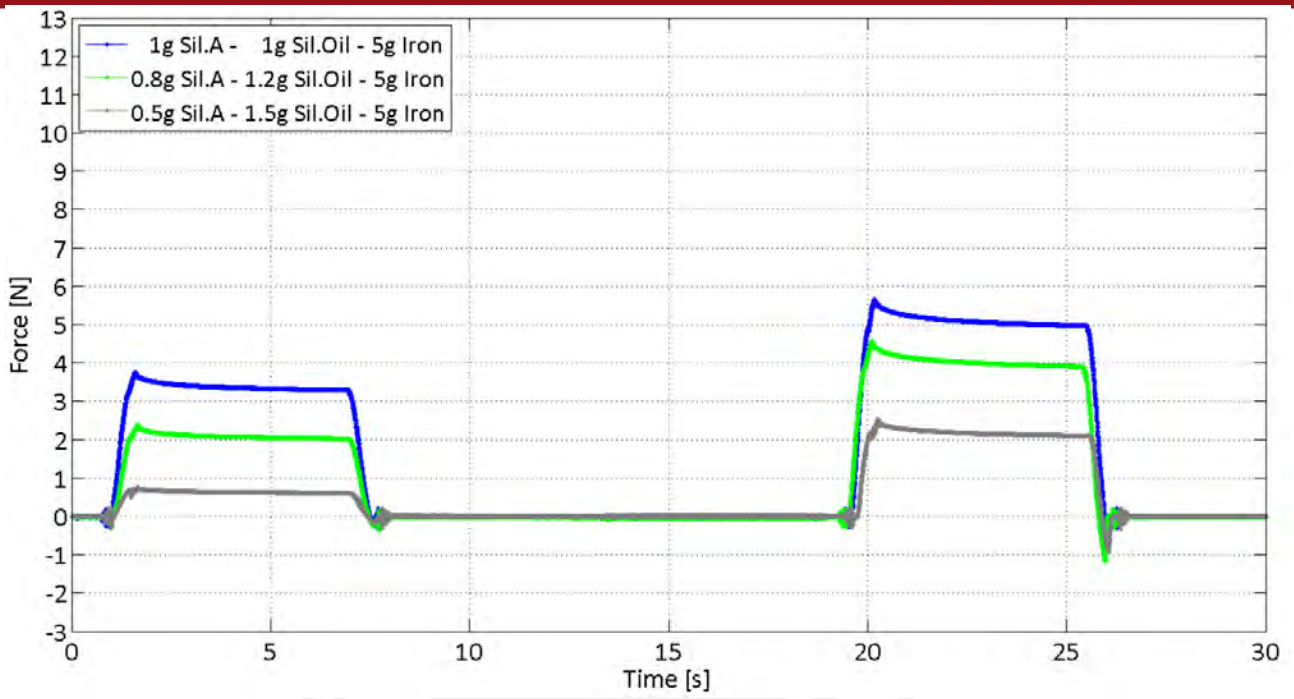

Figure 2.20: Curves force-time for samples 1, 6 and 9, all of them with 5g iron.

From the figure 2.20, it is observed that for the same deformation of 1mm, the forces obtained were lower when the samples had more silicone oil in their composition. This was also expected since the viscosity of the silicone oil is higher (1000 cSt) than the component A (1.05 cSt).

The table 2.6 shows, for these three samples, the percentage of increase of the force by 1mm deformation when the sample is under magnetic field, compared to the force by deformation without magnetic field.

Table 2.6: Force needed to deform 1mm the samples with 5g of iron, with and without the presence of magnetic field.

	Maximum force without magnetic field [N]	**Maximum force under magnetic field [N]**	**Change**
Sample 1	3.745	5.659	51.1%
Sample 6	2.417	4.609	90.7%
Sample 9	0.752	2.515	234.4%

In the table 2.6 is shown that the sample with the highest amount of silicone oil (1.5g) is the one in which becomes biggest the effect of the magnetic field. But at the same time it is observed that the adhesion of surfaces for that mixture is also the highest. The pulling force to the cylinder (around second 26) was very high, even higher than the (opposite of) the maximum force obtained in the first 10 seconds. This is due to the great amount of silicone oil that came to the surface of this sample.

Disregarding the stickiness of the sample with 1.5g silicone oil, it was created one more sample with the same silicone matrix (same ratio of silicone and silicone oil) and more iron (10g), with the hope that with the presence of magnetic field its adhesion decreases due to the expected higher stiffness.

In the figure 2.21 the results for the samples 9 and 10 are compared, both samples with 0.5g of silicone A, 1.5g of silicone oil and 5g and 10g of iron respectively.

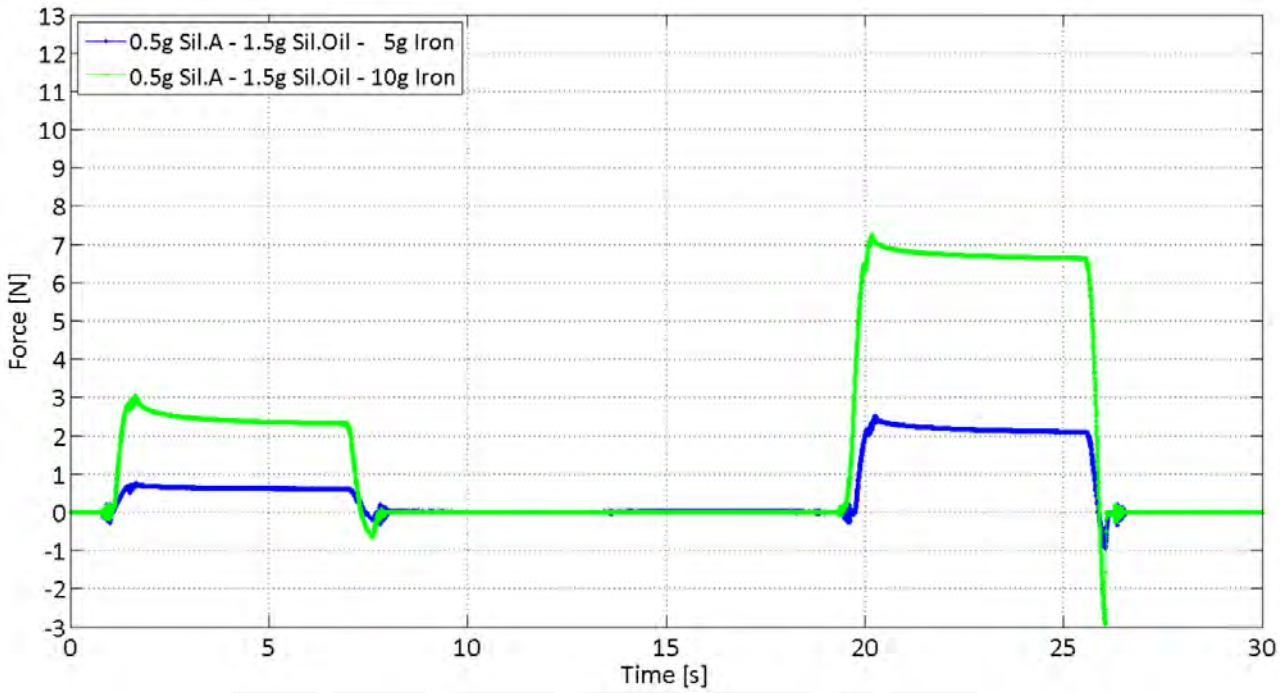

Figure 2.21: Curves force-time for samples 9 and 10, both with 0.5g component A and 1.5g silicone oil.

As it is shown in the figure 2.21, for the sample with 10g iron not only the maximum force by 1mm deformation is higher, also the pulling force due to the adhesion is very high. So, instead of goes down, it has been increased.

The table 2.7 shows, for the two samples with 1.5g silicone oil, the percentage of increment of the force needed to deform 1mm when the sample is under magnetic field, compared to the force needed to deform 1mm without the presence of magnetic field. The effect of the magnetic field on the stiffness change has decreased for the mixture with more amount of iron.

Table 2.7: Force needed to deform 1mm the samples with 0.5g component A and 1.5g silicone oil, with and without the presence of magnetic field.

	Maximum force without magnetic field [N]	**Maximum force under magnetic field [N]**	**Change**
Sample 9	0.752	2.515	234.4%
Sample 10	3.047	7.241	137.7%

As mentioned before, for these samples with ratio 1:3 for component A and silicone oil, a lot of oil came to the surface, this is why the adhesion was higher. Apparently, this concentration exceeds the saturation point of oil in the silicone. As a conclusion, a big amount of silicone oil is not useful for fabricating a samples.

Finally, remains to study the behaviour for samples made with ratio 2:3 for component A and silicone oil, respectively. From the figure 2.19 it is noted that the samples with 8g and 10g are more rigid, however from table 2.5 is also observed that their stiffness is less affected by the presence of magnets. For this reason, the fabricated samples with 0,8g component A and 1,2g silicone oil had 5g, 6g and 7g iron, respectively. These samples are samples 6, 7 and 8 from the table 2.3.

Performing the same tests with these three samples, the force-time curves shown in the figure 2.22 were obtained.

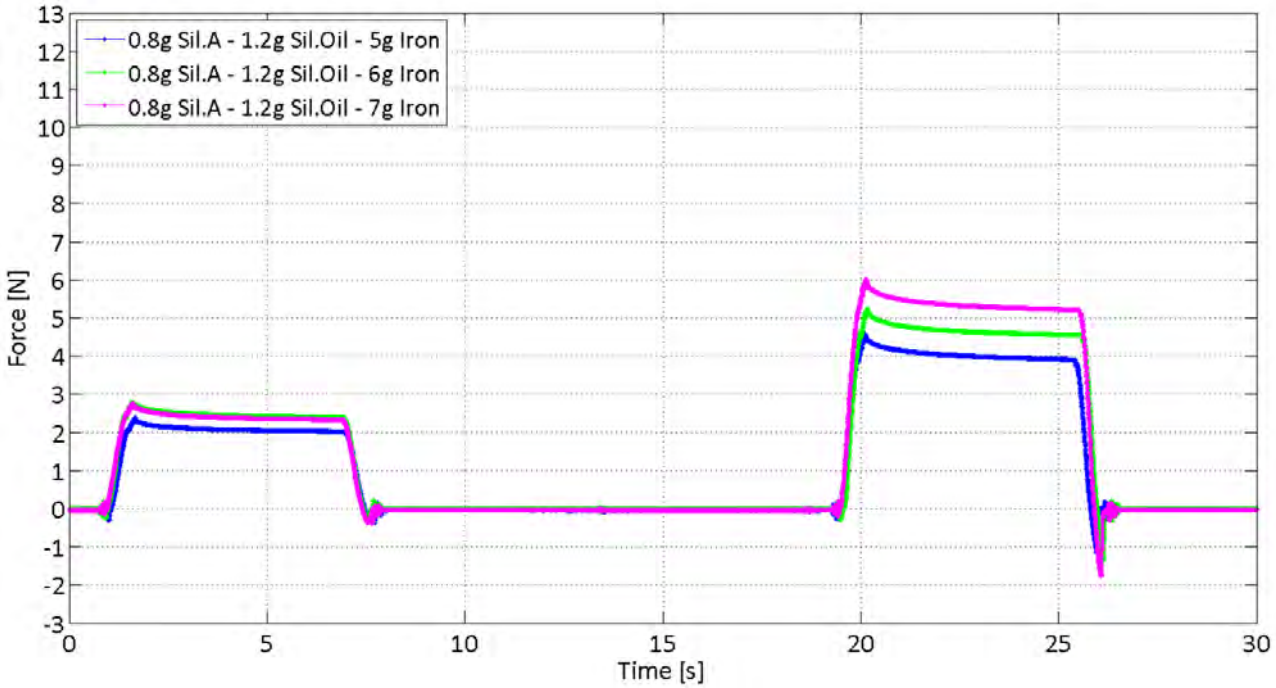

Figure 2.22: Curves force-time for samples 6, 7 and 8, all of them with 0.8g component A and 1.2g silicone oil.

The maximum force obtained by the deformation of 1mm without the action of the magnetic field is greater for the samples with 6g and 7g of iron, although they are very close.

However, the sample containing 7g iron needs a higher force (around 6N) to deform 1mm under magnetic field.

Comparing again the force by deformation without and with the magnets close, as shown on the table 2.8, it is obtained that the stiffness increment is similar for samples with 5g and 6g of iron. For the sample with 7g of iron the effect of the magnetic field is greater and the force needed for 1mm of deformation was about 115% greater than the required to deform 1mm without the presence of magnets.

Table 2.8: Force needed to deform 1mm samples with 0.8g component A and 1.2g silicone oil, with and without the presence of magnetic field.

	Maximum force without magnetic field [N]	**Maximum force under magnetic field [N]**	**Change**
Sample 6	2.417	4.609	90.7%
Sample 7	2.817	5.230	85.6%
Sample 8	2.817	6.050	114.7%

From the results of the experiments of stiffness change with all the samples with different ratio of silicone and silicone oil and the tables from 2.5 to 2.8, the figure 2.23 is plotted, where is shown the stiffness increase depending on the amount of iron and ratio of silicone and silicone oil.

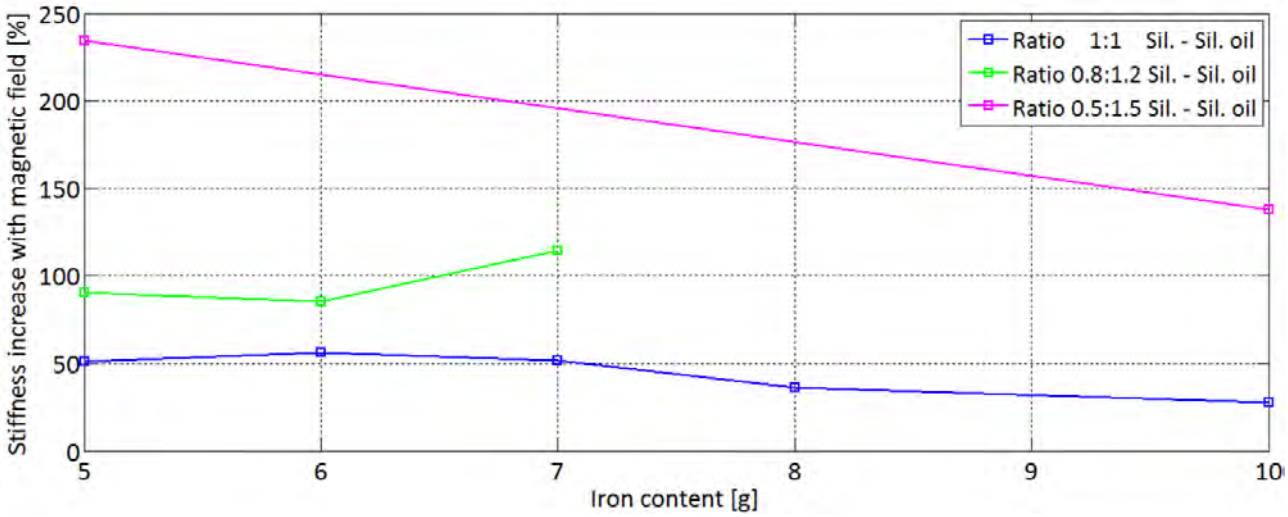

Figure 2.23: Stiffness increment for samples, depending on the amount of iron and ratio of silicone and silicone oil.

From the experiments executed on this section, it is concluded that the sample 8 (0.8g component A Alpa-Sil Classic, 1.2g silicone oil 1000cSt, 7g iron and 0.2g component B) is the one with the best stiffness change and is chosen to deepen the studies of its elastic behaviour under magnetic field. However, the last observation from the figure 2.22 is that this sample has still adhesion on its surface and that point has to be solved in the future.

2.4 Tests for field-induced plasticity

Now that it has been founded the mixture of silicone Alpa-Sil Classic, silicone oil, and iron, that has the best change of its stiffness with the presence of magnetic field, for this section some new test are performed for samples that can be very flexible in the absence of magnets and very rigid under magnetic field.

Some studies already were done for quantitative results of elongation by forces and the change of stiffness with magnetic field [26,33,35]. In this section is only studied qualitatively the results of some samples, to chose the best one for some applications.

2.4.1 Fabrication of samples

These new samples should record the shape of an object that is in contact to them. So, like the samples used for section 2.3, they need to be free of housing on one side, and their size has to be big enough to let the objects be placed on them.

To fabricate the samples for the present section, the same ratio of 0.8g of component A Classic Alpa-Sil, 1.2g of silicone oil 1000cSt, 7g iron and 0.2g of component B was used but in different amounts, as shown in the table 2.9. The procedure for the fabrication was also the same used for samples from section 2.3.

Table 2.9: Dimensions and composition of the samples.

Sample Size	**Diameter [mm]**	**Height [mm]**	**Silicone A [g]**	**Silicone Oil 1000 cSt [g]**	**Iron [g]**	**Silicone B [g]**
Small	40	10	4	6	35	1
Middle	40	15	6	9	52.5	1.5
Big	40	20	8	12	70	2

These three samples were all cylinders with 40mm of diameter and heights equal to 10mm, 15mm and 20mm to study and compare their behaviour. During the tests, all the samples were held in their cast where the mixture was cured. This is illustrated in the figure 2.24.

Figure 2.24: Samples used on field-induced plasticity tests. From left to right 20mm, 15mm and 10mm in height and 40mm diameter for all samples.

2.4.2 Configuration of the test

For this test, the axes of the motorized positioning system were assembled in a way that the end effector has three degrees of freedom, which are the movement in the three axes. The end effector is the object which comes into contact with the sample.
For the experiments, two objects were used: a sphere and a cylinder, both with 20mm diameter as shown in the figure 2.25.

Figure 2.25: Objects inserted to the samples on the experiments, on the left a ball, on the right a cylinder, both with 20mm diameter.

The assembly of the axes and the configuration of the test are shown in the figure 2.26. The magnet used in this test was stronger from the used in the previous sections. This new magnet provided a higher density of magnetic field. The difference is that the sample is only affected by one magnet, from below it and not with two magnets as in the experiments of sections 2.2 and 2.3.

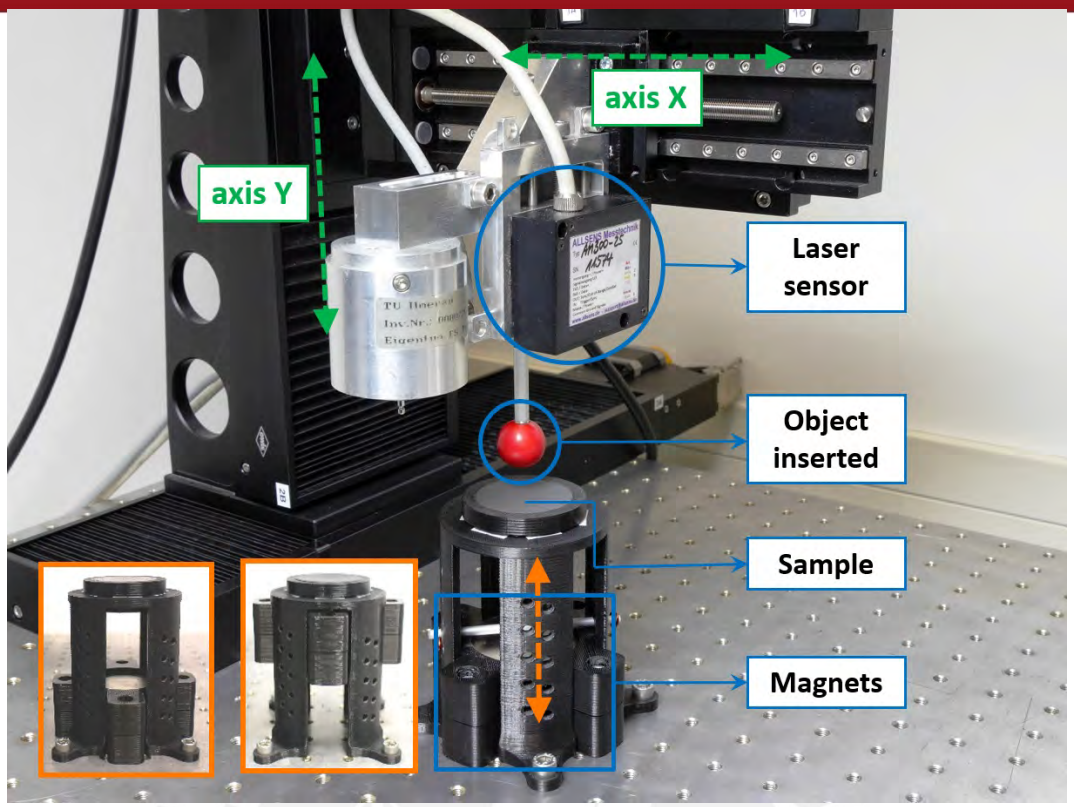

Figure 2.26: Configuration of the motorized positioning system for the tests.

The magnet's housing had four lugs to make easier its movement up and down. The hollow cylinder where the sample and its cast were fixed has four grooves, which served as a guide for moving the magnet and its housing. The initial idea for the experiment was to vary the distance between the magnet and the sample so that the induced magnetic field could had been also varied. That is why it was made some holes of 4mm diameter at certain levels of the cylinder legs to fix the magnet, through a slender cylinder placed above and below the magnet. However, after some initial tests this idea was discarded because the main objective was to compare the behaviour of the sample with and without a magnetic field and also because the magnetic field induced from the magnets was not strong enough to reduce for other tests.

The magnetic field induced to the samples is as shown in the table 2.10. For the tests performed and the results obtained, it is considered that the samples are not under the influence of a magnetic field when the magnets are down (as shown on figure 2.26) because of the low induced magnetic field.

Table 2.10: Magnetic field on the surfaces of samples, with the magnets away and close to them.

Sample	**Magnetic field induced on the samples' surface [mT]**	
	With magnets down	**With magnets up**
Small	28	230
Medium	26	198
Big	23	169

For these experiments the force sensor was not used because it was not the objective to measure the force by deformation. Rather, it has the laser sensor facing the sample, as shown in figure 2.26. Using the laser sensor, was measured the recorded depth on the samples' surface and thus, the recorded shape from the object which came into contact.

2.4.3 Results

As mentioned before, it was measured the recorded shape of the object in contact to the sample by the depth of some points along the sample's surface. As it is shown in the figure 2.27, the sample recorded good the shape from the ball, the imperfections on the surface are due to the adhesion. A similar quality of recorded shape was obtained when the cylinder was inserted on the sample.

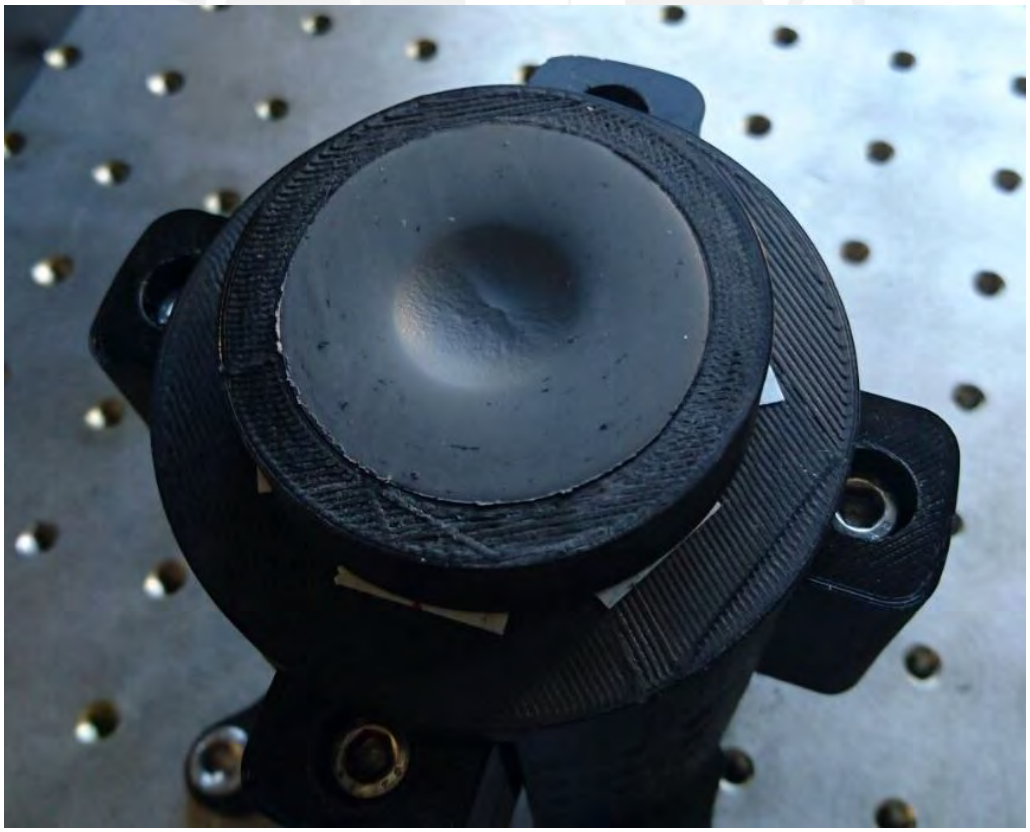

Figure 2.27: Recorded shape on the big sample from insertion of the ball while the magnet was kept near to the sample.

Disregarding the imperfections on the surface and working with the assumption that the recorded shape was a nearly perfect surface of revolution, the recorded shape after the insertion of the ball is represented on the figure 2.28. The region I is the rim created for the mixture pushed out because of the pressure. The region II represents the recorded shape of the ball. A similar revolution shape was recorded with the cylinder.

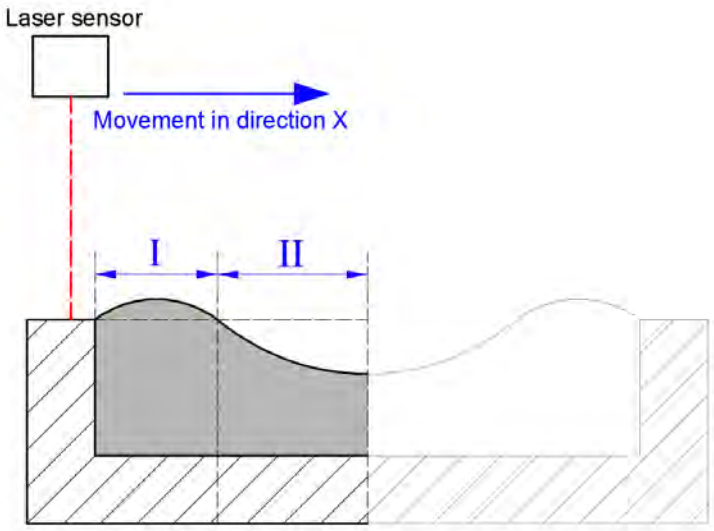

Figure 2.28: Representation of the recorded shape of the ball in one sample; (I) rim created for the mixture pushed out, (II) recorded shape of the ball.

Then the measurement of depth had to be done only for points located on one radius of the sample. For the following figures of results: the axis-X is named the set of points on the radius of the sample where the force sensor measured the depth. The recorded depth was measured for those points until reached the center of the sample. The step for the movement of the force sensor on the axis-X was equal to 0.1mm.

In the experiments three types of tests were performed, which are described below:

Test type I: Tests with middle size sample.
For each object inserted into the middle size sample, it was measured the recorded depth after inserting 1mm, 2mm, 3mm, 4mm, 5mm and 6mm deep on the sample. For each of insertion it was made one test with the sample under the effect of the magnetic field since before the insertion of the object, and one test with the sample under magnetic field after the insertion. In each experiment the recorded surface was measured during the presence of the magnetic field (magnets close to the sample). The specifications for this test are summarized on the table 2.11. In total, 24 experiments for middle size sample were performed.

Table 2.11: Specifications and number of measurements for test type I.

	Specifications	**Number**
Object Inserted	Ball	2
	Cylinder	
Conditions for the magnetic field	Magnetic field after pressure (after inserting the object on the sample)	2
	Magnetic field before pressure (before inserting the object on the sample)	
Depth of the object inside the sample	1mm	6
	2mm	
	3mm	
	4mm	
	5mm	
	6mm	
NUMBER OF MEASUREMENTS		**24**

First was made the tests with the insertion of the ball. In the tests with the ball, first was performed the tests with the action of the magnetic field after insertion, for all the depths (from 1mm to 6mm). The figure 2.29 shows a graphical sequence of the experiment with magnetic field after the insertion of the ball.

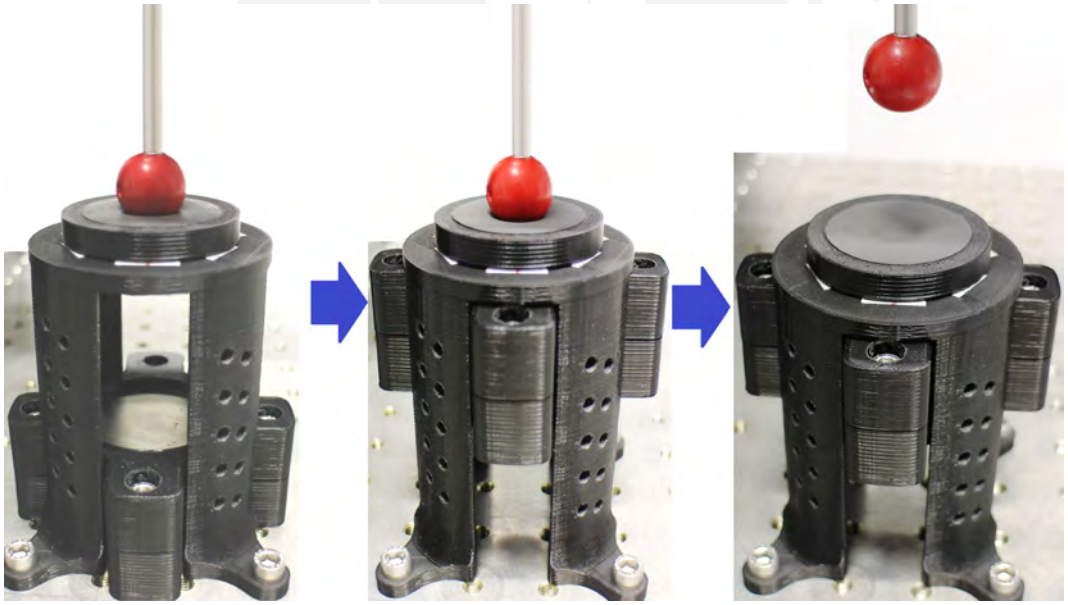

Figure 2.29: Sequence for the experiments with magnetic field after the insertion of the ball.

Then were performed the tests with the magnetic field since before the insertion of the ball. The figure 2.30 shows a graphical sequence of the experiments with magnetic field since before the insertion of the ball.

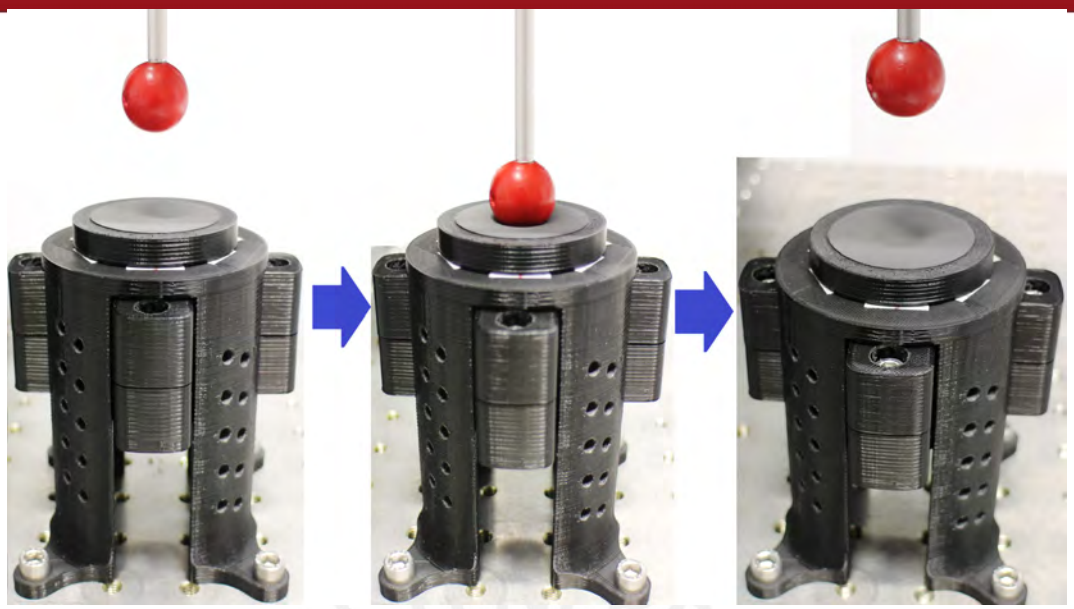

Figure 2.30: Sequence for the experiments with magnetic field since before the insertion of the ball.

After that, were done the experiments with the insertion of the cylinder with the same two sequences.

After the experiment with 3mm of insertion of the cylinder under the effect of the magnetic field since before the insertion, the sample got damaged on its surface because the shape of the cylinder tends to cut the cylinder.

The figure 2.31 shows the results of the measured depths for points along the diameter on the medium sample, for depths of insertion of the ball from 1mm to 6mm, with the magnetic field applied after the insertion of the ball. On this figure and the followings, the recorded depth is shown as negative value in the Y-axis of the graphic, but for the calculation of the percentage of recorded surface the value is considered positive.

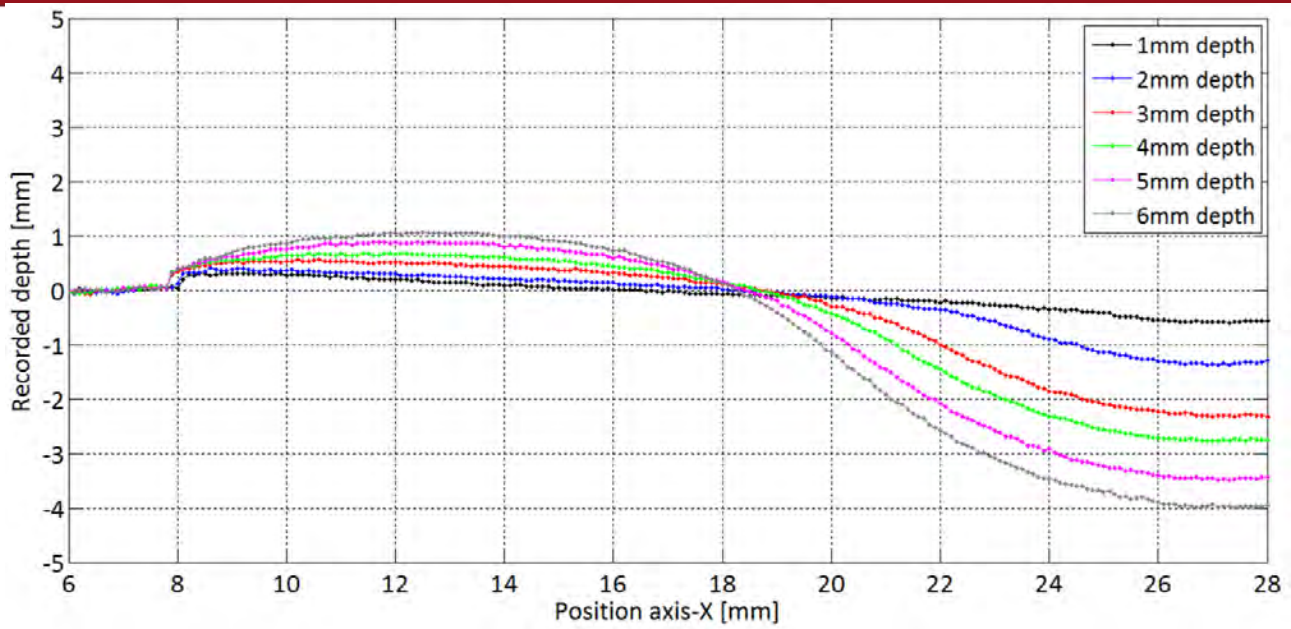

Figure 2.31: Recorded depth on the medium sample after releasing the ball, with the magnetic field applied after the insertion of the ball.

The figure 2.32 shows the results of the measured depths for points along the diameter on the medium sample, for depths of insertion of the ball from 1mm to 6mm, with the magnetic field applied since before the insertion of the ball.

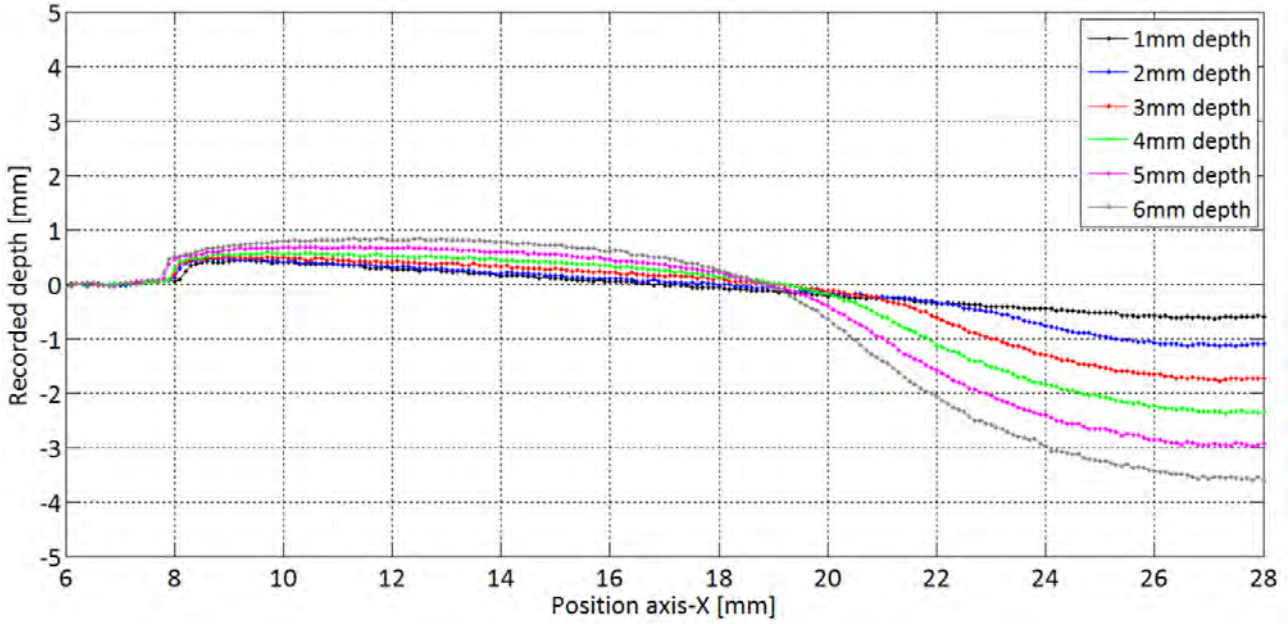

Figure 2.32: Recorded depth on the medium sample after releasing the ball, with the magnetic field applied since before the insertion of the ball.

The figure 2.33 shows the results of the measured depths for points along the diameter

on the medium sample, for depths of insertion of the cylinder from 1mm to 6mm, with the magnetic field applied after the insertion of the cylinder.

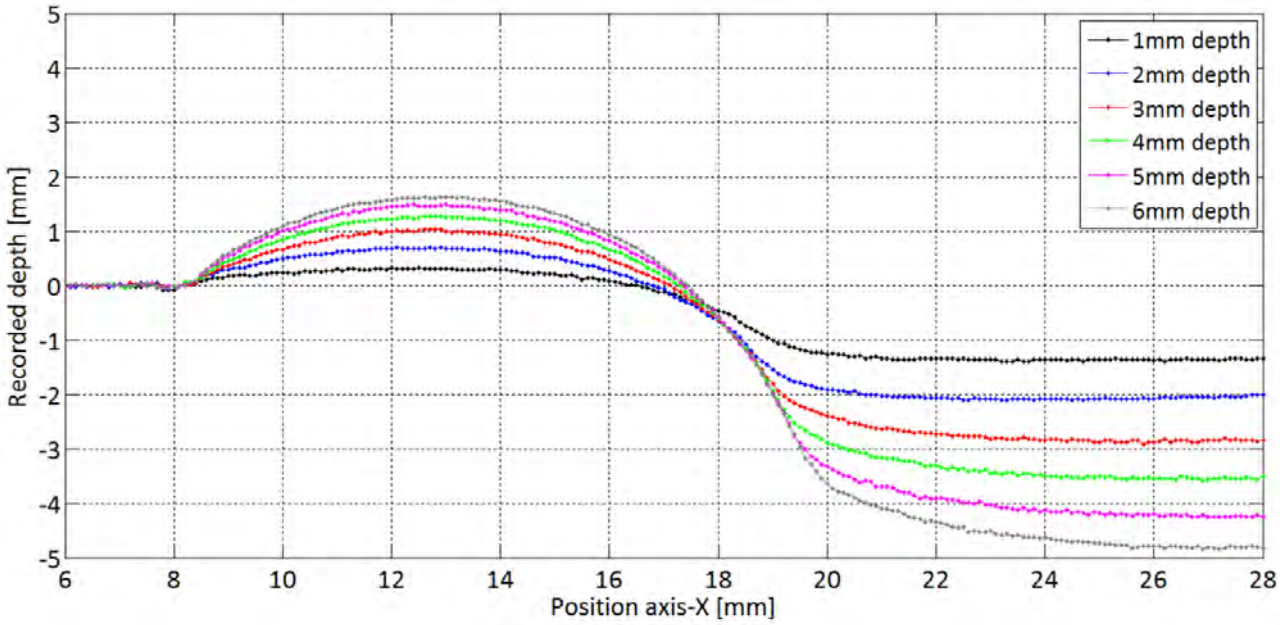

Figure 2.33: Recorded depth on the medium sample after releasing the cylinder, with the magnetic field applied after the insertion of the cylinder.

The figure 2.34 shows the results of the measured depths for points along the diameter on the medium sample, for depths of insertion of the cylinder from 1mm to 6mm, with the magnetic field applied since before the insertion of the cylinder.

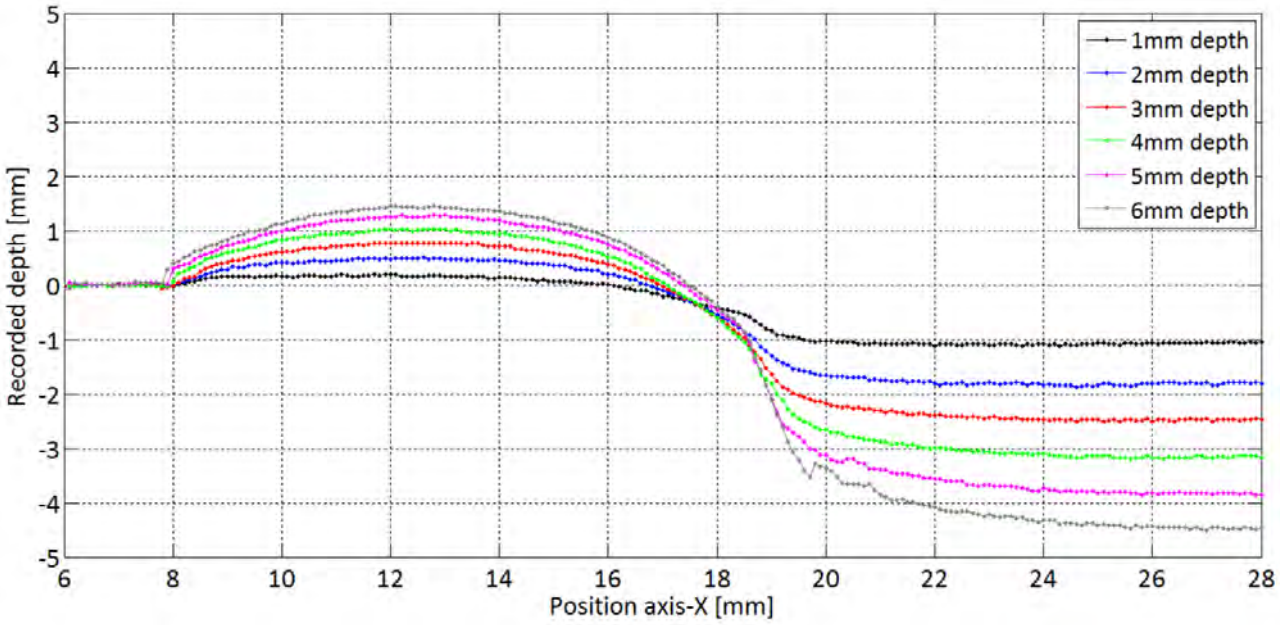

Figure 2.34: Recorded depth on the medium sample after releasing the cylinder, with the magnetic field applied since before the insertion of the cylinder.

The results obtained on the figures 2.31 to 2.34 are summarized on the table 2.12, where is shown the recorded depth for the center of the object inserted into the middle sample (deepest point from each figure) and its proportion to the inserted depth.

Table 2.12: Recorded depth and percentage of recorded depth for tests type I.

Depth	**Ball**				**Cylinder**			
	Magnet Field After Pressure		**Magnet Field Before Pressure**		**Magnet Field After Pressure**		**Magnet Field Before Pressure**	
	Depth recorded [mm]	**%**	**Depth recorded [mm]**	**%**	**Depth recorded [mm]**	**%**	**Depth recorded [mm]**	**%**
1mm	0.593	59.3%	0.627	62.7%	1.381	138.1%	1.113	111.3%
2mm	1.372	68.6%	1.130	56.5%	2.097	104.8%	1.859	93.0%
3mm	2.319	77.3%	1.772	59.1%	2.896	96.5%	2.489	83.0%
4mm	2.763	69.1%	2.360	59.0%	3.562	89.0%	3.178	79.5%
5mm	3.477	69.5%	2.958	59.2%	4.239	84.8%	3.841	76.8%
6mm	3.973	66.2%	3.597	60.0%	4.824	80.4%	4.489	74.8%

From figures 2.31 to 3.34 and the table 2.12, it is observed and concluded:

- By bringing the magnets close to the sample for tests with the magnetic field applied before the insertion, it was seen that the sample sank towards its center.
- In both experiments, with the ball and the cylinder, the sample recorded better the shape with the magnetic field applied after the deformation. This is because before having magnets close, the sample is much more flexible and can be deformed more easily, when the magnets are close the sample is rigid.
- The percentages of recorded depths on the sample is large for tests with insertion of the cylinder 1mm and 2mm depth, becoming even greater than 100
- It is observed that when the depth the object increased, the recorded surface got worse.

Test type II: Tests with 5mm depth on the samples.
For each object inserted, it was measured the recorded depth for 5mm deep of insertion on the three samples. For each sample one test was performed with the sample under the effect of the magnetic field after the insertion of the object, and one test with the sample under magnetic field since before the insertion. For each experiment, the recorded surface was measured during the presence of the magnetic field (magnets close to the sample). These specifications for tests type II are summarized on the table 2.13. In total, 8 new experiments were performed. Adding the results already obtained for the middle size sample, a total of 12 measurements were used to study the results of these tests.

Table 2.13: Specifications and number of measurements for test type II.

	Specifications	**Number**
Sample size	Small	3
	Medium (already done in Test Type I)	
	Big	
Object Inserted	Ball	2
	Cylinder	
Conditions for the magnetic field	Magnetic field after pressure (after inserting the object on the sample)	2
	Magnetic field before pressure (before inserting the object on the sample)	
NUMBER OF MEASUREMENTS		**12**

For each sample, first it was performed the experiments with the insertion of the ball and then the cylinder. For the insertion of each object, first it was made the test with the magnetic field after insertion, and then the test with the magnetic field since before the insertion.

Similar to what happened with tests type I, after experiments inserting the cylinder, the samples got damaged on its surface after the experiments with deformation by the cylinder.

The figure 2.35 shows the set of measured depths for points along the diameter of the samples, for insertion of 5mm depth, with the magnetic field applied after inserting the ball.

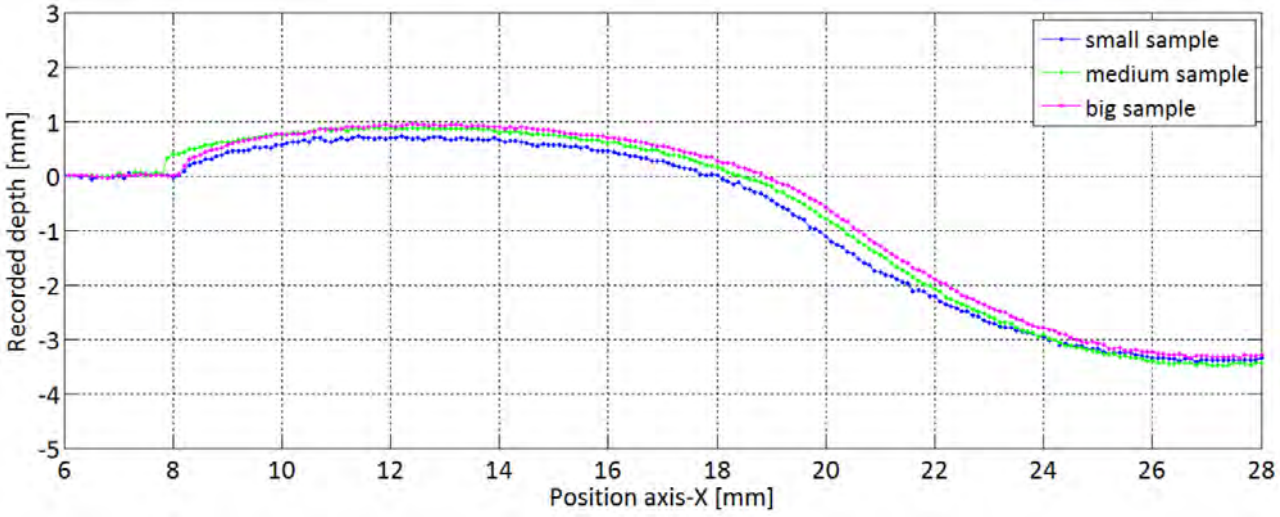

Figure 2.35: Recorded depth after releasing the ball and magnetic field. The magnetic field was applied after the insertion of the ball.

The figure 2.36 shows the set of measured depths for points along the diameter of the samples, for insertion of 5mm depth, with the magnetic field applied since before the insertion of the ball.

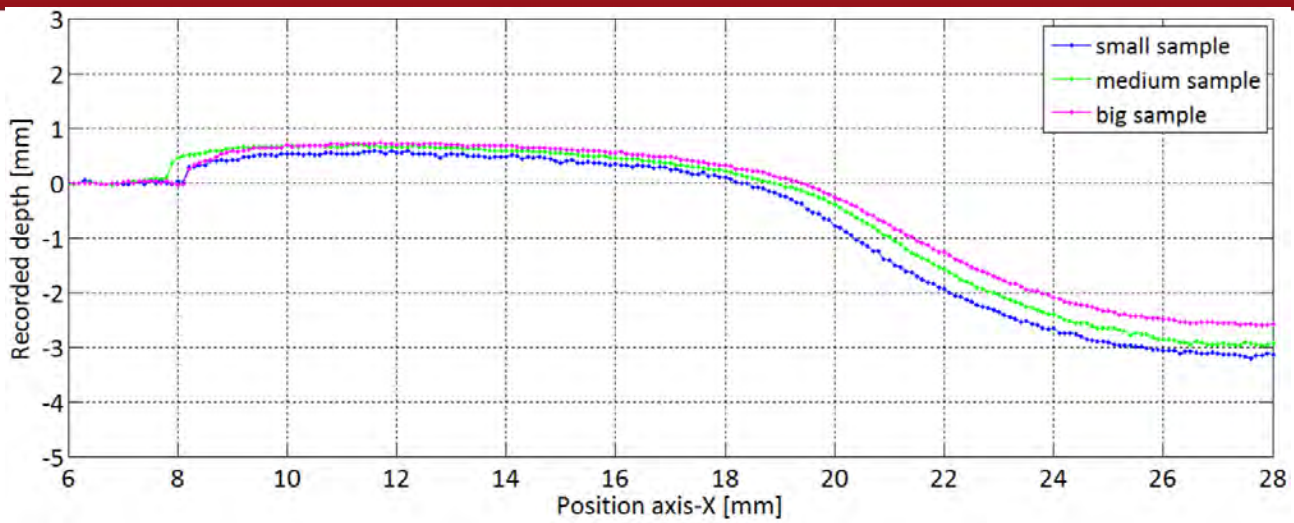

Figure 2.36: Recorded depth after releasing the ball and magnetic field. The magnetic field was applied since before the insertion of the ball.

The figure 2.37 shows the set of measured depths for points along the diameter of the samples, for insertion of 5mm depth, with the magnetic field applied after inserting the cylinder.

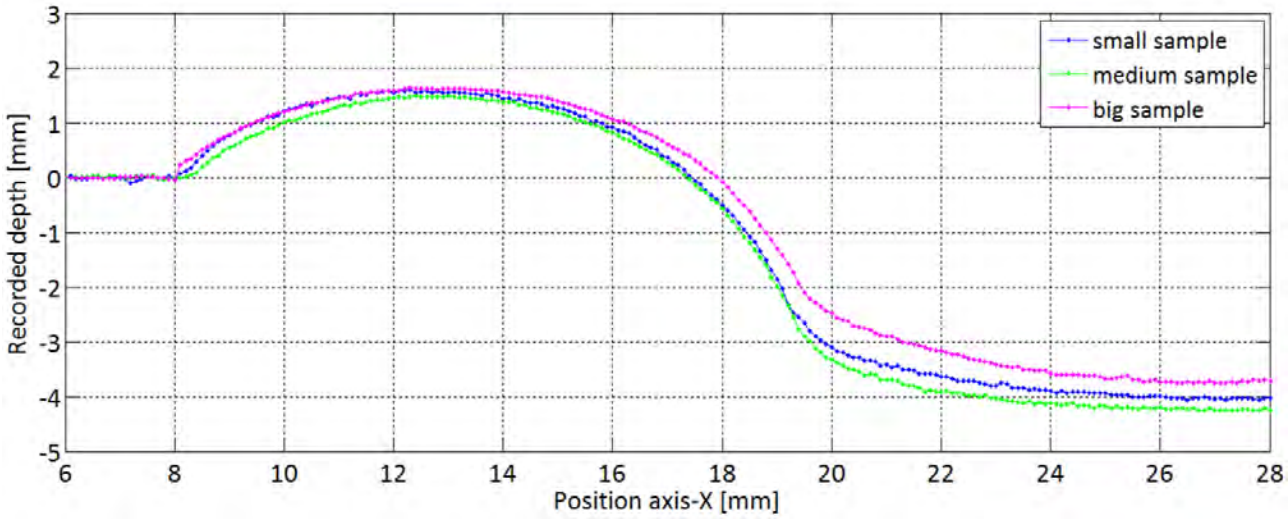

Figure 2.37: Recorded depth after releasing the cylinder and magnetic field. The magnetic field was applied after the insertion of the cylinder.

The figure 2.38 shows the set of measured depths for points along the diameter of the samples, for insertion of 5mm depth, with the magnetic field applied since before the insertion of the cylinder.

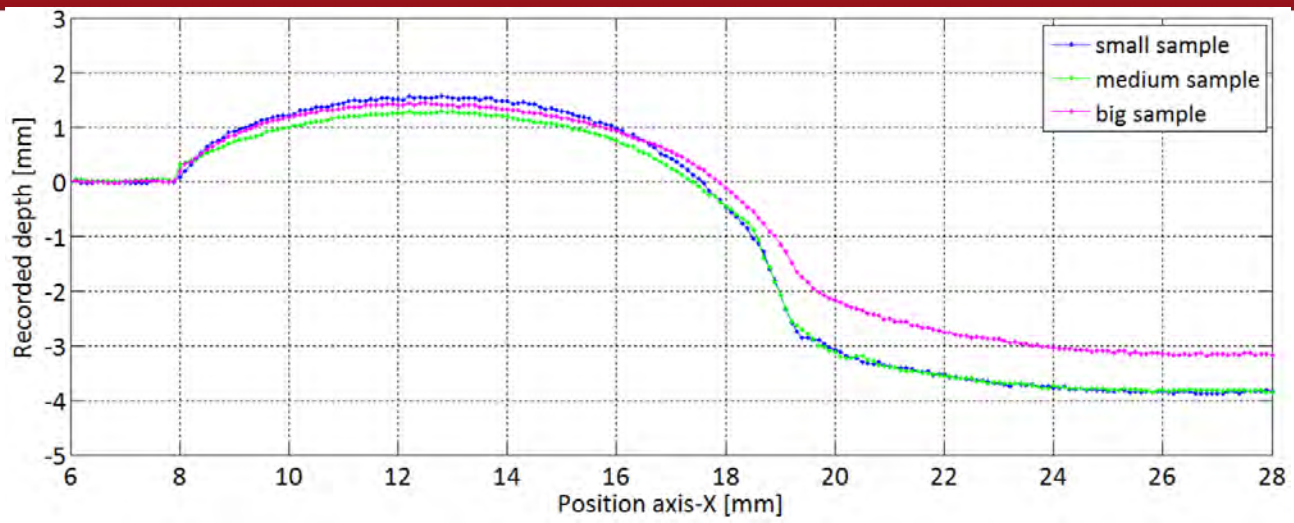

Figure 2.38: Recorded depth after releasing the cylinder and magnetic field. The magnetic field was applied since before the insertion of the cylinder.

The results obtained on the figures 2.35 to 2.38 are summarized in the table 2.14, where is shown the recorded depth for the center of the object inserted into the samples (deepest point from each figure) and its proportion to the 5mm inserted.

Table 2.14: Recorded depth and percentage of recorded depth for tests type II.

Size	**Ball**				**Cylinder**			
	Magnet Field After Pressure		**Magnet Field Before Pressure**		**Magnet Field After Pressure**		**Magnet Field Before Pressure**	
	Depth recorded [mm]	**%**	**Depth recorded [mm]**	**%**	**Depth recorded [mm]**	**%**	**Depth recorded [mm]**	**%**
Small	3.395	67.9%	3.195	63.9%	4.057	81.1%	3.873	77.5%
Medium	3.477	69.5%	2.958	59.2%	4.239	84.8%	3.841	76.8%
Big	3.334	66.7%	2.585	51.7%	3.745	74.9%	3.176	63.5%

From the table 2.14 and figures from 2.35 to 2.38, it can be observed and concluded:

- For all the samples and object inserted, the depth of the object inserted was recorded better with the samples under magnetic field after the pressure.
- For the experiments with the effect of the magnetic field after the pressure, the best result of field-induced plasticity was obtained with the medium sample.
- For the experiments with the effect of the magnetic field since before the pressure, the best result of field-induced plasticity was obtained with the small sample.
- The biggest sample had no good results, because its surface is further from the magnet and the induced magnetic field on it is lower than in the other two samples.

Test type III: Time effect on the field-induced plasticity.
For these experiments just the ball was inserted the samples, the cylinder was not used to avoid damage the samples' surface. The biggest sample was discarded from these experiments since from the tests type II, it was concluded that this sample did not save good the shape of the object in contact. This was probable due to the lower induced magnetic field on its surface, compared to the other samples (see table 2.10).

The ball was inserted a depth of 5mm on the small and medium samples. For each sample it was made the test under the effect of the magnetic field with two conditions: the first by only 10 seconds after inserting the ball, and the second during the whole time after the insertion of the ball. Finally, for each experiment it was measured the recorded surface 1 minute, 10 minutes, 1 hour and 12 hours after the insertion. Also the initial surface before inserting the ball was measured.

The presented specifications for this test are summarized in the table 2.15. A total of 30 measurements were executed.

Table 2.15: Specifications and number of measurements for test type III.

	Specifications	**Number**
Sample size	Small	2
	Medium	
Conditions for the magnetic field	Magnetic field for some seconds after pressure: pressure (object inserted) –>Magnets up –> release pressure (object disengaged) –>Magnets down	2
	Magnetic field the whole time after pressure	
Measuring time	Before starting the test	5
	1 minute after pressure	
	10 minutes after pressure	
	1 hour after pressure	
	12 hours after pressure	
NUMBER OF MEASUREMENTS		**20**

In the figure 2.39 are shown the depths measured along the diameter of the small sample, with the effect of the magnetic field for just 10s after the pressure.

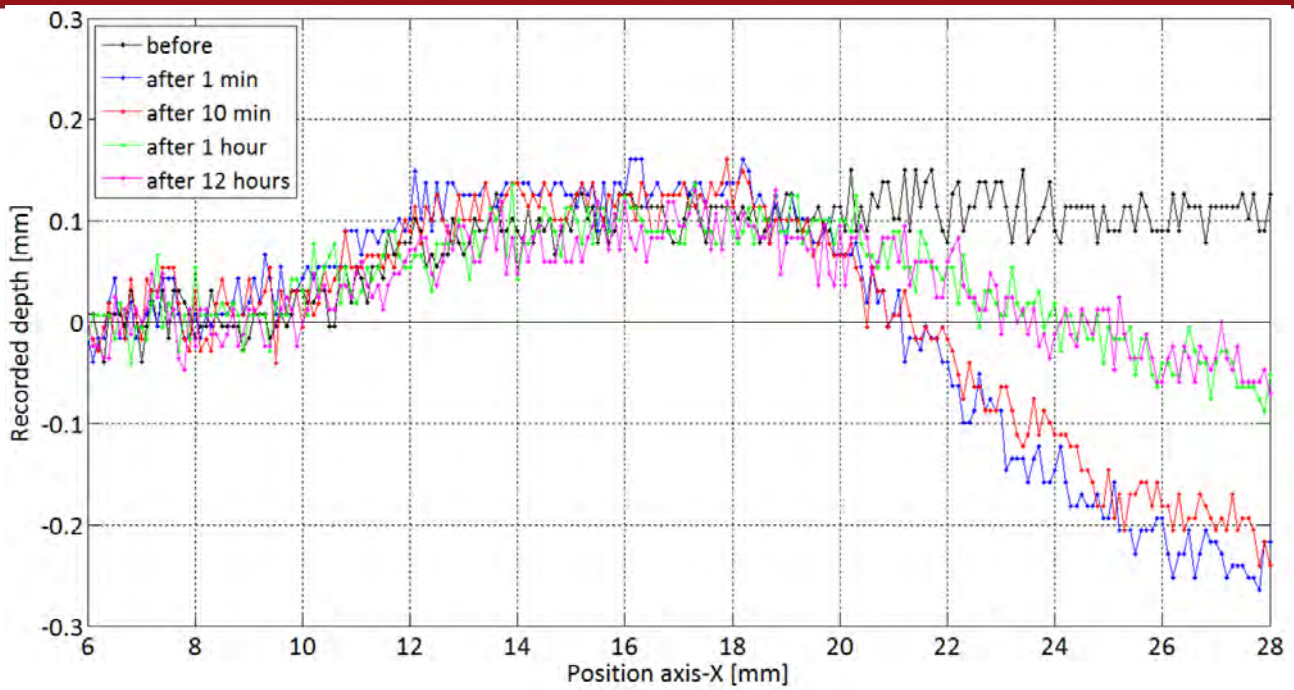

Figure 2.39: Recorded depth on the small sample after releasing the ball and magnetic field. The magnetic field was applied only 10s after the insertion of the ball.

In the figure 2.40 are shown the depths measured along the diameter of the small sample, with the effect of the magnetic field the whole time after the pressure.

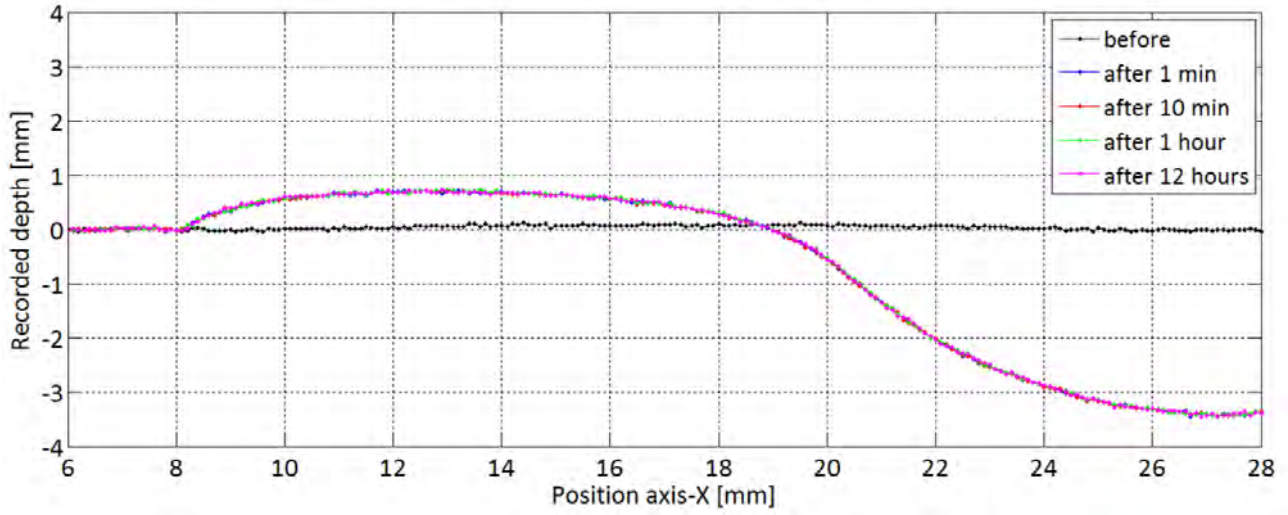

Figure 2.40: Recorded depth on the small sample after releasing the ball and magnetic field. The magnetic field was the whole time after the insertion of the ball.

In the figure 2.41 are shown the depths measured along the diameter of the medium sample, with the effect of the magnetic field for just 10s after the pressure.

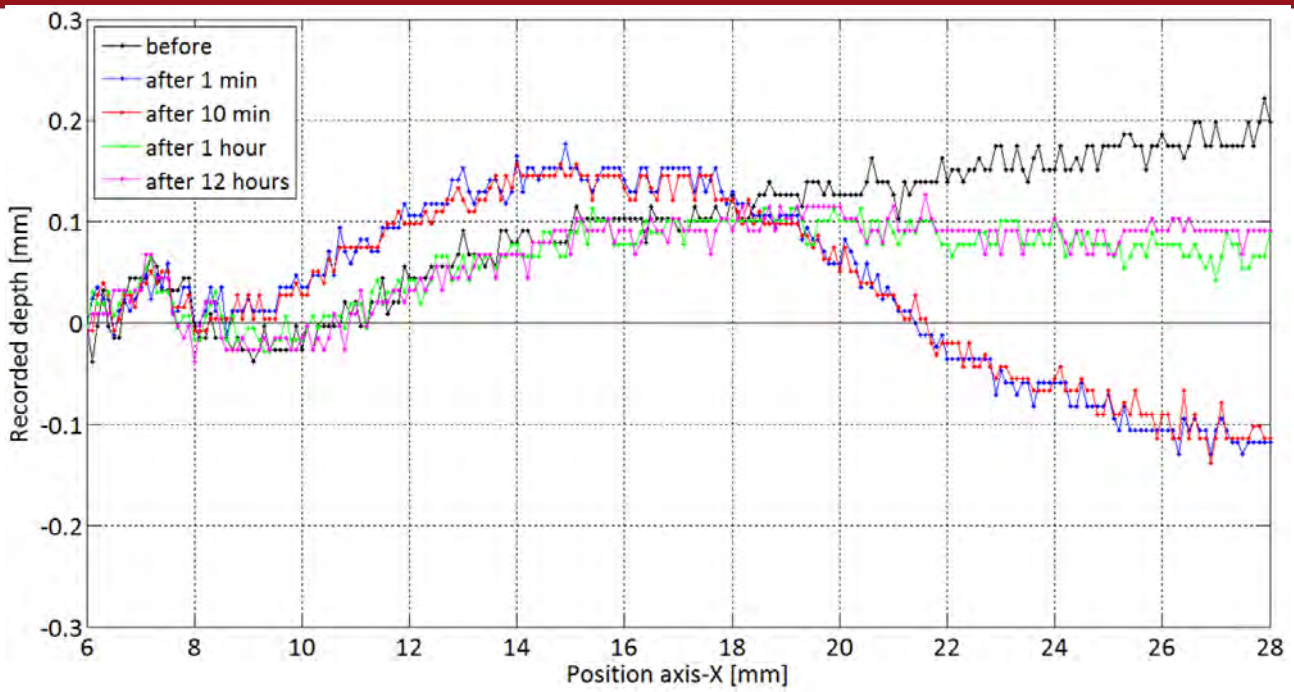

Figure 2.41: Recorded depth on the medium sample after releasing the ball and magnetic field. The magnetic field was applied only 10s after the insertion of the ball.

In the figure 2.42 are shown the depths measured along the diameter of the medium sample, with the effect of the magnetic field the whole time after the pressure.

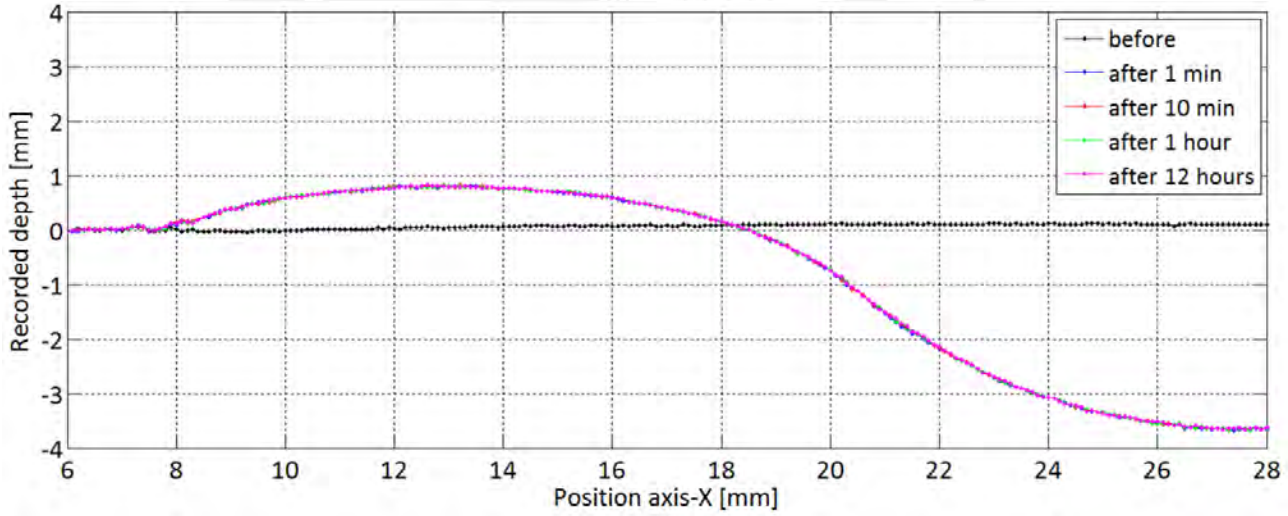

Figure 2.42: Recorded depth on the medium sample after releasing the ball and magnetic field. The magnetic field was the whole time after the insertion of the ball.

For figures 2.40 and 2.42 the samples were still under magnetic field during the measurement, in the other hand for figures 2.39 and 2.41 the magnetic field was relieved during the measurement.

The table 2.16 summarizes the results of the recorded depth from the insertion of the ball after a specified time from the removal of the pressure (see figures 2.39 and 2.41) and under magnetic field for just 10 seconds after the insertion of the ball. In the initial state, the samples had a negative depth because the samples were completely new and on the fabrication it could not be achieved a perfectly flat surface. On the percentages indicated for depth recorded, the calculation is made as indicated by the equation 2.2, dividing the difference in depths (depth measured minus initial depth) over the applied depth (5mm).

Table 2.16: Recorded depth and percentage of recorded depth for tests type III with magnets removed.

Time	**Small sample**		**Medium sample**	
	Depth recorded [mm]	**%**	**Depth recorded [mm]**	**%**
Before	-0.112	0.0%	-0.161	0.0%
1 min	0.264	7.5%	0.130	5.8%
10 min	0.241	7.1%	0.138	6.0%
1 hour	0.088	4.0%	-0.042	2.4%
12 hours	0.070	3.6%	-0.068	1.9%

$$\%\text{Recorded} \quad \text{depth} = \frac{\text{Depth} \quad \text{measured} - \text{Initial} \quad \text{depth}}{\text{Depth} \quad \text{inserted}} \tag{2.2}$$

For instance, the recorded depth for the small sample, 1 hour after removing the magnetic field is:

$$\%\text{Recorded} \quad \text{depth}_{\text{small}-1\text{hour}} = \frac{0.088\text{mm} - (-0.112\text{mm})}{5\text{mm}} = 4\%$$

The results from figures 2.40 and 2.42 are summarized in the table 2.17. There, the sample its considered with perfectly flat surface (depth 0 mm) before the tests. The percentage indicated for the recorded depth is the maximum depth recorded divided by the 5mm inserted.

Table 2.17: Recorded depth and percentage of recorded depth for tests type III with magnets the whole time.

Time	**Small sample**		**Medium sample**	
	Depth recorded [mm]	**%**	**Depth recorded [mm]**	**%**
1 min	3.442	68.8%	3.662	73.2%
10 min	3.425	68.5%	3.653	73.1%
1 hour	3.445	68.9%	3.655	73.1%
12 hours	3.437	68.7%	3.645	72.9%

From figures 2.39 to 2.42 and the tables 2.16 and 2.17, it can be concluded:

- The recorded shape on the samples after releasing the magnetic field effect, was well mitigated during time. The best results were obtained for the middle sample (see table 2.16). I.e., after a while with no magnetic field, the surface of the medium sample were closer to its original condition (just 1.9% of difference in the best case). However, that does not mean that the small sample had a bad result, the worse percentage for that sample was 7.5%, but that just mean 0.376mm of difference to the initial condition.

- The recorded shape on the samples under a constant magnetic field was not affected by the time and was very stable for both samples. The medium sample recorded best the depth of the inserted ball during 12 hours. The recorded depth on this sample just decreased 0.4% in 12 hours.

As a conclusion of all the experiments performed in this section, both samples of the kept the given shape during time with no significant changes, and then they returned to their initial shape easily when the magnetic field was relieved. That can be used shapes of new objects.
The suitable time for the application of the magnetic field was after the deformation of the samples, then the shape could be recorded in better quality.
And the last conclusion is that the percentage of recorded surface could be improved if the adhesion between the two surfaces decreases, then the sample's surface would not being pulled up.

3 Conclusions and future work

From all the tests performed during this work, are presented below the most remarkable conclusions and possible applications for the MSE [29-33] with the results obtained. Also there is a list of some works that were uncompleted because of the time limit of the project. In addition, there are mentioned some problems on the tests and fabrication that can be improved or completely solved in the future.

3.1 Conclusions

The electrical resistance of the samples used on the section 2.2 had a huge change under the effect of magnetic field. Besides, by the end of the same section, was mentioned that the mechanical load applied to the new cylindrical samples had a big influence on the resistance's change. This can be used to create sensors which alert the presence of magnetic field due to their resistance change.

The mechanical behaviour of the mixtures depends not only of the iron contained, but all the components. On the section 2.3 it was founded a mixture with a specified mechanical behaviour under the effect of magnets. Joining this properties and the one from section 2.2, it can be developed a kind of sensor that have a big deformation in the absence of magnets and therefore a high electrical resistance, but when applied a magnetic field it could not be deformed as before and its resistance's change would be decreased.

As concluded on the section 2.4, the MSE can be used for some applications were it is needed to control how stiff or deformable the material is. E.g., it can be performed a gripper that, with the presence of magnetic field is very strong and does not change easily its form, but when the field is released it can reach its original shape easily. Then, can save other object's shapes and return to its own, controlled by the magnetic field.

3.2 Future work

- It is pending to study the solubility of the two types of silicone oil on the silicone matrix. With the results a new sample, with a good mechanical behaviour and low adhesion, could be fabricated.
- A deeper quantitative study of the effect of the magnetic field on the electrical resistance. Mathematical models for the curves obtained of electrical resistance over mechanical load or magnetic field, like the figure 1.8.
- Development of new tests with the influence of mechanical load on the resistance, with the new samples and electrical contacts presented on the subsection 2.2.5.
- Add to the mixtures some thermoplastic materials, to see the behaviour of the sample under a gradient of temperature [25].

- Add some amount of graphite to the tests from section 2.3 to see how it influences the mechanical behaviour with and without magnetic field.

3.3 Improvements

- Make more stable the balance while weighting the amount of components.
- Eliminate electrostatic charges on the recipients and balance during the addition of components for the mixture.
- Decrease the adhesion between the sample and the object inserted for section 2.4. It can be used some powder.
- Improve the fabrication of samples in general. E.g., make more flat the surface of samples for tests of section 2.4.

4 Bibliography

[1]. J. Yiang, S. Sun, H. Du, G. Alici, T. Yan and W. Li. "Fabrication and characterization of magneto-rheological shear-stiffened elastomers". *Frontiers in Materials* (2014), **10**, 2213.

[2]. D. Ivaneyko, V. Toshchevikov, M. Saphiannikova and G. Heinrich. "Mechanical properties of magneto sensitive elastomers unification of the continuum mechanics and microscopic theoretical approaches". *Soft Matter* (2014).

[3]. D. Ivaneyko, V. Toshchevikov and M. Saphiannikova "Dynamic moduli of magneto-sensitive elastomers a coarse-grained network model". *Soft Matter* (2015).

[4]. S. Abramchuk, E. Kramarenko, D. Grishin, G. Stepanov, L. V. Nikitin, G. Filipcsei, A. R. Khokhlov, M. Zrínyi. "Novel highly elastic magnetic materials for dampers and seals: Part I. Preparation and characterization of the elastic materials". *Polym. Adv. Technol.*, (2007), **18**, 513-518.

[5]. X. Zhang, S. Peng, W. Wen and W. Li, "Analysis and fabrication of patterned magnetorheological elastomers". *Smart Mater. Struct.*, (2008), **17**, 045001.

[6]. N. Aspaldin, "Magnetics Materials, Fundamentals and Applications". Second edition. Cambridge University Press, (2011), 17-21.

[7]. J. Adams, "Electromagnetic Theory (IEEE Press Series on Electromagnetic Wave Theory)". McGraw-Hill, (2007), 125-127.

[8]. W. Hosford. "Mechanical Behavior of Materials", 2nd edition. Cambridge University Press, (2009), 244-249.

[9]. M. R. Jolly, J. D. Carlson, B. C. Muñoz, "A model of the behaviour of magnetorheological materials". *Smart Materials and Structures Vol.5* (1996), 607-614.

[10]. J. Koo, F. Khan, D. Jang, H. Jung. "Dynamic characterization and modeling of magneto-rheological elastomers under compressive loadings". *Smart Materials and Structures Vol.19* (2010) 117002 (6pp).

[11] Noll, W. "Chemistry and Technology of Silicones". Academic Press, New York, (1968), chap. 6.

[12]. E. Falcon, B. Castaing, "Electrical conductivity in granular media and Branly's coherer: A simple experiment". *Laboratoire de Physique, Ecole Normale Superieure de Lyon* (2008).

[13]. Y. Wang, S. Xuan, B. Dong, F. Xu, X. Gong, "Stimuli dependent impedance of conductive magnetorheological elastomers". *Smart Materials and Structures Vol.25* (2016) 025003 (10pp).

[14] W. Schatt, K.-P. Wieters, B. Kieback, "Pulvermetallurgie. Technologien und Werkstoffe", 2. Auflage; Springer-Verlag Berlin Heidelberg, (2007), 41.

[15] M. Abshinova, A. Lopatin, N. Kazantseva, J. Viláková, and P. Sáha. "Correlation between the microstructure and the electromagnetic properties of carbonyl iron filled polymer composities". *Elsevier Journal* Vol. 38A, No.12 (2007) 2471-2485.

[16] I. Zivkovic and A. Murk. "Extraction of dielectric and magnetic properties of carbonyl iron powder composites at high frequencies". *Journal of Applied Physics 111* , 114104 (2012).

[17] I. Oltean, D. Motoc. "Factors influencing the electrical conductivity of composites with iron particles". *Optimization of Electrical and Electronic Equipment (OPTIM), 2012 13th International Conference on, Brasov*, (2012), pp. 124-129.

[18] M. Sedlacik, V. Pavlinek, P. Saha, P. Svrcinova, P. Filip. "Polymer coated carbonyl iron particles and their magnetorheological suspensions". *4th WSEAS international conference on Energy and development - environment - biomedicine* , (2011) 289-293.

[19] W. Li, K. Kostidis, X. Zhang, and Y. Zhou. "Development of a Force Sensor Working with MR Elastomers". *IEEE/ASME International Conference on Advanced Intelligent Mechatronics* (2009) 233-238 .

[20] D. Ivaneyko, V. Toshchevikov, M. Saphiannikova and G. Heinrich. "Effects of particle distribution on mechanical properties of magneto-sensitive elastomers in a homogeneous magnetic field". *Condensed Matter Physics* (2012).

[21] C. Ruddy, E. Ahearne and G. Byrne. "A review of magnetorheological elastomers: Properties and Applications". University College Dublin, Ireland. *Advanced Manufacturing Science (AMS) Research Centre* (2014).

[22] Yi Han, Wei Hong, LeAnn E. Faidley. "On the stiffening effect of magneto-rheological elastomers". Iowa State University, USA. Wartburg College, USA. (2014).

[23] YING ZuGuang, NI YiQing, and SAJJADI Masoud. "Nonlinear dynamic characteristics of magneto-rheological visco-elastomers". *Science China: Technological sciences* (2012).

[24] A. Boczkowska and S. Awietjan. "Microstructure and properties of magneto-rheological Elastomers". Chapter 6 from *'Advanced Elastomers-Technology, Properties and Applications'* (2012).

[25] K. Shahrivar, J. Vicente, "Thermoresponsive polymer-based magneto-rheological (MR) composites as a bridge between MR fluids and MR elastomers". *Soft Matter*, (2013), 9, 11451.

[26] N. Ghafoorianfar, X. Wang and F. Gordaninejad. "Combined magnetic and mechanical sensing of magnetorheological elastomers". *Smart Materials and Structures* Vol.23 (2014) 055010.

[27] S.C. Tjong, and Y.-W.Mai. "Physical properties and applications of polymer nanocomposites". (2010) Cambridge, UK: Woodhead Publishing.

[28] S. Murao, K. Hirata, and F. Miyasaka. "Analysis of Variable Stiffness Magnetorheological Elastomer Employing Particle Method and FEM". Osaka University, Japan (2015).

[29] Daniel J. Klingenberg. "Magnetorheology: Applications and Challenges". *AIChE Journal* Vol. 47 No.2 (2001) 246-249.

[30] A. Aczel. "Modelling of an electroactive polymer actuator". *MMaMS Procedia Engineering Vol.48* (2012) 1-9.

[31] H. Böse, R. Rabindranath and J. Ehrlich. "Soft magnetorheological elastomers as new actuators for valves". *Journal of Intelligent Material Systems and Structures* (2011).

[32] I. Guomundsson. "A Feasibility Study of Magnetorheological Elastomers for a Potential Application in Prosthetic Devices". Master of Science. University of Iceland (2011).

[33] D. PetkoviÂ´c and N.D. Pavlovic. "A New principle of Adaptive Compliant Gripper". *Mechanisms, Transmissions and Application. Vol. 3: Mechanisms and Machine Science.* (2012) pp. 143-150.

[34] H. Biernholtz, S. Kenig and H. Dodiuk. "Dielectric, Magnetic and Mechanical Properties of Ferrite Composities". *Polymers for Advanced Technologies* Vol.3 (1992) pp. 125-131.

[35] P. Melenev, Y. Raikher, G. Stepanov, V. Rusakov, and L. Polygalova. "Modeling of the Field-Induced Plasticity of Soft Magnetic Elastomers". *Journal of Physics: Conference Series 149* (2009).

[36] G. Walther, T. Büttner, B. Kieback, T. Weiβgärber. "Properties and sintering behaviour of fine spherical iron powders produced by a new hydrogen reduction process". Fraunhofer Institute for Manufacturing Technology and Advanced Materials IFAM, Branch Lab Dresden, Germany.*Powder Metallurgy Vol. 57, Issue 3.* (2014).

[37] S. Humphries, Jr. "Finite-element Methods for Electromagnetics". Field Precision LLC, (2010), 163-169.

[38] Han Y., Mohla A., Huang X., Hong W. and Faidley L. E., "Magnetostriction and field stiffening of magneto-active elastomers". *Int. J. Appl. Mechanics 7 1550001* (2015).

[39] Biller A. M., Stolbov O. V. and Raikher Y. L., "Modeling of particle interactions in magnetorheological elastomers". *J. Appl. Phys. 116 114904* (2014).

[40] Chen W. W., Sun L. Y., Li X. H. and Wang D. F., "Numerical investigation on the magnetostrictive effect of magnetosensitive elastomers based on a magneto-structural coupling algorithm *Smart Mater. Struct. 22 105012* (2013).

Appendix A Technical data of Alpa-Sil Classic

PRODUKTINFORMATION Stand 06/2006

ALPA-SIL CLASSIC

ALPINA Technische Produkte GmbH

additionsvernetzender 2-Komponenten Siliconkautschuk, der bei Raumtemperatur vulkanisiert

- **vernetzt bei Temperaturen ab 23° C**
- **Problemloses Mischen der Komponenten**
- **einfache Verarbeitung**
- **Gute mechanische Eigenschaften bei niedriger Shore / A- Härte.**
- **Schnelle Verarbeitungs- und Entformzeit.**

Einsatz zum Dublieren in Dental-Laboren und im Modell- und Formenbau.

TECHNISCHE DATEN

	ALPA-SIL Classic A Komponente A	**ALPA-SIL Classic B** Komponente B		
Aussehen	Viskose Flüssigkeit	Viskose Flüssigkeit		
Farbe	transluzent	Blau		
Viskosität	1.050	2.700	MPas	Brookfield HBTD [1])
Dichte	1,05	1,1	g/cm³	DIN 53 479 [1])
	Mischung			
Mischungsverhältnis	100 : 10		Nach Gewicht	
Viskosität			mPa·s	Brookfield HBTD [1])
Topfzeit	7		Minuten	[1])
Entformbar nach	30		Minuten	[1])
	Vulkanisat			
Härte Shore A	6-8			DIN 53 505 [2])
Reißfestigkeit	1,0		Mpa	
Reißdehnung	245		%	DIN 53 504 S 3 A [2])
Weiterreißwiderstand	2,2		N/mm	ASTM D 624 Form B[2])
Linearer Schwund			%	Nach 7 Tagen

Der Platinkatalysator befindet sich in der A-Komponente

[1] = Gemessen im Normalklima DIN 50 014-23/50-2
[2] = Vulkanisat, gemessen nach 14 Tagen Lagerung im Normalklima DIN 50 014-23/50-2

ALPA-SIL CLASSIC

VERARBEITUNG

1. Katalyse
ALPA-SIL CLASSIC Komponente A + B werden in einem bestimmten Verhältnis (siehe technische Daten) miteinander gemischt. Die beiden Komponenten werden mechanisch (z. B. von Hand) oder mit einem Rührgerät gemischt. Um ein Lufteintrag und /oder einen Temperaturanstieg der Masse während des Mischvorgangs zu vermeiden, sollte bei Gebrauch eines Rührgerätes bei niedriger Geschwindigkeit gemischt werden. Die Verwendung einer Dosiermaschine für 2-Komponenten-Systeme ist ebenfalls möglich und empfehlenswert. Weitere Informationen sind auf Anfrage erhältlich. Nach dem Mischen sollte die Masse im Vakuum bei 30 – 50 mbar für ca. 2 Minuten entlüftet werden.

2. Vulkanisation
Bei 23 ° C vulkanisiert das System wie unter technische Daten angegeben. Bei tieferen Temperaturen verlangsamt sich die Vulkanisation durch Erwärmen kann sie dagegen beschleunigt werden.

Anmerkungen:
Der Kontakt mit folgenden Stoffen kann die Vulkanisation verzögern oder verhindern:

- Schwefelhaltige Chlor- oder Butylkautschuke
- Mit Metallsalzen katalysierte LSR- oder RTV-Typen
- Stabilisatoren und Weichmacher
- Aminhärter in Epoxidharzen
- Verschiedene organische Lösemittel, z. B. Ketone, Alkohole, Ether etc.

Im Zweifelsfall sind Vorversuche durchzuführen.

BESONDERE HINWEISE

Lagerung und Haltbarkeit

Bei sachgemäßer Lagerung beträgt die Lagerfähigkeit von Komponente A und B 12 Monate.
Die Produkte unbedingt in ungeöffneten Originalgebinden bei Temperaturen unter 30 ° C und frostfrei lagern.

HINWEISE FÜR DEN ANWENDER

Die in dieser Unterlage enthaltenen Angaben sind das Ergebnis unserer Erkenntnisse und Erfahrungen. Sie entsprechen unserem besten Wissen und sind für die Beratung unserer Kunden bestimmt.
Sie gelten jedoch nur als unverbindliche Hinweise.
Schutzrechte Dritter sind zu beachten.

SICHERHEIT

Bei Umgang mit ALPA-SIL CLASSIC sind die allgemeingeltenden Arbeitsschutzregeln zu beachten.

LIEFEREINHEITEN

ALPA-SIL Classic A :0,9Kg
ALPA-SIL Classic B :0,1Kg
Gebinde:
ALPA-SIL Classic A :4,5Kg
ALPA-SIL Classic B :0,5Kg

Andere Gebindegrößen auf Anfrage

Sicherheitsrelevante Daten entnehmen Sie bitte dem Sicherheitsdatenblatt!

Zur Beachtung: Vorstehende Angaben können nur allgemeine Hinweise sein. Bei den aufgeführten Eigenschaften und Leistungsmerkmalen handelt es sich um circa-Werte, diese sind nicht Teil unserer Produktspezifikation. Wegen der außerhalb unseres Einfluss liegenden Verarbeitungs- und Anwendungsbedingungen und der Vielzahl unterschiedlicher Materialien empfehlen wir, in jedem Fall zunächst ausreichende Eigenversuche durchzuführen. Eine Haftung für konkrete Anwendungsergebnisse kann daher aus den Angaben und Hinweisen in diesem Merkblatt nicht abgeleitet werden.
Ein Gewährleistung wird im Rahmen unserer Verkaufsbedingungen allein für die stets gleichbleibend hohe Qualität unserer Erzeugnisse übernommen. Mit Erscheinen dieser Ausgabe verlieren alle vorherigen technischen Merkblätter ihre Gültigkeit.

ALPINA Technische Produkte GmbH
Breslauer Weg 123
D - 82538 Geretsried • GERMANY
Fon +49(0) 81 71 - 3456 - 0
Fax +49(0) 81 71 - 3456 - 26
Email info@alpina-silicone.de
Web www.alpina-silicone.de

Appendix B Technical data of silicone oil 1000cSt

XIAMETER® from DOW CORNING

XIAMETER® PMX-200 Silicone Fluid, 50-1,000 CS

INCI Name: Dimethicone
Colorless, clear polydimethylsiloxane fluid

FEATURES

- Ease of application and rubout
- Ease of buffing
- Enhances color
- High water repellency
- High compressibility
- High shearability without breakdown
- High spreadability and compatibility
- Low environmental hazard
- Low fire hazard
- Low reactivity and vapor pressure
- Low surface energy
- Good heat stability
- Essentially odorless, tasteless and nontoxic
- Soluble in a wide range of solvents

BENEFITS

For personal care applications

- Skin protection
- Imparts soft, velvety skin feel
- Spreads easily on both skin and hair
- De-soaping (prevents foaming during rubout)

For industrial applications

- High dielectric strength
- High damping action
- Oxidation-, chemical- and weather-resistant

COMPOSITION

- Polydimethylsiloxane polymers
- Chemical composition $(CH_3)_3SiO[SiO(CH_3)_2]nSi(CH_3)_3$

APPLICATIONS

- Active ingredient in a variety of automotive, furniture, metal and specialty polishes in paste, emulsion and solvent-based polishes and aerosols
- Various applications including cosmetic ingredient, elastomer and plastics lubricant, electrical insulating fluid, foam preventive or breaker, mechanical fluid, mold release agent, surface active agent, and solvent-based finishing and fat liquoring of leather

DESCRIPTION

XIAMETER® PMX-200 Silicone Fluid, 50-1,000 CS is a polydimethylsiloxane polymer manufactured to yield essentially linear polymers in a wide range of average kinematic viscosities.

The viscosities generally used in formulating polishes are between 100 and 30,000 cSt. To obtain optimum results, in terms of ease of application and depth of gloss, it is preferable to use a blend of a low-viscosity fluid and a high-viscosity fluid (e.g. 3 parts XIAMETER® PMX-200 Silicone Fluid 100 cSt and 1 part XIAMETER® PMX-200 Silicone Fluid 12,500 cSt). The low-viscosity silicone fluid acts as a lubricant to make polish application and rubout easier, whereas the high-viscosity silicone fluid produces a greater depth of gloss. Since these polymers are inherently water-repellent, they will cause water to bead up on a treated surface rather than penetrate the polish film.

HOW TO USE

XIAMETER® PMX-200 Silicone Fluid, 50-1,000 CS is highly soluble in organic solvents such as aliphatic and aromatic hydrocarbons, and the halocarbon propellants used in aerosols. The fluid is easily emulsified in water with standard emulsifiers and normal emulsification techniques. XIAMETER PMX-200 Silicone Fluid, 50-1,000 CS is insoluble in water and many organic products. Additive quantities as small as 0.1% may suffice where XIAMETER PMX-200 Silicone Fluid, 50-1,000 CS is to be used as a surface agent or for de-soaping creams and lotions. However, 1-10% is needed for applications such as hand creams and lotions to form a more uniform film and effective barrier.

PRODUCT SAFETY INFORMATION

XIAMETER PMX-200 Silicone Fluid, 50-1,000 CS may cause temporary eye discomfort.

PRODUCT SAFETY INFORMATION REQUIRED FOR SAFE USE IS NOT INCLUDED IN THIS DOCUMENT. BEFORE HANDLING, READ PRODUCT AND MATERIAL SAFETY DATA SHEETS AND CONTAINER LABELS FOR SAFE USE, PHYSICAL, ENVIRONMENTAL, AND HEALTH HAZARD INFORMATION. THE MATERIAL SAFETY DATA SHEET IS AVAILABLE ON THE XIAMETER WEB SITE AT WWW.XIAMETER.COM.

TYPICAL PROPERTIES

Specification Writers: These values are not intended for use in preparing specifications. Please contact your local XIAMETER® sales representative prior to writing specifications on this product.

Test	Unit	Result		
		50 cSt	**100 cSt**	**200 cSt**
Appearance		Crystal clear	Crystal clear	Crystal clear
Specific Gravity at 25°C (77°F)		0.960	0.964	0.967
Refractive Index at 25°C (77°F)		1.4022	1.4030	1.4032
Color, APHA		5	5	5
Flash Point, Open Cup	°C (°F)	318 (605)	>326 (>620)	>326 (>620)
Acid Number, BCP		trace	trace	trace
Melt Point	°C (°F)[1,2]	-41 (-42)	-28 (-18)	-27 (-17)
Pour Point	°C (°F)	-70 (-94)	-65 (-85)	-65 (-85)
Surface Tension at 25°C (77°F)	dynes/cm	20.8	20.9	21.0
Volatile Content, at 150°C (302°F)	percent	0.3	0.02	0.07
Viscosity Temperature Coefficient		0.59	0.60	0.60
Coefficient of Expansion	cc/cc/°C	0.00104	0.00096	0.00096
Thermal Conductivity at 50°C (122°F)	g cal/cm·sec·°C	-	0.00037	-
Solubility Parameter[3]		7.3	7.4	7.4
Solubility in Typical Solvents				
Chlorinated Solvents		High	High	High
Aromatic Solvents		High	High	High
Aliphatic Solvents		High	High	High
Dry Alcohols		Poor	Poor	Poor
Water		Poor	Poor	Poor
Fluorinated Propellants		High	High	High
Dielectric Strength at 25°C (77°F)	volts/mil	400	400	400
Volume Resistivity at 25°C (77°F)	ohm-cm	$1.0x10^{15}$	$1.0x10^{15}$	$1.0x10^{15}$
		350 cSt	**500 cSt**	**1,000 cSt**
Appearance		Crystal clear	Crystal clear	Crystal clear
Specific Gravity at 25°C (77°F)		0.969	0.970	0.970
Refractive Index at 25°C (77°F)		1.4034	1.4035	1.4035
Color, APHA		5	5	5
Flash Point, Open Cup	°C (°F)	>326 (>620)	>326 (>620)	>326 (>620)
Acid Number, BCP		trace	trace	Trace
Melt Point	°C (°F)[1,2]	-26 (-15)	-25 (-13)	-25 (-13)
Pour Point	°C (°F)	-50 (-58)	-50 (-58)	-50 (-58)
Surface Tension at 25°C (77°F)	dynes/cm	21.1	21.2	21.2
Volatile Content, at 150°C (302°F)	percent	0.15	0.11	0.11
Viscosity Temperature Coefficient		0.60	0.61	0.61
Coefficient of Expansion	cc/cc/°C	0.00096	0.00096	0.00096
Thermal Conductivity at 50°C (122°F)	g cal/cm·sec·°C	-	0.00038	0.00038
Solubility Parameter[3]		7.4	7.4	7.4
Solubility in Typical Solvents				
Chlorinated Solvents		High	High	High
Aromatic Solvents		High	High	High
Aliphatic Solvents		High	High	High
Dry Alcohols		Poor	Poor	Poor
Water		Poor	Poor	Poor
Fluorinated Propellants		High	High	High
Dielectric Strength at 25°C (77°F)	volts/mil	400	400	400
Volume Resistivity at 25°C (77°F)	ohm-cm	$1.0x10^{15}$	$1.0x10^{15}$	$1.0x10^{15}$

[1]The melt point temperature is a typical value and may vary somewhat due to molecular distribution (especially 50 cSt). If the melting point is critical to your application, then several lots should be thoroughly evaluated.
[2]Due to different rates of cooling, this test method may yield pour points lower than the temperature at which these fluids would melt.
[3]Fedors Method: R.F. Fedors, Polymer Engineering and Science, Feb. 1974.

USABLE LIFE AND STORAGE

Product should be stored at or below 60°C (140°F) in the original unopened containers. The most up-to-date shelf life information can be found on the XIAMETER Web site in the Product Detail page under Sales Specification.

LIMITATIONS

This product is neither tested nor represented as suitable for medical or pharmaceutical uses. Not intended for human injection. Not intended for food use.

LIMITED WARRANTY INFORMATION – PLEASE READ CAREFULLY

The information contained herein is offered in good faith and is believed to be accurate. However, because conditions and methods of use of our products are beyond our control, this information should not be used in substitution for customer's tests to ensure that our products are safe, effective, and fully satisfactory for the intended end use. Suggestions of use shall not be taken as inducements to infringe any patent.

Dow Corning's sole warranty is that our products will meet the sales specifications in effect at the time of shipment.

Your exclusive remedy for breach of such warranty is limited to refund of purchase price or replacement of any product shown to be other than as warranted.

DOW CORNING SPECIFICALLY DISCLAIMS ANY OTHER EXPRESS OR IMPLIED WARRANTY OF FITNESS FOR A PARTICULAR PURPOSE OR MERCHANTABILITY.

DOW CORNING DISCLAIMS LIABILITY FOR ANY INCIDENTAL OR CONSEQUENTIAL DAMAGES.

Appendix C Technical data of silicone oil 5cSt

XIAMETER® from DOW CORNING

Product Information

XIAMETER® PMX-200 Silicone Fluid, 5-20 cSt

Polydimethylsiloxane base fluid

FEATURES

- Good dielectric properties
- High water repellency
- High shearability without breakdown
- High compressibility
- High spreadability
- Low surface tension
- Low fire hazard and reactivity
- Low vapor pressure
- Good heat stability
- Good leveling and easy rubout
- Essentially odorless and nontoxic
- Soluble in a wide range of solvents
- Volatile carrier
- Compatible with a wide range of cosmetic ingredients

BENEFITS

For personal care:
- Soft feel and subtle skin lubricity
- Excellent spreading
- Leaves no residue or buildup
- Transient effect
- Nongreasy feel

For industrial applications:
- Little change in physical properties over a wide temperature span – a relatively flat viscosity-temperature slope, and serviceability from -40°C up to 200°C
- Low surface tension – readily wets clean surfaces to impart water repellency and release characteristics

COMPOSITION

- Polydimethylsiloxane fluid
- Chemical composition $(CH_3)_3SiO[SiO(CH_3)_2]_nSi(CH_3)_3$

APPLICATIONS

- Personal care products such as antiperspirants, deodorants, hair sprays, cleansing creams, skin creams, lotions, bath oils, suntan products, nail polishes
- Industrial applications such as glass vial and lens coatings, household product ingredients, mechanical fluids, penetrating oil ingredients, surface active agents, coatings, electrical insulating fluids and polish ingredients

DESCRIPTION

XIAMETER PMX-200 Silicone Fluid is a polydimethylsiloxane fluid commonly used as a base fluid in personal care products due to its excellent spreading and unique volatility characteristics. It is clear, tasteless, essentially odorless and nongreasy. Unlike other volatile carriers used in the personal care industry, this volatile silicone fluid does not cool the skin when it evaporates, a consequence of its unusually low heat of vaporization.

Commercial bulk-polymerized dimethyl silicone fluids, such as XIAMETER PMX-200 Silicone Fluids, typically contain trace amounts of impurities.

HOW TO USE

XIAMETER PMX-200 Silicone Fluid may be used alone or blended with other cosmetic fluids to provide a fluid base for a variety of cosmetic ingredients. It feature good solubility in most anhydrous alcohols and in many solvents used in cosmetics.

HANDLING PRECAUTIONS

XIAMETER PMX-200 Silicone Fluid may cause temporary eye discomfort.

Use caution when handling volatile fluids at temperatures with 10°C of the quoted flash point.

XIAMETER PMX-200 Silicone Fluids with viscosities below 5 cSt are flammable. Keep away from heat, sparks, open flames and other sources of ignition. Keep container tightly closed.

At elevated temperatures, XIAMETER PMX-200 Silicone Fluids are sensitive to contamination by strong acids, bases, some metallic compounds and oxidizing agents. These contaminants may cause an accelerated rate of volatile byproduct formation. Oxidizing agents can also cause an increase in fluid viscosity. When these conditions may exist, it is recommended that the flash point of the fluids be checked periodically to monitor operational safety. Also, ignitable conditions may exist if the fluid is giving off smoke.

PRODUCT SAFETY INFORMATION REQUIRED FOR SAFE USE IS NOT INCLUDED IN THIS DOCUMENT. BEFORE HANDLING, READ PRODUCT AND SAFETY DATA SHEETS AND CONTAINER LABELS FOR SAFE USE, PHYSICAL AND HEALTH HAZARD INFORMATION. THE SAFETY DATA SHEET IS AVAILABLE ON THE XIAMETER WEBSITE AT XIAMETER.COM, OR FROM YOUR XIAMETER REPRESENTATIVE OR DISTRIBUTOR, OR BY CALLING

TYPICAL PROPERTIES

Test	Unit	Result		
		5.0 cSt	10.0 cSt	20.0 cSt
Appearance		Crystal clear	Crystal clear	Crystal clear
INCI Name		Dimethicone	Dimethicone	Dimethicone
Specific Gravity at 25°C (77°F)		0.913	0.935	0.949
Refractive Index at 25°C (77°F)		1.3960	1.3989	1.4009
Color, APHA		5	5	5
Flash Point, Closed Cup	°C (°F)	134 (272)	211 (411)	246 (474)
Acid Number, BCP		trace	trace	trace
Melt Point	°C (°F)[1,2]	-70 (-94)	-60 (-76)	-52 (-62)
Pour Point	°C (°F)	-100 (-148)	-100 (-148)	-84 (-119)
Surface Tension at 25°C (77°F)	dynes/cm	19.7	20.1	20.6
Volatile Content at 150°C (302°F)	percent	–	–	4.5
Viscosity Temperature Coefficient		0.55	0.56	0.59
Coefficient of Expansion	cc/cc/°C	0.00105	0.00108	0.00107
Thermal Conductivity at 50°C (122°F)	g cal/cm·sec·°C	–	0.00032	0.00034
Solubility Parameter[3]		7.1	7.2	7.3
Solubility in Typical Solvents				
Chlorinated Solvents		High	High	High
Aromatic Solvents		High	High	High
Aliphatic Solvents		High	High	High
Dry Alcohols		Good	Good	Good
Water		Poor	Poor	Poor

[1]The melt point temperature is a typical value and may vary somewhat due to molecular distribution. If the melting point is critical to your application, then several lots should be thoroughly evaluated.
[2]Due to different rates of cooling, this test method may yield pour points lower than the temperature at which these fluids would melt.
[3]Fedors Method: R.F. Fedors, *Polymer Engineering and Science*, Feb. 1974.

YOUR GLOBAL XIAMETER CONNECTION.

USABLE LIFE AND STORAGE

When stored at or below 25°C (77°F) in the original unopened containers, this product has a usable life ranging from 30 to 60 months from the date of production depending on viscosity.

LIMITATIONS

This product is neither tested nor represented as suitable for medical or pharmaceutical uses. Not intended for human injection. Not intended for food use.

HEALTH AND ENVIRONMENTAL INFORMATION

To support customers in their product safety needs, Dow Corning has an extensive Product Stewardship organization and a team of Product Safety and Regulatory Compliance (PS&RC) specialists available in each area.

For further information, please see our website, xiameter.com, or consult your local XIAMETER representative.

LIMITED WARRANTY INFORMATION – PLEASE READ CAREFULLY

The information contained herein is offered in good faith and is believed to be accurate. However, because conditions and methods of use of our products are beyond our control, this information should not be used in substitution for customer's tests to ensure that *Dow Corning*® and XIAMETER® products are safe, effective, and fully satisfactory for the intended end use. Suggestions of use shall not be taken as inducements to infringe any patent.

Dow Corning's sole warranty is that *Dow Corning* or XIAMETER products will meet the sales specifications in effect at the time of shipment.

Your exclusive remedy for breach of such warranty is limited to refund of purchase price or replacement of any product shown to be other than as warranted.

DOW CORNING SPECIFICALLY DISCLAIMS ANY OTHER EXPRESS OR IMPLIED WARRANTY OF FITNESS FOR A PARTICULAR PURPOSE OR MERCHANTABILITY.

DOW CORNING DISCLAIMS LIABILITY FOR ANY INCIDENTAL OR CONSEQUENTIAL DAMAGES.

Appendix D Technical data of iron powder

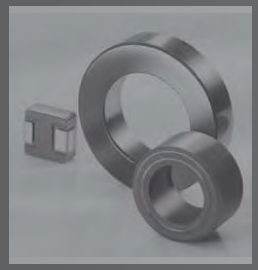

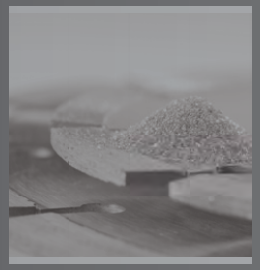

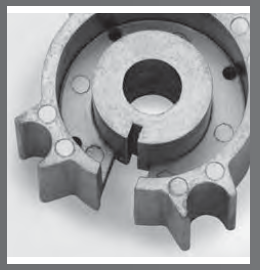

ADVANTAGES OF CIP BY BASF

Carbonyl Iron Powder (CIP) is a key raw material for Metal Injection Molding (MIM). The unique fineness of CIP makes it easily compoundable with high load. It provides high density, excellent strength and surface texture quality in the sintered part. CIP's uniform spherical particle shape generates a high flowability and facilitates high accuracy to size in the final part. Using CIP helps to precisely control the carbon-oxygen ratio of the feedstock.

BASF'S CIP GRADES

BASF's CIP OS and OM grades are the CIP grades mostly used for MIM applications. They offer excellent sintering properties and outstanding batch-to-batch consistency. CIP OS is additionally silicon-coated to improve the flowability of the feedstock.

CIP CC is a hydrogen-reduced grade with very low carbon and nitrogen content. It is widely applied in combination with OS or OM in order to adjust the carbon-oxygen ratio of the feedstock.

Our specialty H grades are employed when highest demands need to be met. The extraordinary fineness of CIP H-grades provides high density and surface texture quality in micro MIM parts.

Our CIP grades for high quality MIM parts

With precisely controlled properties, our well-known high-quality CIP grades contribute to superior MIM parts. BASF's excellent batch-to-batch consistency helps our customers to efficiently run their production processes.

Typical Properties

Grade	Fe min. (%)	C max. (%)	N max. (%)	O max. (%)	d10 (mic.)	d50 (mic.)	d90 (mic.)
CEP OM	97.8	0.75–0.90	0.65–0.90	0.15–0.40	1.7–2.7	3.9–5.2	7.2–9.2
CEP OS	97.5	0.7–0.9	0.5–0.9	0.6–0.9	1.4–2.4	3.4–4.4	6.4–8.4
CEP CC	99.5	0.05	0.01	0.18–0.35	1.7–2.7	3.8–5.3	6.5–10.0
CEP HF	97.7	0.9	0.9	0.5	1.2	2,5	3,5
CEP HQ	97.8	0.6–0.9	0.6–0.9	0.3–0.5	1	2	3
CEP HS	97.5	1	1	0.5		1.8–2.3	

CIP MIM: G-CAM_CIP_0312_MIM_e_03

Please contact us to discuss the requirements of your CIP application.

BASF SE
Carbonyl Iron Powder & Metal Systems
G-CA/MM
67056 Ludwigshafen
Germany

Asia
BASF East Asia
Regional Headquarters Ltd.
Hong Kong, China
Phone: +852 2731 3706

USA
BASF Corporation
Evans City, PA, USA
Phone: +1 724 538 1300

For information, please send an e-mail to:
inorganics@basf.com

Visit our website at:
www.carbonyliron powder.com

BASF
The Chemical Company

Note

Appendix E Technical data of graphite

degussa.
creating essentials

Technical Information No. 1261

PRINTEX® XE2
PRINTEX® XE2-B
DERUSSOL® NA 9/XE2-B

Printex® XE2 and Printex® XE2-B are conductive blacks with extraordinary properties which differ significantly from those of conventional carbon blacks.

This difference is essentially attributed to the porous structure of Printex® XE2 and Printex® XE2-B.

In the case of Printex® XE2 and Printex® XE2-B the major physical properties regarding conductive characteristics of carbon black - such as specific surface area, structure and pore volume - range on an entirely different level than those of conventional carbon blacks. This is shown in the diagram below.

A comparison of the physico-chemical data is shown in **Table 1.**

In general, polymers exhibit a high electrical resistivity. As a result of employing Printex® XE2's and Printex® XE2-B's extraordinary properties, a noticeable drop in the resistivity of polymers is observed at comparatively low concentrations.

The use of Printex® XE2-B results in similar good conductive properties as the use of Printex® XE2, though at increased sulphur and heavy metal contents. A possible influence on the heat ageing properties of plastics has to be taken into consideration.

When producing conductive compounds, only relatively small quantities of Printex® XE2 and Printex® XE2-B are needed.

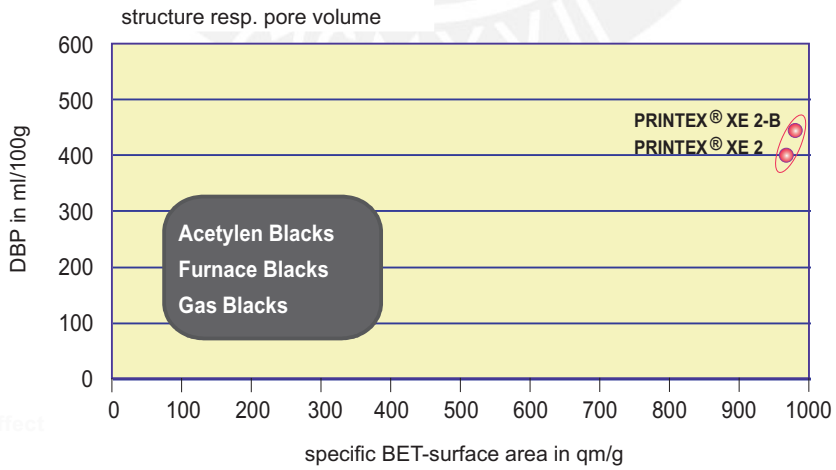

1-1261-2 / Feb05

degussa.
creating essentials

	PRINTEX® XE2	PRINTEX® XE2-B
Iodine absorption mg/g	1075	1125
DBP-absorption ml/100 g	380	420
Sieve residue ppm	≤ 500	≤ 500
Ash content %	≤ 1,0	≤ 2,0
Sulfur content %	≤ 0,4	≤ 0,8
Fleetingness at 105 °C	≤ 1,0	≤ 1,0
pH-value	8	7,8
Vanadium content ppm	approx. 1000	approx. 5000
Nickel content ppm	approx. 500	approx. 2500
Iron content ppm	approx. 300	approx. 1800

Table 1: Physico-chemical data

This is a very important advantage compared to other conductive compounds containing higher concentrations of conventional carbon blacks. This results in the following positive effects:

- decreased influence on the viscosity of liquid systems and polymer melts
- reduced effect on the flow and injection properties of thermoplastic compounds
- less influence on mechanical properties of particular final products
- highly reduced moisture adsorption of the conductive compound when stored under unfavourable weather conditions.

Applications

Printex® XE2 and Printex® XE2-B are mainly used for the manufacture of electrically conductive or antistatic compounds. Low sensitivity to mechanical stress during processing and production is a particular advantage of Printex® XE2 and Printex® XE2-B.

Thermoplastics

Among the leading fields of applications are:

- containers, boxes and trays (not to be used for food)
- tubes and fittings
- flooring compounds (computer rooms, hospitals, etc.)
- plastic films and packaging materials (for explosives and elctronic components)
- heating panels and sheets
- cables (for conductor jacketing and shielding)
- shielding elements (EMI-Shielding)

For instance based on PE, EVA, EEA, PP, PA, PS and copolymers, PVC, PC, POM, PUR, SI, UP, EP, etc.

Elastomeres

In this case Printex® XE2 and Printex® XE2-B are applied to produce rubber goods such as:

- conveyor belts and transmission belts
- flooring compounds
- cables (for conductor jacketing and shielding)
- technical rubber goods
- tanks for transportation and fuel
- hoses
- special tires and rollers

For instance, based on NR, SBR, EPDM, CPR, BR and nitrile rubber etc.

degussa.
creating essentials

Other Special Applications

Further applications of Printex® XE2 and Printex® XE2-B are the electrically conductive modification of:

- adhesives and sealants
- papers for use in conductor insulation and cash registers
- paints and coatings
- printing inks
- resin-modified mineral systems such as knifing fillers, floor pavements, concrete, mortar, etc.

Processing Recommendations

Printex® XE2 and Printex® XE2-B provides equivalent conductivity at a mere one-third to one-quarter of volume by weight, compared to that of conventional carbon blacks.

In thermoplastics, for instance, amounts of about 5 -15 % by weight of Printex® XE2 and Printex® XE2-B are sufficient to achieve resistivity values in the range of $< 10^2\ \Omega$ **cm**.

In rubber compounds, Printex® XE2 and Printex® XE2-B are preferably used in combination with other carbon blacks (2-6 phr). However, it can also be used as the sole component at 20-30 phr.

	PRINTEX® XE2	PRINTEX® XE2-B
Electrical resistivity in PP 8 wt. % carbon black	43 Ω cm	42 Ω cm
Filter pressure value (15 % carbon black, 85 % PE), 42 µm Sieb	0.077 bar cm^2/g	0.076 bar cm^2/g
Microtome cut (Number of particles: according to 5 cm^2 und 2,5 % carbon black-content)		
20 µm	21	180
30 µm	1	79
40 µm	1	1
50 µm	1	2
60 µm	1	0
> 60 µm	0	0

Table 2

DERUSSOL® NA 9 / XE2-B

Pigment black dispersions have proven successful for many years for the antistatic finishing of aqueous binder/filler systems. A great advantage here must be seen in the possibility of dust-free metered addition of the carbon black. In addition, no intensive dispersing is necessary because the dispersion already contains the carbon black in well distributed form. In order to ensure the stability of carbon black dispersions, they contain carefully matched wetting agent systems.

Designation:	**Derussol® NA 9/XE2-B**
Carbon black-content:	9 %
Solid matter content:	23 %
Wetting agent :	anionic/non-ionic

degussa.
creating essentials

The presence of cation-active substances, especially multivalent cations, for example of iron and aluminium, various wetting agent systems, the pH value, etc. can result in a flocculation of the carbon black.

During the testing of the dispersion, it must be considered that the concentration of the carbon black used, lies below the concentration used for conventional conductivity blacks. The amount of water introduced via the dispersion should be considered in the formulation.

An aqueous dispersion based on Printex XE2 is available on request as a special product, too.

Before the processing, the containers must be stirred. Since temperatures below + 1° C and over + 30° C can possibly result in a flocculation, appropriate storage conditions must be maintained. Under normal conditions carbon black dispersions can be stored for at least four months.

Product Forms Supplied

Printex XE2 and Printx XE2-B are supplied as pelletized carbon black in 5 kg PE-LD bags.

Carbon black dispersions are offered in 100 kg open-head drums with PE-liners or in 1000 l containers.

Literature List

Information regarding product safety are published in our Material Safety Data Sheets.

No.	Titel
SR 7	Degussa Pigment Blacks and Pigment Black-Preparations for Plastics
TI 1185	Pigment Blacks for Plastics

For further information please contact:

Applied Technology

Degussa AG
Business Unit
Advanced Fillers & Pigments
Anwendungstechnik
D-63403 Hanau-Wolfgang
Germany

Tel: +49 (6181) 59-2902
Fax: +49 (6181) 59-4995

E-Mail: jutta.zimmermann@degussa.com
E-Mail: konrad.rockstein@degussa.com
E-Mail: wolfgang.oertel@degussa.com
http://www.degussa-fp.com

Sales

Degussa AG
Business Unit
Advanced Fillers & Pigments
Weißfrauenstraße 9
D-60287 Frankfurt am Main,
Germany

Tel: +49 (69) 218-2119
Fax: +49 (69) 218-2853

E-Mail: marcus.lauer@degussa.com
http://www.degussa-fp.com

Or your local Degussa Representative

Appendix F Technical data of silicone glue

WACKER

CREATING TOMORROW'S SOLUTIONS

ELASTOSIL® E41

Siliconkautschuke, RTV-1

ELASTOSIL® E41 is a flowable,
one-component silicone rubber with very good mechanical properties,
which cures at room temperature under the influence of atmospheric moisture.

Typische Allgemeine Eigenschaften

Eigenschaft	Prüfmethode	Wert
Dichte bei 23 °C	DIN 53217	1,078 g/cm³
Dichte bei 23 °C, in Wasser	DIN EN ISO 1183-1 / ISO 2781	1,12 g/cm³
Hautbildungszeit bei bei 23 °C / 50 % RLF		10 - 20 min
Härte Shore A	DIN 53505 / ISO 868	40
Reißdehnung	DIN 53504 S1 / ISO 37	350 %
Reißfestigkeit	DIN 53504 S1 / ISO 37	6 N/mm²
Viskosität, dynamisch bei 23 °C	Brookfield	65000 mPa.s
Weiterreißwiderstand	ASTM D 624	11,5 N/mm

Die Angaben stellen Richtwerte dar und sind nicht zur Erstellung von Spezifikationen bestimmt.

ANWENDUNGEN

> Industriekleber

Links

> Technisches Datenblatt

> Sicherheitsdatenblatt

Appendix G Tests for electrical change under magnetic field

Table G.1: Positions and movements for tests type I.

Position	Distance of magnet 1 and the sample [mm]	Force applied [N]	Distance of magnet 2 and the sample [mm]	Waiting time for measurement after reached position [s]
Position 1	23.0	0	23.0	0
Position 2	0.5	0	0.5	0
Position 3	23.0	0	23.0	0
Position 4	0.5	0	0.5	0
Position 5	23.0	0	23.0	0
Position 6	0.5	0	0.5	0
Position 7	23.0	0	23.0	0

Table G.2: Positions and movements for tests type II. The measurement was done only for the positions in gray color.

Position	Distance of magnet 1 and the sample [mm]	Force applied [N]	Distance of magnet 2 and the sample [mm]	Waiting time for measurement after reached position [s]
Position 1	23.0	0	23.0	0
Position 2	0.5	0	0.5	0
Position 3	23.0	0	23.0	0
Position 4	0.5	0	0.5	0
Position 5	23.0	0	23.0	0
Position 6	0.5	0	0.5	0
Position 7	23.0	0	23.0	0
Position 8	0.5	0	0.5	0
Position 9	23.0	0	23.0	0
Position 10	0.5	0	0.5	0
Position 11	23.0	0	23.0	0
Position 12	0.5	0	0.5	0
Position 13	0.5	10	0.5	0
Position 14	0.5	0	0.5	0
Position 15	23.0	0	23.0	0

Table G.3: Positions and movements for tests type III. The measurement was done only for the positions in gray color.

Position	**Distance of magnet 1 and the sample [mm]**	**Force applied [N]**	**Distance of magnet 2 and the sample [mm]**	**Waiting time for measurement after reached position [s]**
Position 1	23.0	0	23.0	0
Position 2	0.5	0	0.5	0
Position 3	23.0	0	23.0	0
Position 4	0.5	0	0.5	0
Position 5	23.0	0	23.0	0
Position 6	0.5	0	0.5	0
Position 7	23.0	0	23.0	0
Position 8	0.5	0	0.5	0
Position 9	23.0	0	23.0	0
Position 10	0.5	0	0.5	0
Position 11	23.0	0	23.0	0
Position 12	0.5	0	0.5	0
Position 13	23.0	0	23.0	0
Position 14	23.0	10	23.0	0
Position 15	23.0	0	23.0	0